TWO-PHASE MULTI-OBJECTIVE EVOLUTIONARY APPROACH FOR SHORT-TERM OPTIMAL THERMAL GENERATION SCHEDULING IN ELECTRIC POWER SYSTEMS

by

DAPENG LI

B.S., Xi'an University of Technology, 2001
M.S., Shanghai University, 2004

AN ABSTRACT OF A DISSERTATION

submitted in partial fulfillment of the requirements for the degree

DOCTOR OF PHILOSOPHY

Department of Electrical and Computer Engineering
College of Engineering

KANSAS STATE UNIVERSITY
Manhattan, Kansas

2010

Abstract

The task of short-term optimal thermal generation scheduling can be cast in the form of a multi-objective optimization problem. The goal is to determine an optimal operating strategy to operate power plants, in such a way that certain objective functions related to economic and environmental issues, as well as transmission losses are minimized, under typical system and operating constraints. Due to the problem's inherent complexity, and the large number of associated constraints, standard multi-objective optimization algorithms fail to yield optimal solutions.

In this dissertation, a novel, two-phase multi-objective evolutionary approach is proposed to address the short-term optimal thermal generation scheduling problem. The objective functions, which are based on operation cost, emission and transmission losses, are minimized simultaneously.

During the first phase of this approach, hourly optimal dispatches for each period are obtained separately, by minimizing the operation cost, emission and transmission losses simultaneously. The constraints applied to this phase are the power balance, spinning reserve and power generation limits. Three well known multi-objective evolutionary algorithms, NSGA-II, SPEA-2 and AMOSA, are modified, and several new features are added. This hourly schedule phase also includes a repair scheme that is used to meet the constraint requirements of power generation limits for each unit as well as balancing load with generation. The new approach leads to a set of highly optimal solutions with guaranteed feasibility. This phase is applied separately to each hour long period.

In the second phase, the minimum up/down time and ramp up/down rate constraints are considered, and another improved version of the three multi-objective evolutionary algorithms, are used again to obtain a set of Pareto-optimal schedules for the integral interval of time (24 hours). During this phase, the hourly optimal schedules that are obtained from the first phase are used as inputs.

A bi-objective version of the problem, as well as a three-objective version that includes transmission losses as an objective, are studied. Simulation results on four test systems indicate that even though NSGA-II achieved the best performance for the two-objective model, the

improved AMOSA, with new features of crossover, mutation and diversity preservation, outperformed NSGA-II and SPEA-2 for the three-objective model. It is also shown that the proposed approach is effective in addressing the multi-objective generation dispatch problem, obtaining a set of optimal solutions that account for trade-offs between multiple objectives. This feature allows much greater flexibility in decision-making. Since all the solutions are non-dominated, the choice of a final 24-hour schedule depends on the plant operator's preference and practical operating conditions. The proposed two-phase evolutionary approach also provides general frame work for some other multi-objective problems relating to power generation as well as in other real world applications.

TWO-PHASE MULTI-OBJECTIVE EVOLUTIONARY APPROACH FOR SHORT-TERM OPTIMAL THERMAL GENERATION SCHEDULING IN ELECTRIC POWER SYSTEMS

by

DAPENG LI

B.S., Xi'an University of Technology, 2001
M.S., Shanghai University, 2004

A DISSERTATION

submitted in partial fulfillment of the requirements for the degree

DOCTOR OF PHILOSOPHY

Department of Electrical and Computer Engineering
College of Engineering

KANSAS STATE UNIVERSITY
Manhattan, Kansas

2010

Approved by:

Co-Major Professor
Sanjoy Das

Approved by:

Co-Major Professor
Anil Pahwa

Copyright

Abstract

The task of short-term optimal thermal generation scheduling can be cast in the form of a multi-objective optimization problem. The goal is to determine an optimal operating strategy to operate power plants, in such a way that certain objective functions related to economic and environmental issues, as well as transmission losses are minimized, under typical system and operating constraints. Due to the problem's inherent complexity, and the large number of associated constraints, standard multi-objective optimization algorithms fail to yield optimal solutions.

In this dissertation, a novel, two-phase multi-objective evolutionary approach is proposed to address the short-term optimal thermal generation scheduling problem. The objective functions, which are based on operation cost, emission and transmission losses, are minimized simultaneously.

During the first phase of this approach, hourly optimal dispatches for each period are obtained separately, by minimizing the operation cost, emission and transmission losses simultaneously. The constraints applied to this phase are the power balance, spinning reserve and power generation limits. Three well known multi-objective evolutionary algorithms, NSGA-II, SPEA-2 and AMOSA, are modified, and several new features are added. This hourly schedule phase also includes a repair scheme that is used to meet the constraint requirements of power generation limits for each unit as well as balancing load with generation. The new approach leads to a set of highly optimal solutions with guaranteed feasibility. This phase is applied separately to each hour long period.

In the second phase, the minimum up/down time and ramp up/down rate constraints are considered, and another improved version of the three multi-objective evolutionary algorithms, are used again to obtain a set of Pareto-optimal schedules for the integral interval of time (24 hours). During this phase, the hourly optimal schedules that are obtained from the first phase are used as inputs.

A bi-objective version of the problem, as well as a three-objective version that includes transmission losses as an objective, are studied. Simulation results on four test systems indicate that even though NSGA-II achieved the best performance for the two-objective model, the

improved AMOSA, with new features of crossover, mutation and diversity preservation, outperformed NSGA-II and SPEA-2 for the three-objective model. It is also shown that the proposed approach is effective in addressing the multi-objective generation dispatch problem, obtaining a set of optimal solutions that account for trade-offs between multiple objectives. This feature allows much greater flexibility in decision-making. Since all the solutions are non-dominated, the choice of a final 24-hour schedule depends on the plant operator's preference and practical operating conditions. The proposed two-phase evolutionary approach also provides general frame work for some other multi-objective problems relating to power generation as well as in other real world applications.

Table of Contents

List of Figures

List of Tables

Acknowledgements

First and foremost, I would like to thank my advisors Dr. Sanjoy Das and Dr. Anil Pahwa for their supervision, advice, and guidance throughout this research work. From the very early stage of this research to the last step to put the finishing touch to this dissertation, they provided me lots of great suggestions. Next, I would like to thank outside chairman Dr. Steven Eckels and my graduate committee members, Dr. Ruth Douglas Miller and Dr. Shing I Chang, for providing valuable advices to enrich this research work. I also would like to thank all the faculty and staff of Electrical and Computer Engineering Department in Kansas State University. They are always willing to offer help at any time. It is also a pleasure to thank all the friends I met at Manhattan, Kansas. It was them that made my graduate studies at K-State a colorful and exciting experience. Finally, I would like to express my deep gratitude to my beloved families. This dissertation would not have been possible without their understanding, encouragement, support and endless love. I love you ever so much.

CHAPTER 1 - Introduction

1.1 Significance of the Optimal Thermal Generation Scheduling

A typical electric power system performs three different tasks: the generation, transmission and distribution of electrical energy. Electrical energy is produced by various power generation plants, such as fossil-fuelled plants, hydroelectric plants, wind plants, nuclear power plants, solar power plants, and geothermal power plants, *etc.* This electrical energy is then transmitted over great distances at high voltages (typically 110 kV or 345 kV), using alternating current (AC), direct current (DC) or a combination of both. The distribution system comprises of a network that delivers the electric power to the customers at the required relatively low voltages (*i.e.* 120 V or 240 V).

The responsibility of power system operators includes the task of ensuring the economic operation of the plant. This is because it is important to produce electric energy to meet the load while keeping the cost as low as possible. The long term costs are minimized through judicious power system planning, which includes cost-effective and reliable strategies for the expansion of the generation, transmission and distribution systems to meet the load requirements 5 to 30 years into the future. Over shorter periods of time, when the network topology does not change, the can be brought down by optimal generation scheduling. This task is one of finding the optimal operating strategy to operate power plants in such a way as to minimize certain objective while satisfying various system and operating constraints over a given period. The objective functions may include economic costs, system security, or other costs [1]. When the only involved is the operation cost, the optimal generation scheduling problem is identical to the unit commitment (UC) problem. It is well known that human activities follow fixed patterns, in different electricity consumptions during different hours in a day. Usually, the load demands high during the daytime and early evening because people use more electricity to operate machines, keep lights on, cook food and so forth. Conversely, the load demands are low during night as people are asleep. In addition, the electricity usage is heavier during weekdays than in weekends [2-3]. It might be necessary to keep all the generators online to meet the customer demands during the peak hours, but operate some generators at their minimum levels in off-peak hours, or even switch them off. Thus, to minimize the total system-wide operation cost, the UC

problem is to decide which generators should be on and which generators should be off and for how long, while satisfying various system and operating constraints [2].

Even though it is desirable to develop optimal operating schedules considering both economic and technical constraints over a very long period [4], factors such as uncertainty in hourly load forecasting and generator outage status over a long planning horizon, exponentially increased computing time, fuel price fluctuations, maintenance time and crew constraints, disallow this option [5]. Therefore, recent attention has focused on short-term generation scheduling. It is shown that for large utility companies, even a 0.5% decrease in the fuel cost, a principal component of the operation cost, can save millions of dollars each year [6].

Although green energy, such as wind, solar and hydro power, are receiving more attention due to increased concern for environmental protection, fossil fuelled power plants burning coal, oil and natural gas still produce a large share of electricity supply. This is due to the fact that the renewable energy is not enough to sustain the huge electricity needs in modern society. These thermal plants release carbon dioxide (CO_2), sulfur dioxide (SO_2), nitrogen oxides (NO_x), methane (CH_4), hydro fluorocarbons (HFCs), per fluorocarbons (PFCs) and sulfur hexafluoride (SF_6). CO_2 is the main greenhouse gas resulting in global warming, while SO_2 and NO_x are key atmospheric pollutants that cause acid rain.

Following the Clean Air Act Amendments of 1990 (CAAA90) applied to the environmental protection [7], electric power companies adopted some practices to reduce the atmospheric emissions of the thermal power plants. The strategies used to reduce emissions include installation of pollution cleaning equipment, replacement of aged fuel-burners and generator units, the use of low emission fuels as well as taking into account emission dispatch during generation scheduling [7-8]. For example, tall chimneys were adopted as a way to reduce emission concentrations at ground level [9]. As a short-term alternative to achieve the emission targets without any investment in new pollutant cleaning equipment, minimum emission dispatch and emission-constrained economic dispatch were proposed [10-11]. In addition, minimizing emission along with operation cost during economic and environmental dispatch, which can be formulated mathematically as a multi-objective optimization problem, has been getting more attention [12-14]. However, from an operational planning standpoint, these papers mainly concentrate on the economic dispatch problem, which determines the outputs of all the online with the aim of keeping the generation cost at the minimum, but does not decide which units

should be committed for each hour of the day, to limit emissions to desirable levels. In recent with the increasing concern on environment protection, the realistic questions that system operators face are:

- How are units to be committed, and the total generation shared by them?
- How can daily emission limits be determined?
- How can a set of criteria be established to meet the emission requirements?

Transmission lines carry the current and transport the energy in the electric power system. According to Kirchhoff's laws, voltage drops from one end of the line to the other end due to the resistance, and energy lost occurs when transmitting the electricity from one electrical bus to the other one. Losses can be estimated as the difference between the amounts of energy produced by power plants and that consumed by end customers (load). Such power system losses in the United States amount to billions of kWh annually. Based on the statistical data, the transmission and distribution losses in the USA were approximately 7.2% in 1995 and 6.5% in 2007 [15-16]. These losses are accompanied by additional greenhouse gas emissions.

Improving the technologies and efficiency of the transmission system is increasingly important to make utilities generate less power and lower their atmospheric emissions than before to meet the load demands. Reducing the transmission losses is a key component and would benefit both the industry and consumers, while at the same time, reducing the sector's air pollution and carbon footprint. Specific efforts have been made to improve the transmission of electricity. These include using high voltage direct current transmission, controlling transmission line flows by system optimization, and replacing a conductor with one of a larger diameter or changing to a material with less resistance. Of these approaches, the effective integration of system optimization of the generation cost, emissions and transmission losses can lead to an optimal thermal generation schedule to best utilize the transmission system, and save a significant amount of money for utilities by reducing generation requirements to meet the actual load demands, which also could reduce emissions of greenhouse gases and air pollutants.

1.2 A Survey of Methods of Optimal Thermal Generation Scheduling

The principle objective of optimal generation scheduling problem for power utilities is to schedule the generation units effectively over a given time horizon while meeting forecasted load demand and a variety of operating constraints, such as spinning reserve requirements, minimum

up/down time constraints, *etc*. When the only goal of scheduling the generation units is to minimize operation cost, this problem becomes the well-known UC problem. Various numerical techniques have been developed to address the UC problem. Some of these methods have been discussed in [4]. These techniques, which can be classified as deterministic and meta-heuristic approaches, are reviewed next.

1.2.1 Deterministic Approaches

Deterministic approaches include priority list, dynamic programming, mixed integer programming, branch-and-bound method, and Lagrangian relaxation.

The priority list is obtained through exhaustive enumeration of all the unit combinations for different load conditions [17]. Lee used the commitment utilization factor and the classical economic index average full-load cost to determine the priority order of the generation units [18]. Unfortunately, this method cannot be applied to large systems.

Dynamic programming has been employed to solve generation scheduling problems for specific power systems [19]. When applied to UC problems, its chief advantage is its capability to handle larger scale problems as well as the flexibility in modeling the requirements of specific utilities [20].

Mixed integer programming was applied to the UC problem by rejecting the infeasible subsets to reduce the solution search space [21]. Takriti and Birge have studied the integer programming method on the UC problem based on the extension and modification of the branch-and-bound method [22]. However, it was found that the mixed integer programming based approaches take extremely long computation time when it is applied to UC problems with more detailed nonlinear models [23].

A branch-and-bound based approach incorporating all time dependent constraints without the needs of a priority ordering of generation units was developed [24]. The branch-and-bound method was also applied to the thermal generating scheduling [25]. However, as this method has to deal with the economic dispatch problem recursively to determine the upper bounds, it is computationally expensive [26].

By using the method of Lagrangian multipliers, a Lagrangian function can be obtained by relaxing the power balance and generation constraints and adding them to the cost function [27]. Lagrangian relaxation has the advantage of being easily modified to incorporate specific

characteristics of new unit constraints, and was used by some utilities [28]. Okuno *et al.* an effective Lagrangian relaxation based method to optimally schedule spinning reserve by relaxing the demand, spinning reserve and ramp rate constraints [29].

1.2.2 Meta-Heuristic Approaches

More recently, there has been an ever increasing interest in the area of meta-heuristic approaches and their applications in the engineering field. Meta-heuristic based methods have provided efficient and powerful approaches to obtain the global or near global optimum in power system optimization problems. These approaches include expert systems, fuzzy logic, artificial neural networks, tabu search, simulated annealing (SA), genetic algorithm (GA), and evolutionary programming.

An expert system to help power system operators with generation scheduling was proposed in [30]. Expert system also has been applied to the short-term large UC problem in real time [31]. Due to the uncertainty of demand and outages of generators, different fuzzy logic based approaches have been proposed to tackle the UC problem when the load demand and other variables are not precise [32].

Kasangaki *et al.* proposed a stochastic Hopfield network for the optimal generation costing problem [33]. An augmented neural network model with newer interconnections that include discrete and continuous values was proposed in [34].

Mori and Matsuzaki proposed to embed the priority list into Tabu search for the UC problem [35]. Bai and Shahidehpour have investigated the hydro-thermal, scheduling problem by applying Tabu search and a decomposition method to increase the computing accuracy of dynamic programming [36].

Originally proposed by Kirkpatrick, Gela, and Vecchi in 1982, simulated annealing is a probabilistic method that simulates the physical process of annealing, in which a material is initially heated at a high temperature and then is slowly cooled usually for softening and making the material less brittle [37]. SA was applied to UC problems with a technique of improving the probability of generating feasible solutions [38]. Wong and Fung applied SA to the short-term hydro-thermal scheduling problem [39].

Genetic algorithms were first introduced by John Holland [40]. GA based approaches been used as a popular search and optimization tool during recent years. It is motivated by the

principles of natural selection. A GA employs a population of candidate solutions and produces new solutions by the reproduction operator, such as crossover and mutation, to keep the good solutions surviving and eliminate bad solutions base on each solution's fitness, through the selection process. Several GA approaches for the solution of UC problems have been developed with the difference in the methods of representing chromosome and encoding the problem search space, and fitness evaluation. A new GA-based algorithm has been investigated on the large size UC problem [41]. Sheble *et al.* have investigated the performance of GA to solve a long-term problem with the time period from one to seven days [42]. A parallel GA was proposed for the problem [43]. Mantawy *et al.* have proposed an approach to integrate GA, SA and Tabu search the UC problem [44].

Evolutionary programming is a method that is very similar to the GA approach. Yang *et al.* applied evolutionary programming to the economic dispatch problem for units with non-smooth fuel cost functions [45]. Juste *et al.* proposed an evolutionary programming algorithm in which populations of contending solutions are evolved through random changes [20].

1.3 Why Use Multi-Objective Evolutionary Algorithms?

Most applications in electric power systems involve more than one objective to be optimized. For the optimal generation scheduling problem, the objectives are to minimize the generation cost of producing each MW of the energy, to reduce the atmospheric pollution that thermal power plants emit, and to keep the losses of transmission lines as minimum as possible, *etc.* This is a typical multi-objective optimization problem. Many multi-objective optimization problems are highly convex and nonlinear. Hence these problems cannot be addressed readily using classical optimization techniques, in which gradient-based methods are most popular ones. However, some difficulties have been revealed by many researchers for these classical methods when dealing with the real world application problems [46]:

- The initial solutions chosen by user have a significant effect on the convergence performance to the optimal solutions.
- Algorithms are not effective in solving the problems having a discrete search space.
- Most algorithms are problem-specified.
- It is possible for an algorithm to get stuck to a suboptimal solution.
- Parallel implementations for these algorithms are not efficient.

Compared with conventional optimization techniques, nature-inspired algorithms are very popular approaches for multi-objective optimization, as they are derivative-free methods, which converge quickly to Pareto-optimal solutions. Evolutionary algorithms (EAs) are probably the most important nature-inspired multi-objective optimization algorithms. These algorithms are based on Darwinian mechanisms of natural selection. There are two important goals for a multi-objective evolutionary algorithm (MOEA): It must produce samples that are as close as possible to the problem's true Pareto front. Moreover it must also produce samples that sample the front at regularly spaced intervals. These two features are called *convergence* and *diversity*. A MOEA not only should converge quickly to the Pareto front, but also maintain diversity.

Conventional multi-objective optimization methods convert multiple objectives into a single objective function by multiplying each objective with a pre-defined weight, which is called weighted sum method. However, this preference-based weighting strategy is subjective to the decision maker, and it is known for the deficiency that it cannot find certain Pareto-optimal solutions when the objective space is nonconvex. Moreover, this approach cannot find multiple solutions in a single run. Compared with the weighted sum method, MOEAs are a better choice, as they do not need any pre-defined preference information, and are able to find many different trade-off solutions which are Pareto-optimal. Various EAs, such as Horn *et al.*'s niched-Pareto genetic algorithm [47], Srinivas and Deb's non-dominated sorting genetic algorithm [48], Zitzler and Thiele's strength Pareto evolutionary algorithm [49], Knowles and Corne's Pareto-archived evolution strategy [50], have been applied to real multi-objective optimization problems.

Deb *et al.* proposed a more efficient version, which is called NSGA-II, by adopting the following effective techniques which included the following features [51]:

- A fast non-dominated sorting approach to sort a population into different nondomination levels.
- A new diversity preserving mechanism in which the crowding-distance computation was employed.
- A constraint-handling method in which an infeasible solution always be dominated by a feasible one.

Zitzler *et al.* proposed SPEA-2 as an improvement over the strength Pareto evolutionary algorithm, with a better search performance by incorporating several new features, which are [52]:

- An improved fitness assignment scheme which takes into account the number of

solutions a solution dominates and is dominated by.

- A nearest neighbor density estimation technique for better diversity estimation.
- A new archive truncation method to preserve boundary solutions.

Archived multi-objective simulated annealing (AMOSA) is another powerful and up-to-date simulated annealing-based multi-objective optimization algorithm [53]. AMOSA incorporates a domination based approach to determine the probability of acceptance of a new solution, and an archive to retain tradeoff solutions of the problem, throughout the computation.

Of all multi-objective optimization algorithms, NSGA-II and SPEA-2 showed excellent results through conducted experiments on many multi-objective optimization problems, while AMOSA is a very new one, with significantly lower computational complexity. All three schemes are effective in finding Pareto-optimal solutions with good diversity. Thus these three algorithms are selected to solve the short-term optimal thermal generation scheduling problem which needs to minimize several objective functions simultaneously.

1.4 Scope of This Dissertation

This dissertation is focused on the study of proposed two-phase multi-objective evolutionary approach applied to the short-term optimal thermal generation scheduling problem. Chapter 2 gives an overview of multi-objective optimization with focus on the principles of domination and Pareto optimality, followed by a survey of applications of multi-objective optimization in power systems. Chapter 3 provides detailed descriptions of the working of GA and SA, which can be easily used for multi-objective optimization by adopting the of Pareto-optimal set. Chapter 3 also presents the principles of three major multi-objective evolutionary algorithms, which are NSAG-II, SPEA-2 and AMOSA[1]. In Chapter 4, the emission cap and trade policy in electric power systems is introduced, and the detailed formulation of the mathematical model that represents the multi-objective short-term optimal thermal generation scheduling is described thereafter. In Chapter 5, the novel two-phase multi-objective approach is proposed to solve the short-term optimal thermal generation scheduling problem. In the first phase, this approach formulates the hourly-optimal scheduling problem as a nonlinear constrained multi-objective optimization problem which simultaneously minimizes operation

[1] Simulated annealing algorithm is loosely classified as an evolutionary algorithm. Furthermore, in this dissertation it also incorporates several standard evolutionary operators, such as crossover and mutation.

emission and transmission losses, while satisfying constraints such as power balance, spinning reserve and power generation limits. Three MOEAs, NSGA-II, SPEA-2 and AMOSA, are to get the optimal solutions for each hourly time interval, and a repair method is used to meet the constraint requirements of power generation limits for each unit as well as balancing load with generation. In the second phase, the minimum up/down time and ramp up/down rate constraints are considered, and the three MOEAs are used again to obtain a set of Pareto-optimal schedules from the hourly-optimal schedules obtained in the first phase, for the integral interval of time (24 hours). In order to investigate the performance of the proposed two-phase multi-objective evolutionary approach, Chapter 6 presents simulation results from all case studies applied on test systems. The improvement of AMOSA is also presented. The results obtained by incorporating the three MOEAs into the two-phase approach are compared with one another. Finally in Chapter 7, it is concluded that the proposed approach is effective in addressing the short-term optimal thermal generation scheduling problem, obtaining a set of optimal solutions that account for trade-offs among multiple objectives. This feature allows much greater in decision-making. Since all the solutions are Pareto-optimal, the choice of a final 24-hour schedule depends on the plant operator's preference and practical operating conditions. In the proposed two-phase multi-objective evolutionary approach has a good perspective on other mixed-integer programming problem as long as the model can be fitted into this general framework.

CHAPTER 2 - Multi-Objective Optimization

In many real world problems particularly in engineering design and business decision-making, more than one objective may be required to be taken into account. For example, a customer wanting to buy a new car potentially may consider six objectives: price, comfort, fuel consumption, power, size, and safety. While some of these objectives, such as price and fuel consumption would be minimal in the ideal product, others, such as comfort and size should be as high as possible. There is no single "best" solution that can achieve all these goals simultaneously, which may often be mutually conflicting. When an optimization problem involves simultaneously minimizing or maximizing two or more objective functions, which are in conflict with each other, the process of finding one or more optimal solutions is called multi-objective optimization [46].

This chapter gives a brief overview of multi-objective optimization with a focus on the principles of domination and Pareto optimality. In addition, a survey of applications of multi-objective optimization in power systems is provided.

2.1 Multi-Objective Optimization

Without the loss of generality, it is assumed that each objective function is to be minimized in the multi-objective optimization problem. Mathematically, the general multi-objective optimization problem can be defined as:

$$Minimize \quad f_m(\mathbf{x}), \qquad m = 1,2,\dots,M; \tag{2.1}$$

$$subject\ to \quad g_j(\mathbf{x}) \geq 0, \qquad j = 1,2,\dots,J; \tag{2.2}$$

$$h_k(\mathbf{x}) = 0, \qquad k = 1,2,\dots,K; \tag{2.3}$$

$$x_i^L \leq x_i \leq x_i^U, \quad i = 1,2,\dots,n; \tag{2.4}$$

where $\mathbf{x} = [x_1, x_2, \dots, x_n]^T$, and x_i^L and x_i^U are the lower and upper bound of the decision variables x_i. The task of multi-objective optimization is to find the vector $\mathbf{x}^* = [x_1^*, x_2^*, \dots, x_n^*]^T$ that minimizes the vector objective function with M objective functions $\boldsymbol{f} = [f_1(\mathbf{x}), f_2(\mathbf{x}), \dots, f_M(\mathbf{x})]^T$, while satisfying the J inequality constraints and K equality constraints. The duality principle can be used to covert an original objective for maximization an objective for minimization.

Since the objective functions $f_m(\mathbf{x})$ may include mutually conflicting ones, there is no single optimum solution that is minimum along each objective. Therefore in multi-objective optimization problems, the goal is to seek good compromise solutions (*i.e.* trade-off surfaces) rather than a single solution.

If the multiple objective functions are transformed into an aggregated single objective function by using weighted sum method, or addressed by placing bounds on the objective values as in the ε-constraint method, a number of difficult issues are encountered [46]. First, there is only one search space, *i.e.* the decision variable space, in a single objective optimization, whereas in a multi-objective optimization problem, the objective function forms a separate objective-function space. Furthermore, when converting several objective functions to a single one, some parameters need be set up artificially. For example, the weights for each objective when using weighted sum method, and the ε values when using ε-constraint method, need to be defined. Lastly, the only goal for single objective optimization is to find only a single optimum solution, while in multi-objective optimization, an entire set of trade-off solutions needs to be obtained. As there are no convergence guarantees in general, and because multi-objective optimization algorithms can yield only a finite, fixed number of solutions, the output is a set of solutions that are very close to the true trade-off surface (which is called the Pareto front, as discussed later). Issues related to multi-objective optimization are discussed next.

2.2 Pareto Optimality

Within any multi-objective framework, it is not easy to distinguish a good solution from an inferior one. This is because in multi-objective optimization problems, the objective functions are often conflicting, and no one solution can be said to be better than other with respect to all objective functions. Thus a solution that is better along one objective, may evaluate to a worse value along another objective.

Under these circumstances, it is convenient to invoke the concept of domination. The task of the multi-objective optimization problem turns into finding a set of the Pareto-optimal solutions by applying domination relationship between solutions. Without the loss of generality, throughout this chapter, we assume that all the objectives are to be minimized.

Definition 2.1 (*Domination*) Let $\mathbf{x_1}$ and $\mathbf{x_2}$ be two feasible solutions (decision vectors) a multi-objective optimization problem. We say that $\mathbf{x_1}$ dominates $\mathbf{x_2}$(written as $\mathbf{x_1} \prec \mathbf{x_2}$) *iff*

1) $f_i(\mathbf{x_1}) \leq f_i(\mathbf{x_2}), \quad \forall\, i \in \{1,2,\ldots,M\}$, and

2) $f_j(\mathbf{x_1}) < f_j(\mathbf{x_2}), \quad \exists\, j \in \{1,2,\ldots,M\}$.

The above definition states that given two solutions, $\mathbf{x_1}$ and $\mathbf{x_2}$, it is said that $\mathbf{x_1}$ dominates $\mathbf{x_2}$ if and only if $\mathbf{x_1}$ is at least as good as $\mathbf{x_2}$ along all the objectives, and $\mathbf{x_1}$ is better than $\mathbf{x_2}$ along at least one objective.

Three scenarios arise when two solutions $\mathbf{x_1}$ and $\mathbf{x_2}$ are compared with each other based the definition above, which are: $\mathbf{x_1}$ dominates $\mathbf{x_2}$ ($\mathbf{x_1} \prec \mathbf{x_2}$), or $\mathbf{x_1}$ is dominated by $\mathbf{x_2}$ ($\mathbf{x_2} \prec \mathbf{x_1}$), or $\mathbf{x_1}$ and $\mathbf{x_2}$ do not dominate each other ($\mathbf{x_1} \not\prec \mathbf{x_2}$ and $\mathbf{x_2} \not\prec \mathbf{x_1}$). If $\mathbf{x_1}$ dominates $\mathbf{x_2}$, $\mathbf{x_1}$ is called the non-dominated solution within the set $\{\mathbf{x_1}, \mathbf{x_2}\}$. The dominance relation is transitive, which means if $\mathbf{x_1} \prec \mathbf{x_2}$ and $\mathbf{x_2} \prec \mathbf{x_3}$, then $\mathbf{x_1} \prec \mathbf{x_3}$.

Definition 2.2 (*Non-dominated set*) Given a set of solutions S, The *non-dominated set* of solutions S' are those that are not dominated by any solutions of the set S.

If S is the entire search space, the non-dominated set S' is called *Pareto-optimal set*. The solutions within the Pareto-optimal set are called *Pareto-optimal solutions*. The image of the Pareto-optimal set in the space of objective functions is referred to as the *Pareto front*.

.

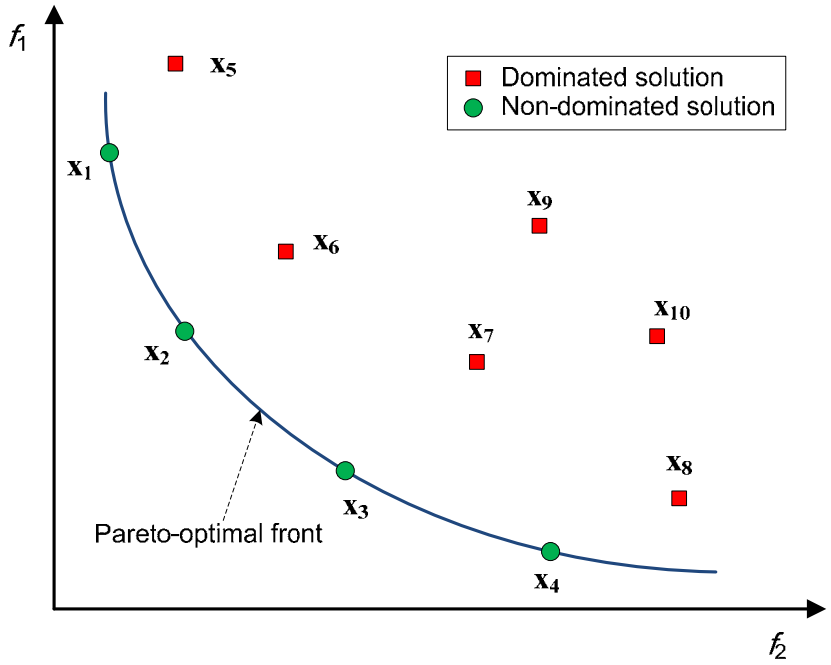

Figure 2.1 Dominated/non-dominated solutions and Pareto front

All feasible solutions of a bi-objective optimization problem are shown in objective space in Figure 2.1. The two objectives to be minimized are denoted by f_1 and f_2. Solution $\mathbf{x_2}$ is better than solution $\mathbf{x_6}$ for both objectives, thus solution $\mathbf{x_2}$ dominates solution $\mathbf{x_6}$, or it can be said that solution $\mathbf{x_6}$ is dominated by solution $\mathbf{x_2}$. While solution $\mathbf{x_2}$ is worse than solution $\mathbf{x_3}$ along objective f_1, but better than solution $\mathbf{x_3}$ along objective f_2, hence solution $\mathbf{x_2}$ and solution $\mathbf{x_3}$ do not dominate each other. Solutions within the non-dominated set $\{\mathbf{x_1}, \mathbf{x_2}, \mathbf{x_3}, \mathbf{x_4}\}$ constitute the Pareto front, which is the surface connected by all non-dominated solutions.

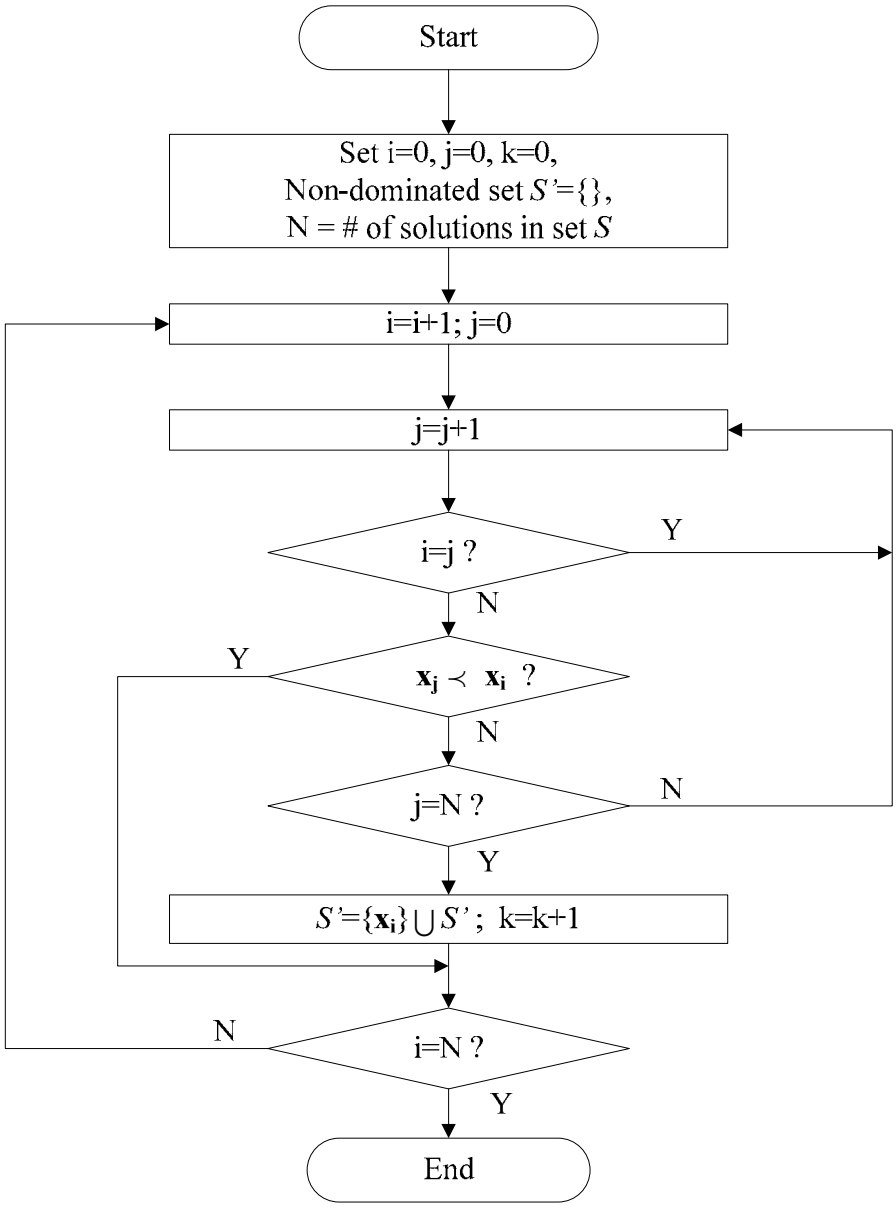

Figure 2.2 The procedure to find the non-dominated set

There are different approaches to find the non-dominated set, and the most intuitive and straightforward one is described in figure 2.2.

2.3 Goals of Multi-Objective Optimization

It is desired that any multi-objective optimization algorithm:

1) converges as close to the true Pareto front as possible, and

2) provides Pareto front samples as uniformly as possible.

These two goals are the two crucial aspects of the multi-objective optimization.

Figure 2.3 shows four different sets of solutions of the multi-objective optimization problem with different performance of convergence and diversity.

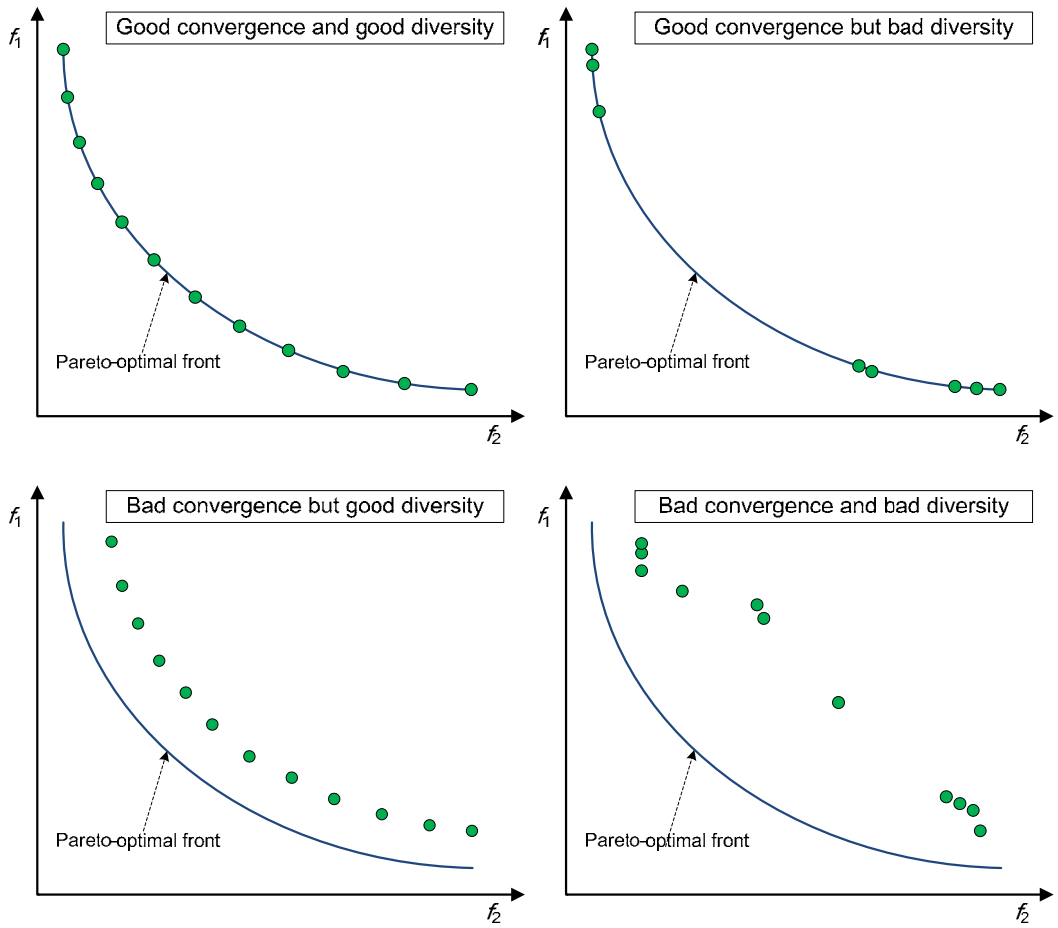

Figure 2.3 Convergence and diversity of multi-objective optimization solutions

2.4 Multi-Objective Optimization in Electric Power Systems

In recent years there has been increasing interest in applying multi-objective optimization approaches to power system problems. A variety of techniques, such as the ε-constrained method, the weighted sum method, goal-attainment, MOEAs, multi-objective particle swarm optimization, and artificial immune systems have been proposed for various multi-objective optimization problems.

It was demonstrated that in power systems there are several advantages of multi-objective optimization techniques [54], which are: 1) the ability to handle different objectives simultaneously; 2) simplification of the decision making process, and 3) the ability to see the relationship between different objectives from the Pareto front. In this manner, power system operators can obtain the most appropriate solution considering a variety of factors.

Chiang *et al.* applied the ε-constraint method to solve multi-objective optimal network reconfiguration problems in distribution systems [55]. In the ε-constraint method, one of the objective functions is selected as the primary objective function and all the other objective functions are converted into inequality constraints bounded by some allowable levels ε, so that the multi-objective optimization problem is treated as a single objective optimization problem. However, this method requires multiple runs to generate a set of Pareto-optimal solutions.

In multi-objective economic-emission dispatch problems, the economic and the environmental objectives have been combined linearly by using a weighted sum method to form a single objective function [56-57].

While the weighted sum approach has been used frequently in the past, it has three major disadvantages: 1) it cannot find Pareto-optimal solutions on the concave regions of the Pareto front (if any); 2) a uniformly distributed set of weight vectors does not necessarily lead to an even spread of Pareto-optimal solutions; 3) it requires multiple runs to obtain a set of Pareto-optimal solutions by varying weight coefficients.

The goal-attainment method has been applied to multi-objective optimization for single-tuned harmonic filter planning in industrial distribution systems [58]. With the use of interior point methods together with goal programming and linearly combined objective functions as a single one, a new multi-objective optimal power flow technique was proposed to

optimize active and reactive power dispatch while maximizing voltage security in power systems [59].

EA inherently explores a population of solutions simultaneously by employing selection operators. EA is independent of the complexity of problems, *i.e.* the solution space can include nonconvex regions, and the objective functions need not to be differentiable. These features make EA very attractive for multi-objective optimization, to determine an entire set of Pareto-optimal solutions, in a single run.

A niched Pareto genetic algorithm was applied to multi-objective environmental-economic dispatch problem [60]. Abido used the strength Pareto evolutionary algorithm to solve multi-objective optimal VAR dispatch problem [61] and economic/emission dispatch problem [12]. SPEA-2 is an improved version which eliminates the potential weaknesses of its predecessor SPEA and incorporates several new features. Li, Das and Pahwa proposed a new two-phase multi-objective evolutionary approach to solve the optimal thermal generation scheduling problem, and compared the performance of SPEA-2 and AMOSA [62]. NSGA-II is probably the most popular MOEA showing great potential in solving multi-objective optimization problems in power systems. Li, Pahwa and Das proposed implementing the NSGA-II for solving the multi-objective optimal strategy problem in day-ahead electricity market [63]. Yang and Chang have applied NSGA-II to the optimization of maintenance schedules and extents for composite power systems [64].

The multi-objective particle swarm optimization is an extensive version of the single-objective particle swarm optimization with redefinition of global and local best solutions, to handle multi-objective optimization problems. Particle swarm optimization is a population based heuristic search technique inspired by social behavior of bird flocking or fish schooling [65]. A study of stochastic economic emission load dispatch through a modified particle swarm optimization algorithm was presented in [13]. Pindoriya and Singh proposed a multi-objective particle swarm optimization based approach to study day-ahead optimal self-scheduling of generators under electricity price forecast uncertainty [66].

Recently, the artificial immune system has been widely used to solve the optimization problems by applying some features of human immune system, such as clonal selection. Slimani and Bouktir proposed using multi-objective artificial immune system for solving economic power dispatch of power system with pollution control [67]. Ahuja, Das and Pahwa proposed a

hybrid algorithm based on artificial immune system and ant colony optimization for distribution system reconfiguration, which is formulated as a multi-objective optimization problem with the aim of minimizing real losses, keeping transformer load balancing and minimizing voltage deviation [68].

The optimization process in SA resembles the annealing process of metals. The molten metal is cooled from a high temperature slowly until it is solidified at a low temperature. There have been attempts in extending SA to multi-objective optimization by aggregating all the objectives into one by taking their weighted sum. For example, in [69], Wong *et al.* combined multiple objectives of generation dispatch into one by using weighted sum method, and then applied the SA method to this single-objective optimization problem. By incorporating Pareto-domination methods, a frame work for multi-objective simulated annealing has been proposed [70], [53]. Li, Das and Pahwa applied the AMOSA to solve the multi-objective optimal generation scheduling problem with the environmental considerations [62].

CHAPTER 3 - Overview of Evolutionary Algorithms

This chapter gives an overview of evolutionary algorithms, *i.e.* genetic algorithms, evolutionary programming and evolutionary strategies. This is followed by more detailed descriptions of GAs and SA. Finally, this chapter outlines the three multi-objective evolutionary algorithms, non-dominated sorting genetic algorithm II, strength Pareto evolutionary algorithm 2 and archived multi-objective simulated annealing.

3.1 Introduction

As mentioned previously, the two goals of multi-objective optimization are to find a set of solutions that are as close as possible to the Pareto front with a good diversity.

EAs employ a population of solution candidates to find the optimal solutions, which is an efficient way to find multiple Pareto-optimal solutions simultaneously in a single simulation run. This characteristic inherently makes EAs suitable for multi-objective optimization. However, to extend the ideas of single-objective EAs to multi-objective cases, two design issues have to be addressed to satisfy the above goals of multi-objective optimization [71], which are:

1) developing an effective set of evolutionary operators for selection, crossover, and mutation, and
2) methods to maintain population diversity.

Moreover, to prevent good solutions from being lost, additional elite-preserving operators can be used so that the elites of any generation are guaranteed to be present in the next. Early researchers have developed some MOEAs which do not use any elite-preserving operator. These algorithms include niched Pareto genetic algorithm and non-dominated sorting genetic algorithm. However, elite preservation enable the high probability of creating better offspring, and Rudolph has reported that GAs with elitism converge to the global optimal solution of some functions [72]. Therefore, more recent MOEAs such as NSGA-II and SPEA-2, *etc.* incorporate elite-preserving strategies. AMOSA is a SA-based multi-objective optimization algorithm, which naturally uses elitism by keeping an archive of best solutions that are found at each iteration.

3.2 Overview of Evolutionary Algorithms

EAs aim to obtain optimal solutions by continuously making improvements to a population of candidate solutions starting with an initial, usually randomly generated one. It applies stochastic evolutionary operators to the solutions in the population in each generation, to obtain new ones. Using the Darwinian principle of survival of the fittest, only the better solutions, evaluated according to some fitness measures, are allowed to enter the next generation. EAs differ from many traditional optimization techniques in that they are population-based approaches, making them inherently parallelizable. EAs have shown success in a variety of domains including numerical function optimization, combinatorial optimization, adaptive control and machine learning.

The general scheme of an evolutionary algorithm is described in figure 3.1.

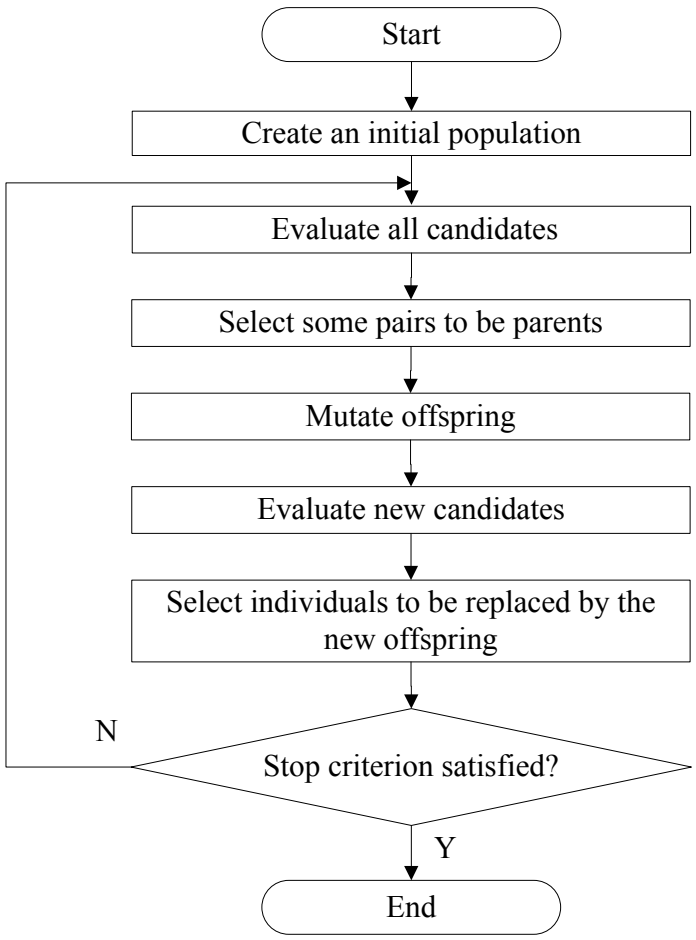

Figure 3.1 The general scheme of an evolutionary algorithm

EAs consist of three basic schemes: genetic algorithms, evolutionary strategies and evolutionary programming. These three algorithms, although originating from the same basic algorithmic skeleton, differ in details such as the way of selecting the best solutions, creating new solutions from existing ones, and the data structures used to represent those solutions.

A GA is initialized with a set of solutions (represented by chromosomes) called population. The data structure that represents the solutions can be binary or real parameters according to the attributes of the problem. Each solution is evaluated to see how good it is represented by its fitness, and is allocated the opportunity to reproduce offspring in such a way that the more suitable it is the more chances it has to reproduce. This procedure is repeated until the stop criterion, *i.e.* total number of iterations or improvement of the best solution, is satisfied.

The early evolutionary strategy uses real parameters and does not have the crossover-like operator, which is different from GA. However, more recent do include crossover. Various versions of evolutionary strategies can be differentiated based on the number of parents involved in the procreation of an offspring, and whether selection takes place only among the offspring or among the offspring and parents together. Evolutionary strategies can be applied in all fields of optimization including continuous, discrete, combinatorial search spaces without and with constraints as well as mixed search spaces.

Evolutionary programming is a predominantly mutation-based evolutionary algorithm which is applied to discrete search spaces. There are a few differences between evolutionary programming and GAs. In evolutionary programming, the solution representation is dependent on the problem, while GAs usually encode solutions as strings of genes. Additionally, evolutionary programming uses mutation as the main search operator, while GAs include both crossover and mutation operators for the same purpose.

Particle swarm optimization is another nature-inspired optimization approach that is motivated by social behavior of organisms such as bird flocking and fish schooling. It is also a population-based search procedure. Unlike GA, particle swarm optimization does not apply evolutionary search operators, but uses other ones that are motivated by swarm behavior instead [65].

Another swarm intelligence based technique ant colony optimization, was initially proposed by Marco Dorigo in 1992 [73]. Ant colony optimization has been applied to a broad

range of hard combinatorial problems, such as scheduling problems, vehicle routing problems, *etc.* [74-75].

While swarm intelligence provides an excellent alternative approach for optimization, unfortunately, Particle swarm optimization being primarily a continuous optimization cannot be used in this research. Ant colony optimization, although intended for combinatorial optimization, has not been very successful in multi-objective optimization. Therefore this research is limited to genetic algorithms and simulated annealing algorithm. Further details of these approaches follow.

3.3 Genetic Algorithms

There are a variety of GAs proposed in recent years but in essence all the algorithms follow a standard format as shown in figure 3.2.

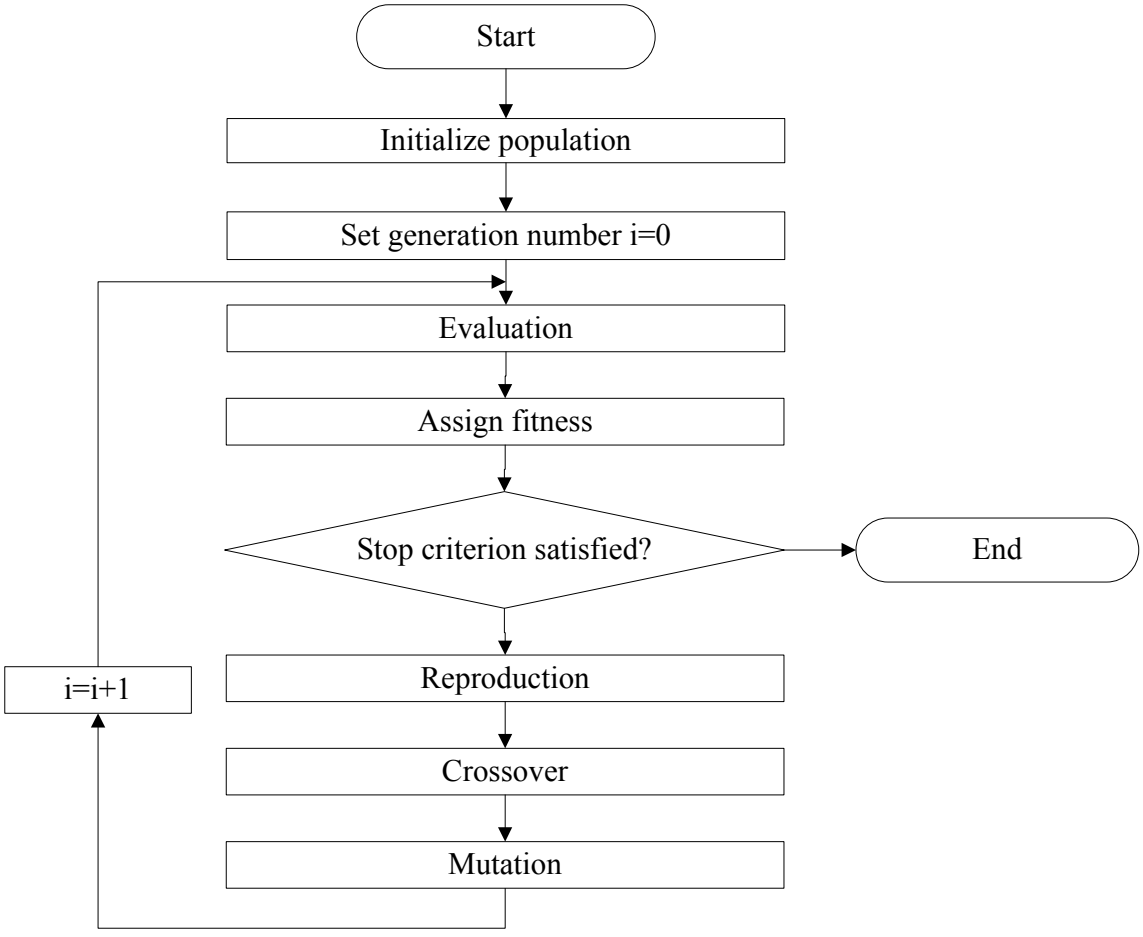

Figure 3.2 The flowchart of a typical GA

3.3.1 Chromosome Representation

A typical GA usually begins with a randomly selected population of chromosomes. These chromosomes are representations of the possible solutions of the problem. Each chromosome consists of a number of genes, which can be encoded in various ways, such as binary bits, real numbers and characters, *etc.*, depending on the nature of the problem. Figure 3.3 shows the binary and real-number representations of two chromosomes.

Binary representation:

Chromosome 1	0	0	1	0	0	1
Chromosome 2	0	0	0	0	1	0

Real-number representation:

Chromosome 1	7.00	8.34	2.60
Chromosome 2	2.00	4.22	6.88

Figure 3.3 Binary and real-number chromosome representations

Binary-coded GAs are naturally used in problems having a discrete search space. However, in handling a continuous search space problem, binary-code GA has several difficulties. One difficulty is the well known issue of Hamming cliffs. The other bottleneck of the binary-coded GA is the inability of a chromosome to represent a solution with arbitrary precision. These two aspects of binary-coded GAs often render them ineffective in some situations. Therefore, real-coded GAs are ideally suited to handle problems where the search space is continuous.

3.3.2 Fitness Evaluation

The fitness evaluation is to measure the quality of the represented solution (chromosome). The fitness function is always problem dependent and reflects the goodness of a candidate solution. In a single-objective optimization problem, the fitness is nothing more than the objective function to be minimized.

With the chromosome representation and the fitness function defined, GAs proceed to generate a population of solutions randomly (initialization), and then improve it through repetitive application of selection, crossover and mutation operators.

3.3.3 Selection

The selection operator is used to identify a set of parents for the mating pool. Here, multiple copies of better solutions are allowed, while inferior ones are probabilistically removed. Tournament selection and proportionate selection are the two most common selection schemes.

In tournament selection, a group of solutions of constant size are picked randomly from the population and a "tournament" is carried out among them to locate the best one, which enters the mating pool. This process is repeated until the pool is filled. In binary tournament selection, the group size is kept at 2. It is clear that the larger the group size the higher probability the selection is biased towards fitter solutions.

Proportionate selection, also known as roulette-wheel selection, is another way of choosing potentially useful solutions from the population in a way that is proportional to their fitness. The better the solutions are, the more is their likelihood to be selected. Unfortunately, due to the probabilistic nature of selection, there is no guarantee that the fittest solutions will enter the next generation with either tournament or roulette-wheel selection.

3.3.4 Crossover

Following selection, a crossover operator is applied to randomly paired chromosomes in the mating pool. This operator is applied with a fixed probability (0.8 is a good first choice), while the remainder of the selected solutions enter the next generation without being crossed over. Crossover is modeled after reproduction in nature, which involve two parent genotypes and yield one or two offspring genotypes. As in nature, crossover combines parts of solutions from two existing chromosomes (parents) to produce the offspring. The crossover operator is the main search operator in the GA. Depending on the choice of chromosomal representation, several methods are available.

3.3.4.1 Crossover Methods for Binary-Coded GA

For solutions with binary variables, only portions of the solutions are exchanged between the solutions during the crossover operation. Different methods are adopted based on the number of cross points.

A solution consists of several variables. In single-point crossover, after one crossover position is selected uniformly at random, variables from the beginning of the vector representing the first of the two parents, up to the crossover point are copied onto the offspring, while the rest

is copied from the second parent. Figure 3.4 illustrates this process. In two-point crossover, two crossover positions are selected uniformly at random, and the variables in the parents between the two points are exchanged to produce two new offspring, which is shown in figure 3.5. Single-point and two-point crossover can be extended to multi-point crossover

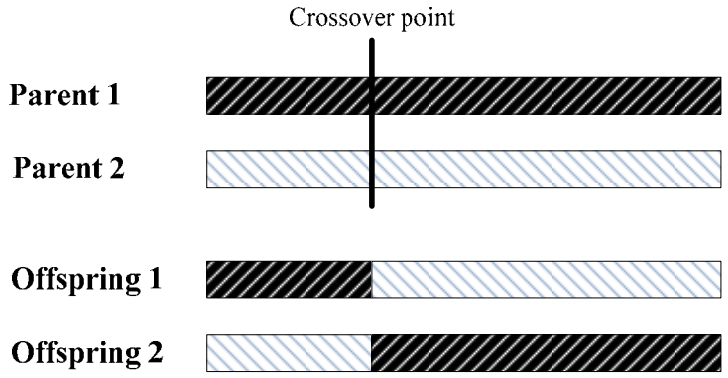

Figure 3.4 The single-point crossover method

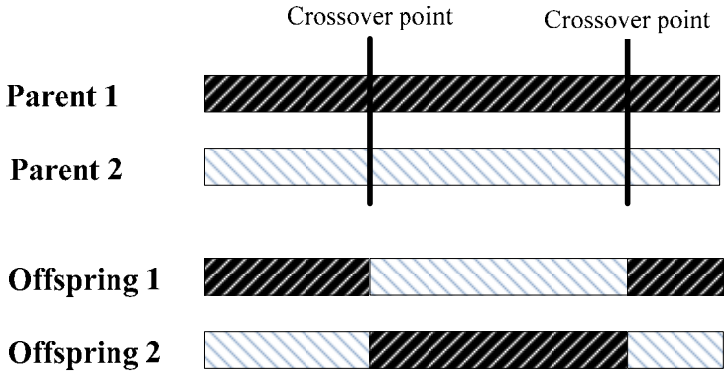

Figure 3.5 The two-point crossover method

3.3.4.2 Crossover Methods for Real-Coded GA

For solutions with real-number variables, crossover methods are different from those used for solutions with binary variables. Real-coded GAs directly manipulate two or more real numbers to generate one or more real numbers as offspring [46].

Simulated binary crossover (SBX) for real-parameter variables was proposed by Deb and Agrawal [76]. SBX simulates the operation of the single-point crossover on binary strings. At

first, a uniformly distributed random number *u* between 0 and 1 is created. To model single-point crossover in binary-coded GAs, an offspring is created following the probability distribution shown below:

$$P(\beta) = \begin{cases} 0.5(\eta_c + 1)\beta^{\eta_c}, & if\ \beta \leq 1; \\ 0.5(\eta_c + 1)\frac{1}{\beta^{\eta_c+2}}, & otherwise. \end{cases} \tag{3.1}$$

where β is defined as:

$$\beta = \left|\frac{y_2 - y_1}{x_2 - x_1}\right| \tag{3.2}$$

and y_1 and y_2 are offspring variables created from the parent variables, x_1 and x_2. In equation (3.1), η_c controls the probability of the distance between the parent variable and offspring variable. The quantity β_q below, is calculated by equating the area under the probability curve to *u*.

$$\beta_q = \begin{cases} (2u)^{\frac{1}{\eta_c+1}}, & if\ u \leq 0.5; \\ \left(\frac{1}{2(1-u)}\right)^{\frac{1}{\eta_c+1}}, & otherwise. \end{cases} \tag{3.3}$$

Finally, two offspring variables y_1 and y_2 are computed using equations (3.4) and (3.5) below.

$$y_1 = 0.5[(1 + \beta_q)x_1 + (1 - \beta_q)x_2] \tag{3.4}$$

$$y_2 = 0.5[(1 - \beta_q)x_1 + (1 + \beta_q)x_2] \tag{3.5}$$

Some other crossover methods for real-coded GAs, such as blend crossover operator and simplex crossover, were also proposed in recent years [77-78].

3.3.5 Mutation

After selection and crossover, solutions undergo a process of mutation. The purpose of mutation is to maintain diversity within the population and avoid premature convergence to local minima. Mutation is applied to each solution only with a certain mutation probability, which should usually be set fairly low, *i.e.* 0.01, as a high value can interfere with the search process by perturbing already obtained good solutions.

3.3.5.1 Mutation Methods for Binary-Coded GA

With binary representation, a bit-wise mutation operator simply inverts the value of the chosen gene (0 goes to 1 and 1 goes to 0). This mutation is also called flip mutation.

3.3.5.2 Mutation Methods for Real-Coded GA

In real-coded GAs, the mutation operator is designed to impart a small local perturbation to the solutions.

Gaussian mutation, which is a common form of this operator when using real-coded chromosomes, adds a zero-mean random value that follows a Gaussian distribution, to a variable x_i as follows:

$$y_i = x_i + N(0, \sigma_i) \tag{3.6}$$

where σ_i is a user-defined parameter. The new variable is clipped if it crosses the lower or upper bounds.

Polynomial mutation follows a polynomial probability distribution function [KM96]:

$$y_i = x_i + \left(x_i^U - x_i^L\right) \overline{\delta}_i \tag{3.7}$$

where the parameter $\overline{\delta}_i$ is calculated from the polynomial probability distribution:

$$\mathrm{P}(\delta) = 0.5(\eta_m + 1)(1 - |\delta|^{\eta_m}) \tag{3.8}$$

$$\overline{\delta}_i = \begin{cases} (2\mathrm{r_i})^{\frac{1}{\eta_m + 1}} - 1, & \text{if } \mathrm{r_i} < 0.5 \\ 1 - [2(1 - \mathrm{r_i})]^{\frac{1}{\eta_m + 1}}, & \text{if } \mathrm{r_i} \geq 0.5 \end{cases} \tag{3.9}$$

where η_m is a fixed user-defined parameter.

Several other mutation operators such as uniform mutation and non-uniform mutation have also been proposed recently [110].

3.4 Non-Dominated Sorting Genetic Algorithm II

Although several evolutionary algorithms for multi-objective optimization have been proposed, NSGA-II is one of the most common methods. The NSGA-II algorithm maintains a population of parents, P_g, of size *NP*. In each iteration *g* of the algorithm, the parents are merged with a population of *NP* offspring, Q_g obtained from the previous iteration. This merged set, $R_g = P_g \cup Q_g$ is then subject to a process of non-dominated sorting, wherein the individual solutions are assigned individual ranks. The ranking scheme makes use of domination relationship among solutions. Ranks are assigned to each solution in R_g, using an algorithm called non-dominated sorting, such that solutions that have the same rank do not dominate one another. Each solution is assigned a lower rank than another that it dominates, and, in turn, is ranked higher than ones dominating it. The non-dominated solutions in the population are assigned a rank of zero.

The least ranked *NP* solutions, which are considered to the elites, are then retained by NSGA-II as the parent population of the next iteration, P_{g+1}, while the remaining solutions are discarded. Ties are resolved by invoking crowding distance evaluation. A bounding hypercube around each solution in the objective function space that does not enclose any other solution is considered. Neighboring solutions will be located at some of the corners of this hypercube. The perimeters of these hypercubes around each of the solutions of identical rank are used as measures of diversity. Solutions whose bounding hypercubes have a larger perimeter are considered to be located in sparser regions than those with smaller ones, and are preferred.

The parents P_{g+1}, selected in this manner are then subject to crossover and mutation to obtain *NP* offspring, which become the offspring population Q_{g+1} of the next iteration. To create new offspring, SBX operator and polynomial mutation operator are used.

3.4.1 Fast Non-Dominated Sorting

The purpose of fast non-dominated sorting [51] is to rank a set of solutions where those within each rank are mutually not dominating, while lower ranked solutions dominate one or more of a higher rank. This approach is described below.

```
BEGIN
S : the solution set.
Z_i : the set of solutions dominated by solution x_i.
dc_i : the domination counter of solution x_i.
k : the front counter.
Ω_k : the set of solutions belonging to the kth front.
FOR each solution x_i ∈ S
    Z_i = ∅
    dc_i = 0
    FOR each solution x_j ∈ S
       IF (x_i ≺ x_j) THEN
          Z_i = Z_i ∪ {x_j}
      ELSE IF (x_j ≺ x_i) THEN
          dc_i = dc_i + 1
```

```
        ENDIF
    ENDFOR
    IF (dc_i = 0) THEN
        x_{i,rank} = 1
        Ω_1 = Ω_1 ∪ {x_i}
    ENDIF
ENDFOR
k = 1
WHILE (Ω_k ≠∅)
    W = ∅
    FOR each solution x_i ∈ Ω_k
        FOR each solution x_j ∈ Z_i
            dc_j = dc_j + 1
            IF dc_i = 0 THEN
                x_{j,rank} = k + 1
                W = W∪ {x_j}
            ENDIF
        ENDFOR
    ENDFOR
    k = k+ 1
    Ω_k = W
ENDWHILE
END
```

Three non-dominated fronts found by the fast non-dominated sorting approach are shown in figure 3.6.

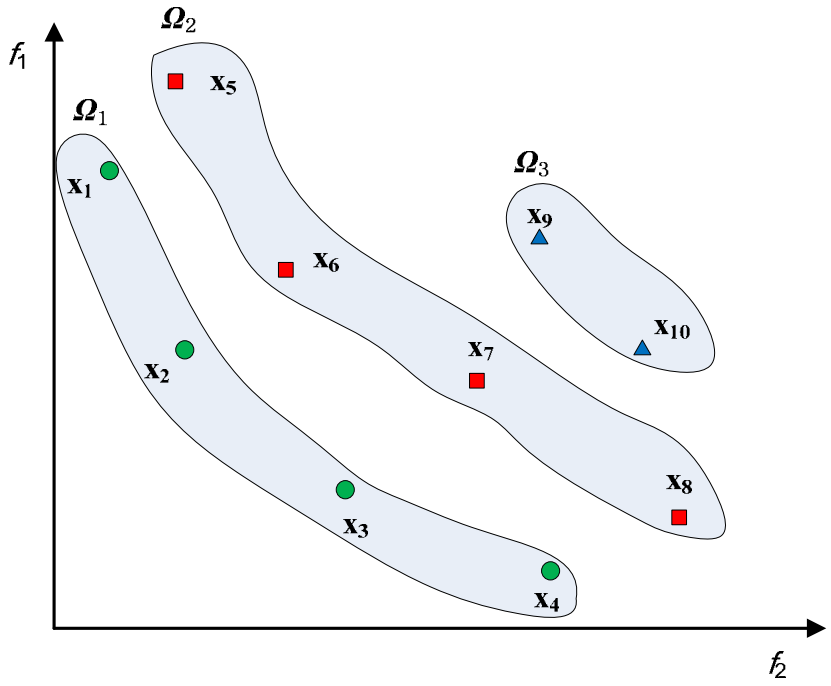

Figure 3.6 Non-dominated fronts

3.4.2 Selection and Diversity Preservation

In tournament selection, a few solutions are selected at random and the fittest is selected for crossover. NSGA-II uses a two-step comparison operator to determine the better of two solutions. A solution $\mathbf{x_i}$ is better than another solution $\mathbf{x_j}$ if solution $\mathbf{x_i}$ has a better rank than $\mathbf{x_j}$, or if they have the same rank but solution $\mathbf{x_i}$ has a better crowding distance than solution $\mathbf{x_j}$. The procedure of calculating crowding distance is [51]:

BEGIN

$|\Omega|$: the total number of solutions in the non-dominated set Ω.

H_i^m: the crowding distance for solution $\mathbf{x_i}$ *along the objective* m, where $i = 1, 2, \ldots, |\Omega|$.

H_i: the crowding distance for solution $\mathbf{x_i}$, where $i = 1, 2, \ldots, |\Omega|$.

FOR (i=1;i<=$|\Omega|$;i++)

    $H_i = 0$

```
ENDFOR
FOR each objective m
    Ω = sort (Ω, m)
    H1 = H|Ω| =∞
    FOR (i=2;i<=(|Ω|-1);i++)
        Hi = Hi + (Hi+1^m - Hi-1^m)/(fm^max - fm^min)
    ENDFOR
ENDFOR
END
```

During the sorting process the boundary points are assigned infinite distance values so that they are always selected. As shown in figure 3.7, the crowding distance for solution $\mathbf{x_i}$ is actually the half of the perimeter of the cuboid enclosed with the nearest sorted two neighboring solutions $\mathbf{x_{i-1}}$ and $\mathbf{x_{i+1}}$.

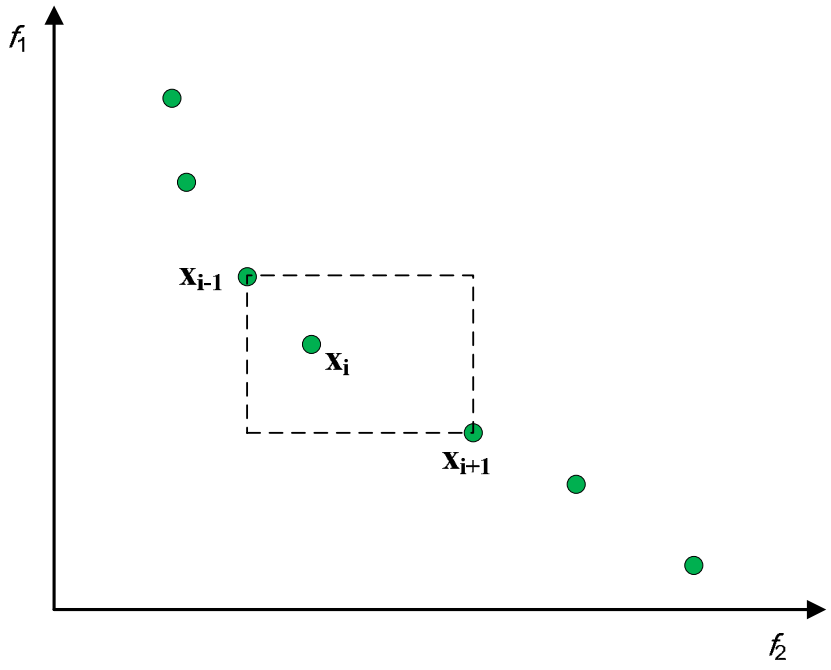

Figure 3.7 Calculation of crowding distance

3.4.3 Crossover and Mutation

In NSGA-II, SBX and polynomial mutation (described earlier) are used.

3.4.4 Constraint Handling

To handle the equality and inequality constraints in the constrained multi-objective optimization problems, the concept of *constrain-domination* is used. A solution $\mathbf{x_i}$ is said to *constrain-dominate* a solution $\mathbf{x_j}$ if any of the following conditions is true [46]:

1) Solution $\mathbf{x_i}$ is feasible and solution $\mathbf{x_j}$ is not.

2) Solutions $\mathbf{x_i}$ and $\mathbf{x_j}$ are both infeasible, but solution $\mathbf{x_i}$ has a smaller overall constraint violation.

3) Solutions $\mathbf{x_i}$ and $\mathbf{x_j}$ are both feasible and solution $\mathbf{x_i}$ dominates solution $\mathbf{x_j}$.

3.4.5 Overall Procedure

An outline of NSGA-II is provided below:

BEGIN

Initialize parent population P_g with size of NP.

$|\Omega_i|$: the total number of solutions that have the rank Ω_i.

WHILE (g < max generation) **DO**

Step 1: Create offspring population Q_g using tournament selection, crossover and mutation.

Step 2: Merge parent and offspring populations and create $R_g = P_g \cup Q_g$.

Step 3: Assign each solution in R_g a rank Ω_i using non-dominated sorting approach, where i = 1, 2, ….

Step 4: Select all solutions with ranks from Ω_1 to Ω_k into new population P_{g+1}, so that $\sum_{i=1}^{k}|\Omega_i| < NP$ and $\sum_{i=1}^{k+1}|\Omega_i| \geq NP$.

Step 5: Add the most widely distributed (NP - $\sum_{i=1}^{k}|\Omega_i|$) solutions into P_{g+1} by performing the crowding distance sorting for all the solutions that have the rank Ω_{k+1}.

Step 6: $g = g + 1$.

ENDWHILE

END

The procedure to select *NP* solutions from the merged population R_g, to form the new population P_{g+1}, is shown in figure 3.8.

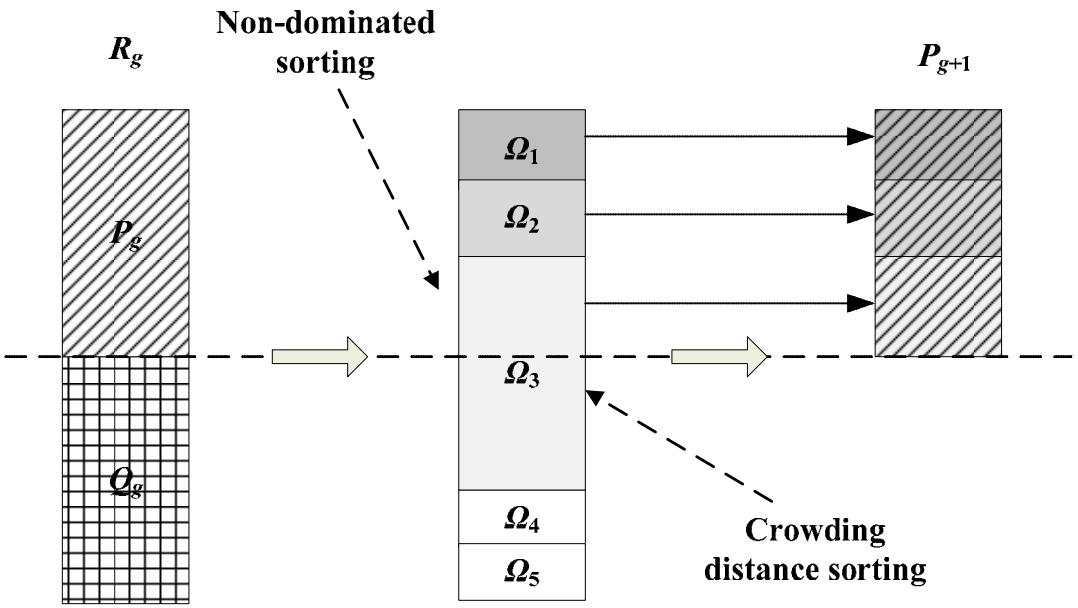

Figure 3.8 Recombination operation in NSGA-II

3.5 Strength Pareto Evolutionary Algorithm 2

SPEA-2 is an improved version of the original strength Pareto evolutionary algorithm. Compared with the original version, the SPEA-2 incorporates a fine-grained fitness assignment strategy, a density estimation technique, and an enhanced archive truncation method.

3.5.1 Overall Procedure

The procedure of SPEA-2 is described as follows [52].

BEGIN

Set archive size as N' and generation number $g = 0$.

Initialize parent population P_g with size of NP and an empty archive $P_g' = \emptyset$.
S': the non-dominated set which is the final output.
WHILE (g < max generation) **DO**
  Step 1: Calculate fitness values of solutions in P_g and P_g'.
  Step 2: Environmental selection: all non-dominated solutions in P_g and P_g' are copied to P_{g+1}'.
    IF ($|P_{g+1}'| > N'$) **THEN**
      Reduce P_{g+1}' to size NP by means of the truncation operator.
    ELSEIF ($|P_{g+1}'| < N'$) **THEN**
      Fill P_{g+1}' with dominated solutions in P_g and P_g'.
    ENDIF
  Step 3: Perform binary tournament selection on P_{g+1}' to fill the mating pool.
  Step 4: Create new population P_g using crossover and mutation to the mating pool.
  Step 5: $g = g + 1$.
ENDWHILE
$S' = P_{g+1}'$.
END

3.5.2 Fitness Assignment

The fitness of a solution is calculated based on the strength value of the solutions by which it is dominated, where the strength value of a solution is defined as the number of solutions that it dominates in the current population. Ties of solutions with the same fitness are resolved by invoking the concept of diversity, which is measured using a nearest neighbor density estimation method.

The fitness value of a solution $\mathbf{x_i}$ comprises of two terms, the raw fitness value, $RF(\mathbf{x_i})$, and the density metric, $DM(\mathbf{x_i})$. This is shown in the following equation [52].

$$F(\mathbf{x_i}) = RF(\mathbf{x_i}) + DM(\mathbf{x_i}) \tag{3.10}$$

The raw fitness value $RF(\mathbf{x_i})$ is a function of other solutions' strength values $SV(\mathbf{x_i})$:

$$RF(\mathbf{x_i}) = \sum_{\mathbf{x_j} \in P_g \cup P'_g, \mathbf{x_j} \prec \mathbf{x_i}} SV(\mathbf{x_j}) \tag{3.11}$$

$$SV(\mathbf{x_i}) = |\{\mathbf{x_j} | \mathbf{x_j} \in P_g \cup P'_g \wedge \mathbf{x_i} \prec \mathbf{x_j}\}| \tag{3.12}$$

where $|\cdot|$ denotes the cardinality of the set. The raw fitness value $RF(\mathbf{x_i})$ of an non-dominated solution $\mathbf{x_i}$ is equal to 0, means that no solution is better than the solution $\mathbf{x_i}$. The higher the raw fitness value $RF(\mathbf{x_i})$ is, the more solutions dominate $\mathbf{x_i}$.

The raw fitness $RF(\mathbf{x_i})$ may fail when most solutions do not dominate each other, and therefore many solutions having identical raw fitness values. In this situation, additional density information is needed to discriminate those solutions. The density $DM(\mathbf{x_i})$ is calculated as follows:

$$DM(\mathbf{x_i}) = \frac{1}{d_i^k + 2} \tag{3.13}$$

where d_i^k is the distance between solution $\mathbf{x_i}$ and its k-th nearest solution, and $k = \sqrt{NP + N'}$.

Since $d_i^k \geq 0$, the density $DM(\mathbf{x_i})$ is always less than 1. Because the raw fitness value $RF(\mathbf{x_i})$ of an non-dominated solution is equal to 0, the minimum fitness values $F(\mathbf{x_i})$ is assigned to each non-dominated solutions with the first rank.

3.5.3 Environmental Selection

In environmental selection, after all the non-dominated solutions in P_g and P'_g are copied into the archive set P'_{g+1}, three scenarios arise [52]:

1) The size of the non-dominated set is exactly equal to the archive size N'. In this case, the environmental selection is completed.

2) The size of the non-dominated set is less than the archive size N'. In this case, we simply add the best $(N' - |P'_{g+1}|)$ dominated solutions in P_g and P'_g, based on their fitness values, to the archive to fill the gap.

3) The size of the non-dominated set is greater than the archive size N'. In this case, an archive truncation procedure is employed to iteratively remove solutions from P'_{g+1} until $|P'_{g+1}| = N'$. At each iteration that solution $\mathbf{x_i}$ is chosen for removal for which $\mathbf{x_i} \leq_d \mathbf{x_j}$ for all $\mathbf{x_j} \in P'_{g+1}$ with

$$\mathbf{x_i} \leq_d \mathbf{x_j} : \Leftrightarrow \begin{matrix} \forall\, 0 < k < \left|P'_{g+1}\right| : d_i^k = d_j^k \ \vee \\ \exists\, 0 < k < \left|P'_{g+1}\right| : [(\forall\, 0 < l < k :\ \ d_i^l = d_j^l) \wedge d_i^k < d_j^k] \end{matrix} \tag{3.14}$$

Using this method, the solution which has the minimum distance to another solution is chosen for removal at each stage. In case there are more than one solution with minimum distance, the tie is broken by seeking the second smallest distances, and so forth.

3.6 Archived Multi-Objective Simulated Annealing

AMOSA is based on the SA and aims to solve the multi-objective optimization problem. It also uses an archive to store the non-dominated solutions.

3.6.1 Simulated Annealing Algorithms

Simulated annealing process is similar to the annealing process of metals and glass. In physical annealing, the glass is heated to a high temperature so that the glass is a liquid and the atoms can move relatively freely. Then the temperature is slowly lowered so that the atoms are able to relax into the most stable orientation, a state of thermal equilibrium. During the cooling process, any random change of the configuration of atoms results in the change of system energy, ΔE. The new configuration is accepted if $\Delta E \leq 0$, but only is accepted with a certain probability if $\Delta E > 0$. The most common probability function is called Boltzmann distribution:

$$P(\Delta E) = e^{-\Delta E / k_b T'} \tag{3.15}$$

where k_b is the Boltzmann's constant and T' is the temperature. It has two important features: the higher the ΔE, the lower the probability to accept the new configuration, and the higher the T', the higher the probability of uphill moves.

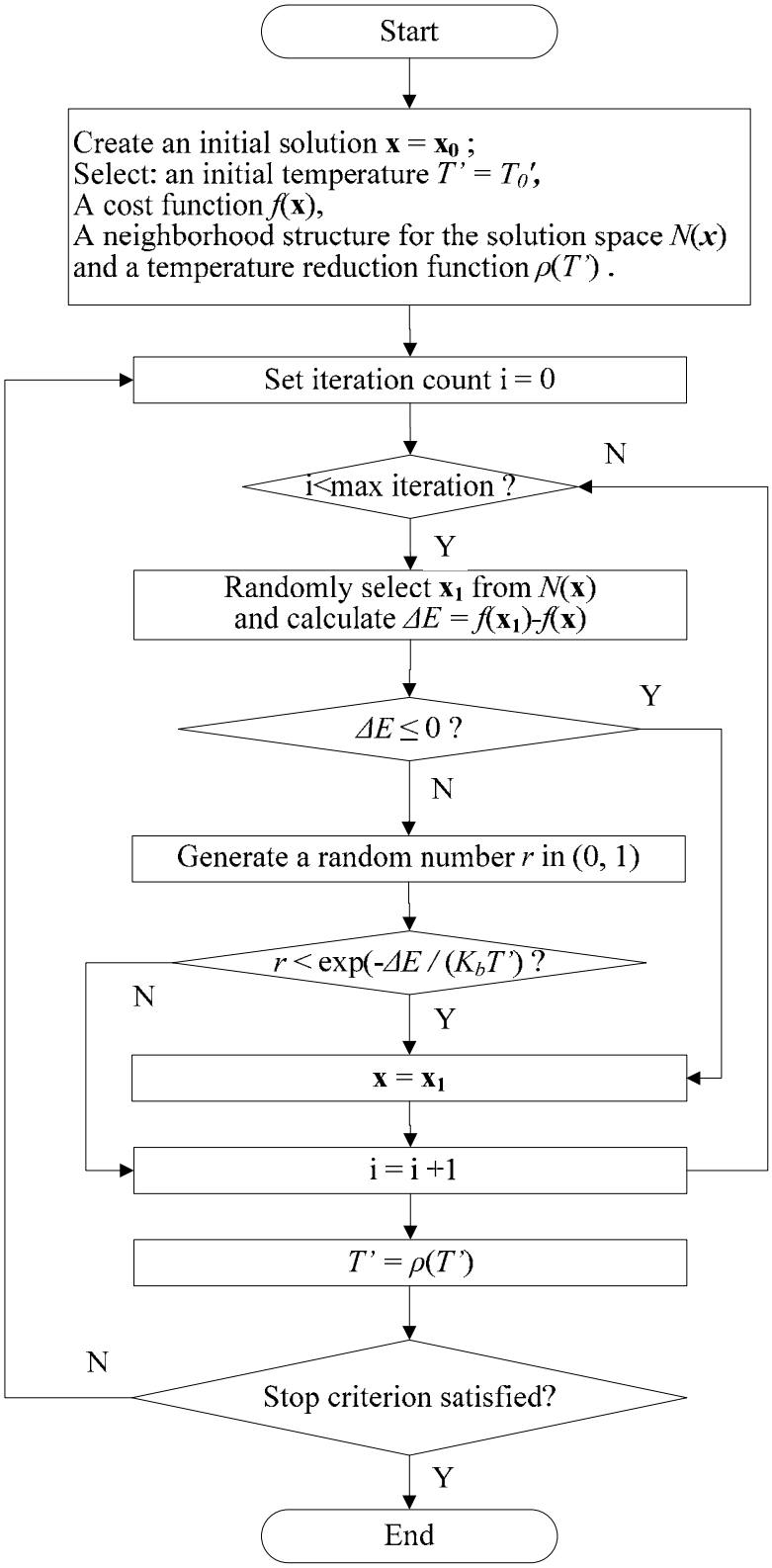

Figure 3.9 The procedure of the simulated annealing algorithm

Figure 3.9 shows the procedure of the simulated annealing algorithm. Various cooling schedules $\rho(T')$ can be used to reduce the temperatures, such as

$$\rho(T') = \varepsilon T' \tag{3.16}$$

where ε between 0.8 and 0.99, and

$$\rho(T') = T'/(1+\eta T'), \tag{3.17}$$

where η is a very small positive number around 0, and

$$\rho(T') = \xi^{(n-1)} T_0' \tag{3.18}$$

where ξ is a scaling factor less than 1, and n is the cooling step counter. T_0' is the initial temperature.

SA works as a hill-climbing search method that allows moves in less good goal directions by a probabilistic method to escape local minima. One of the main drawbacks of simulated annealing is its slower rate of convergence. This is because the temperature has to be lowered at a slow rate in order to avoid the algorithm from getting trapped in local minima.

3.6.2 AMOSA

A number of solutions, equal to $\zeta \times SL$ ($\zeta > 1$) are initially generated, where SL is the maximum size to which the archive may be filled. A simple hill-climbing technique is applied to these solutions until the archive is filled with HL non-dominated solutions. One of the solutions, called $\mathbf{x_{cur}}$, is selected randomly from the archive as the initial solution, and the temperature is initialized to $T'=T'_{max}$. A new solution, called $\mathbf{x_{new}}$, is generated by perturbing $\mathbf{x_{cur}}$. The domination status of $\mathbf{x_{new}}$ is checked with the $\mathbf{x_{cur}}$ as well as solutions in the archive. Three different cases may arise based on the domination relations between $\mathbf{x_{cur}}$ and $\mathbf{x_{new}}$. The amount by which one dominates the other is used to calculate the acceptance probability of a new solution, thereby distinguishing "more dominated" solutions from "less dominated" ones. Whenever the number of non-dominated solutions in the archive exceeds SL, a clustering technique is used to reduce the archive size to HL.

The above process is repeated *iter* times for each temperature T'. The temperature is then reduced to a value $\varepsilon T'$, where the factor ε represents the cooling rate, whose value lies between 0 and 1. The algorithm terminates after the temperature reaches its minimum limit, T'_{min}.

3.6.2.1 Amount of Domination

The amount of domination between two solutions $\mathbf{x_i}$ and $\mathbf{x_j}$ is defined as [53]:

$$\Delta D(\mathbf{x_i}, \mathbf{x_j}) = \prod_{m=1, f_m(\mathbf{x_i}) \neq f_m(\mathbf{x_j})}^{M} \frac{|f_m(\mathbf{x_i}) - f_m(\mathbf{x_j})|}{f_m^{max} - f_m^{min}} \quad (3.19)$$

Figure 3.10 illustrates the amount of domination between the two solutions for a two objective case, which is equal to the area of the shaded rectangle.

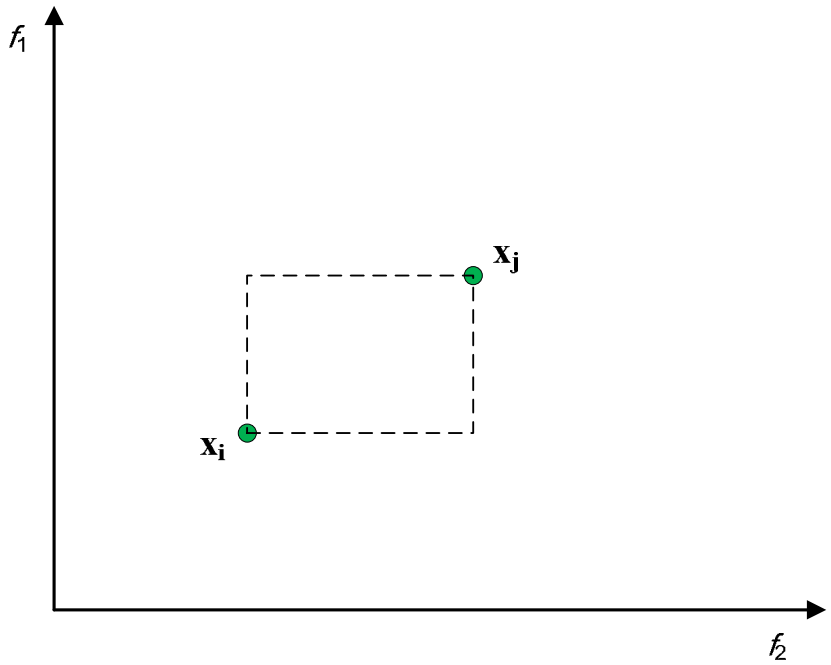

Figure 3.10 Amount of domination between two solutions

3.6.2.2 Overall Procedure

One of the main advantages of AMOSA is in its lower computational complexity in comparison to NSGA-II and SPEA-2. When the parameters *SL* and *HL* follow a linear relationship with the archive size, $N=|P'|$, the complexity per iteration of AMOSA is $O(M(N+\log(N)))$ in comparison to $O(MN^2)$ for NSGA-II and $O(MN^3)$. The procedure for AMOSA [53] is given as follows:

```
BEGIN
Set T'max, T'min, HL, SL, iter, ε, T'=T'max.
Initialize the archive P'.
Randomly choose a solution from P' as xcur.
WHILE (T' > T'min) DO
   FOR (i=0; i<iter; i++)
```

$\mathbf{x_{new}}$ = *perturb*($\mathbf{x_{cur}}$)

IF ($\mathbf{x_{cur}} \prec \mathbf{x_{new}}$)

IF ($\mathbf{x_{new}}$ is dominated by k ($k \geq 0$) solutions in P')

Set $\mathbf{x_{new}}$ as $\mathbf{x_{cur}}$ with probability of

$P = \frac{1}{1+\exp(\Delta D_{avg} * T')}$, where

$\Delta D_{avg} = \frac{\left(\sum_{i=1}^{k} \Delta D(\mathbf{x_i}, \mathbf{x_{new}})\right) + \Delta D(\mathbf{x_{cur}}, \mathbf{x_{new}})}{(k+1)}$

ENDIF

ENDIF

IF ($\mathbf{x_{cur}} \nprec \mathbf{x_{new}}$ and $\mathbf{x_{new}} \nprec \mathbf{x_{cur}}$)

IF ($\mathbf{x_{new}}$ is dominated by k ($k \geq 1$) solutions in P')

Set $\mathbf{x_{new}}$ as $\mathbf{x_{cur}}$ with probability of

$P = \frac{1}{1+\exp(\Delta D_{avg} * T')}$, where

$\Delta D_{avg} = \sum_{i=1}^{k} \Delta D(\mathbf{x_i}, \mathbf{x_{new}})$

ENDIF

IF ($\mathbf{x_{new}}$ is non-dominating with all the solutions in P')

Set $\mathbf{x_{new}}$ as $\mathbf{x_{cur}}$ and add $\mathbf{x_{new}}$ to P'.

IF $|P'| > SL$

Reduce the size of P' to HL by applying the clustering method.

ENDIF

ENDIF

IF ($\mathbf{x_{new}}$ dominates k ($k \geq 1$) solutions in P')

Set $\mathbf{x_{new}}$ as $\mathbf{x_{cur}}$ and add $\mathbf{x_{new}}$ to P'.

Remove all the k dominated solutions from P'.

ENDIF

ENDIF

IF ($\mathbf{x_{new}} \prec \mathbf{x_{cur}}$)

IF ($\mathbf{x_{new}}$ is dominated by k ($k \geq 1$) solutions in P')

Set solutions corresponding to ΔD_{min} as $\mathbf{x_{cur}}$ with probability of

$P = \frac{1}{1+\exp(-\Delta D_{min})}$, where

ΔD_{min} = minimum of the difference of domination amounts between the $\mathbf{x_{new}}$ and the k solutions;

else set $\mathbf{x_{new}}$ as $\mathbf{x_{cur}}$.

ENDIF

IF ($\mathbf{x_{new}}$ is non-dominating with the solutions in P')

Set $\mathbf{x_{new}}$ as $\mathbf{x_{cur}}$ and add $\mathbf{x_{new}}$ to P'.

IF ($\mathbf{x_{cur}}$ is in P')

remove it from P'.

ELSE IF $|P'| > SL$

Reduce the size of P' to HL by applying the clustering method.

ENDIF

ENDIF

IF ($\mathbf{x_{new}}$ dominates k ($k \geq 1$) solutions in P')

Set $\mathbf{x_{new}}$ as $\mathbf{x_{cur}}$ and add $\mathbf{x_{new}}$ to P'.

Remove all the k dominated solutions from P'.

ENDIF

ENDIF

ENDFOR

$T' = \varepsilon T'$

ENDWHILE

IF $|P'| > SL$

Reduce the size of P' to HL by applying the clustering method.

ENDIF

END

CHAPTER 4 - Short-Term Optimal Thermal Generation Scheduling

4.1 Introduction

The main goal of optimal generation scheduling is to schedule the generators in such a way as to minimize certain objective functions, while satisfying various system and operating constraints over a given period. The objective functions may include economic costs, system security, or other costs [1].

With the CAAA90 being applied to environmental protection in Unites States, utility companies have been reducing the atmospheric emissions of the thermal power plants using various strategies [79-80]. Emissions rates can be adjusted according to the levels of pollution control, the characteristics of the fuels undergoing combustion, power plant efficiency and emission dispatching. As a short-term alternative to achieve the emission targets without investment for new pollutant cleaning equipment, emission dispatching is an effective strategy to keep the emission below a certain level.

The SO_2 allowance trading program in CAAA90 has generally been viewed as a success in its goal to achieve emission reductions using a cap and trade policy. In this program, on the basis of historical fuel consumption, the emission trading system first allocate the marketable emission permits (allowances) to power plant operators free of charge. Subsequently, the operators are allowed to either include their own emissions as part of their allowances, or make a profit by selling them to others. Power plants with low emission reduction opportunity cost are allowed to sell unused allocated allowances. On the contrary, some plants may choose to purchase more allowances from others to cover their own emission excess [81]. In general, the annual allocation of allowances to each utility does not change over time. Utilities are required to measure and report emissions to the regulatory agency at the end of the operational year in order to balance the emissions with their allocated allowances. Each day if the operators have a set of different schedules, which are trade-off between operation cost and emission, they acquire a firm understanding of the environmental performance of the power plants on a daily basis, and can exercise flexibility in adopting different schedule for each day, to comply with their standards.

During the process of transferring power supplied by generators via the transmission system, some of the energy is lost due to the resistance of the transmission lines and other

equipments. Most of this lost energy is converted to heat. The total loss in the transmission network can be approximated by the B-matrix loss formula, in which the loss is a function of all the generator outputs. Given a certain transmission network, the system operator must find an economical way to dispatch all the generators in order to improve the transmission efficiency.

An appropriate coordination among operation cost, emission and transmission losses can result in not only significant cost savings but also compliance with the emission caps. Thus, to find the generation scheduling taking operation cost, emission as well as transmission losses into account has received increasing attention.

This chapter gives a brief overview of the emission cap and trade policy in electric power systems and the detailed problem formulation of the multi-objective short-term optimal thermal generation scheduling is described thereafter.

4.2 Emission Cap and Trade

In this dissertation, although any emission source could be readily included for the study, only NO_x emission is considered. One of the most important hazards of NO_x is that it can lead to the formation of ground-level ozone, causing both acute and chronic respiratory ailments. In addition, NO_x also contributes to regional haze, eutrophication of water bodies, *etc.* To help Northeast and mid-Atlantic region reduce harmful groud-level ozone, in 1990 the U.S. Congress established the Ozone Transport Commission (OTC) under the Clean Air Act Amendments. Utility companies have been reducing the atmospheric emissions of the thermal power plants by various strategies [82-83]. With the aim to reduce summertime NO_x emissions, the OTC NO_x Budget Program was implemented from 1999 to 2002，and has since been replaced by the NO_x Budget Trading Program under the *NO_x State Implementation Plan (SIP) Call*, a broader federal program issued by the U.S. Environmental Protection Agency, involving 22 eastern states and the District of Columbia. The OTC NO_x Budget Program has generally been viewed as a success to achieve NO_x reductions using a *cap-and-trade* policy. The apportionment of total budget allowances among the OTC states, or the establishment of the state caps, was accomplished in a uniform manner based on heat input. However, methods to allocate allowances to regulated sources, *i.e.* electricity generating units, were determined by each state individually. For example, some states such as Delaware, New Hampshire, New York, Pennsylvania, and the District of Columbia had fixed allocations from 1999 to 2002, while some other states such as Connecticut,

Maryland, and New Jersey adjusted their allocations periodically based on various factors [84].

After receiving marketable emission permits (allowances), power plant operators are allowed to either cover their own emissions by their allowance, or to make profit by selling them to others. One benefit of the cap-and-trade program is that if the allowance market is well-designed, those with the lowest cost emission reduction opportunities would sell the unwanted allocated allowances for a profit. Meanwhile, some other plant owners may purchase additional allowances to cover emission excess. Finally it is expected that all the power plants acquire the necessary allowance they need, while the net emission comply with the emission caps at the lowest possible cost [85]. In general the annual allocation of allowances to each utility does not change over time, and utilities need to measure and report emissions to the regulatory agency regularly to balance the emissions with the allowances they have.

4.3 Problem Formulation

The following notation is used throughout the dissertation：

$\alpha_i, \beta_i, \gamma_i, \varphi_i, \tau_i$	Characteristic coefficients of unit *i*'s emission
a_i, b_i, c_i	Characteristic coefficients of unit *i*'s fuel cost
h_{it}^{off}	Number of continuous time intervals that a unit *i* has remained OFF before current period *t*
h_{it}^{on}	Number of continuous time intervals that a unit *i* has remained ON before current period *t*
i, j, k	Index of units
t	Index of time period
λ	Market price for the emission allowance
B_{ij}, B_{0i}, B_{00}	The coefficients of the B matrix loss formula
CSC_i	Cold start cost of unit *i*
CSH_i	Cold start hours of unit *i*
D_t	System load demand in period *t*
E	Total emission produced by all units for the entire time interval *T*
Ecap	Emission cap of all the units for the entire time interval *T*
E_t	Emission produced by all units in period *t*
F	Total operation cost for the entire time interval *T* considering emission

	allowance trading
FC_{it}	Fuel cost of unit *i* in period *t*
F_e	Emission cost caused by purchasing or selling additional emission allowance
F_0	Total operation cost for the entire time interval *T* without emission allowance trading
F_{0t}	Operation cost of all units in period *t*
HSC_i	Hot start cost of unit *i*
MD_i	Minimum down time of unit *i*
MU_i	Minimum up time of unit *i*
NG	Number of units
P_{it}	Power output in period *t*
P_i^{max}	Maximum generation limit of unit *i*
P_i^{min}	Minimum generation limit of unit *i*
P_{loss}	Total transmission losses for the entire time interval *T*
$P_{loss,t}$	Total transmission losses in period *t*
R_t	Reserve requirement in period *t*
RD_i	Ramp-down limit of unit *i*
RU_i	Ramp-up limit of unit *i*
SDC_i	Shutdown cost of unit *i* in period *t*
STC_i	Startup cost of unit *i* in period *t*
S0	Set of off-line units
S1	Set of on-line units
T	Entire time interval, in this paper, 24 hours
U_{it}	0/1 variable which states OFF/ON status of unit *i* in period *t*

We will assume that the time period considered is T=24 hours, *i.e.* one day. The short-term optimal thermal generation scheduling attempts to minimize the operation cost, emission and transmission losses while satisfying different system and operating constraints.

4.3.1 Objective Functions

1) The total operation cost F_0, including fuel costs, startup costs, and shutdown costs for the entire period, is given by:

$$F_0 = \sum_{t=1}^{T} \sum_{i=1}^{NG} [FC_{it} + STC_{it} + SDC_{it}] \tag{4.1}$$

Generally, the fuel cost of a thermal unit in any given time interval is a function of the generator power output. Most frequently used cost function is quadratic polynomial and expressed as follow.

$$FC_{it} = (a_i + b_i P_{it} + c_i {P_{it}}^2) U_{it} \tag{4.2}$$

Turning a unit on will incur start-up costs. Startup cost is a function of the number of hours during which the unit has been off. If the thermal unit has been off for a long period, a cold start-up cost is applied. If the unit has been recently turned off (temperature of the boiler is still high), a hot start-up cost is applied. The startup cost function is in the form of equation below.

$$STC_{it} = ST_{it}(1 - U_{i(t-1)}) U_{it} \tag{4.3}$$

$$ST_{it} = \begin{cases} HSC_i & if\ h_{it}^{off} \le CSH_i + MD_i \\ CSC_i & if\ h_{it}^{off} > CSH_i + MD_i \end{cases} \tag{4.4}$$

The shut-down cost is usually a constant value for each unit, which is given below.

$$SDC_{it} = SD_{it}(1 - U_{it}) U_{i(t-1)} \tag{4.5}$$

As explained previously, if the emission allowances are enforced, the operators have the option to buy the deficit from the market or sell the excess to the market, resulting in an additional emission cost:

$$F_e = (E - Ecap)\lambda \tag{4.6}$$

where E is the total emission produced in the entire duration of T hours, $Ecap$ is the emission cap allowed in T hours, and λ is the market price for the emission allowance. Note that F_e could be negative if the total emission produced by all units in T hours is below $Ecap$, which means the plant operator benefits from selling the excess emission allowance to others, thereby curtailing the total operation cost. Although the structure and supply-demand behavior of the emission allowance market have an effect on the quantities of allowances exchanged, this is not the emphasis of this dissertation. It is assumed that the plant operator is capable of selling the excess allowance successfully through other means. Based on this assumption, the revised operation cost can be represented by:

$$F = F_e + F_0 \tag{4.7}$$

2) The form of the NO_x emission function model depends on the parameter estimating techniques used to approximate the amount of NO_x emission [IFM94] [RSTH88] [RHK06]. Some researchers used second order polynomial functions or a combination of polynomial and exponential terms. However, we found that the average emission rate range yielded by using either of them based on testing systems deviated too much from the real-world NO_x emission rates reported in [PConline]. Meanwhile, the combination of polynomial and sinusoidal terms is more appropriate to be used compared with the above two forms. Thus the total NOx emission produced by all units in T hours is expressed by a combination of polynomial and sinusoidal terms of the following form [IFM94]:

$$E = \sum_{t=1}^{T} \sum_{i=1}^{NG} \{[\alpha_i + \beta_i P_{it} + \gamma_i {P_{it}}^2 + \varphi_i \sin(\tau_i P_{it})] U_{it}\} \tag{4.8}$$

3) The transmission losses can be expressed as a function of unit power outputs using the B-matrix loss formula:

$$P_{loss} = \sum_{t=1}^{T} P_{loss,t} \tag{4.9}$$

$$P_{loss,t} = \sum_{i=1}^{NG} \sum_{j=1}^{NG} P_{it} B_{ij} P_{jt} + \sum_{i=1}^{NG} B_{0i} P_{it} + B_{00} \tag{4.10}$$

4.3.2 Constraints

1) Power balance:

If the transmission losses are not considered, the generated power from all the committed units must be sufficient enough to meet the load demand, which is defined as,

$$\sum_{i=1}^{NG} P_{it} = D_t \tag{4.11}$$

When the transmission losses are considered, the power balance equation becomes:

$$\sum_{i=1}^{NG} P_{it} = D_t + P_{loss,t} \tag{4.12}$$

2) Spinning reserve:

To maintain system reliability, committed units must be able to supply more than the load demand in order to prevent power shortages in case a unit fails or an unexpected increase in load occurs. The spinning reserve is considered to be a prespecified amount or a given percentage of the forecasted peak demand. It must be sufficient enough to meet the loss of the most heavily loaded unit in the system. This has to satisfy the equation given in (4.13).

$$\sum_{i=1}^{NG} P_i^{max} U_{it} \geq D_t + R_t \tag{4.13}$$

3) Power generation limits:

Unit rated minimum and maximum capacities must not violate.

$$P_i^{min} U_{it} \leq P_{it} \leq P_i^{max} U_{it} \tag{4.14}$$

4) Minimum up time:

If a unit has already been turned on, it has to be on for a certain period before it can be shut down.

$$\left(h_{i(t-1)}^{on} - MU_i\right)(U_{i(t-1)} - U_{it}) \geq 0 \tag{4.15}$$

5) Minimum down time:

If a unit has already been shut down, it has to be turned off for a certain minimum period before it can be restarted.

$$\left(h_{i(t-1)}^{off} - MD_i\right)(U_{it} - U_{i(t-1)}) \geq 0 \tag{4.16}$$

6) Ramp up rate:

For each unit, output is limited by ramp up rate at each hour.

$$P_{it} - P_{i(t-1)} \leq \left[1 - U_{it}\left(1 - U_{i(t-1)}\right)\right] RU_i + U_{it}\left(1 - U_{i(t-1)}\right) P_i^{min} \tag{4.17}$$

7) Ramp down rate:

For each unit, output is limited by ramp down rate at each hour.

$$P_{i(t-1)} - P_{it} \leq \left[1 - U_{i(t-1)}(1 - U_{it})\right] RD_i + U_{i(t-1)}(1 - U_{it}) P_i^{min} \tag{4.18}$$

8) Unit initial status:

The initial status of each unit at the beginning of the scheduling period must be taken into account. It indicates how long the unit has been on/off.

CHAPTER 5 - Two-Phase Multi-Objective Evolutionary Approach

5.1 Introduction

In this chapter, the two-phase multi-objective evolutionary approach proposed in this research, is introduced to solve the short-term optimal thermal generation scheduling problem. In the first phase, this approach formulates the hourly-optimal scheduling problem as a nonlinear constrained multi-objective optimization problem which simultaneously minimizes operation cost, emission and transmission losses, while satisfying constraints such as power balance, spinning reserve and power generation limits. Three MOEAs, NSGA-II, SPEA-2 and AMOSA, with additional steps necessary to guarantee feasibility, are investigated separately to get optimal solutions for each hourly time interval. A repair method is used in conjunction with the optimization algorithm to meet the constraint requirements of power generation limits for each unit as well as balancing the load demand. In the second phase, the minimum up/down time and ramp up/down rate constraints are considered, and three MOEAs are applied again to obtain a set of Pareto-optimal schedules from the hourly-optimal schedules obtained in the first phase, for the integral interval of time (24 hours). Detailed aspects of the proposed method are discussed below.

5.2 First Phase (Hourly Schedules)

The hourly-optimal dispatch problem is formulated as a nonlinear constrained multi-objective optimization problem which simultaneously minimizes operation cost, emission and transmission losses, subject to the usual constraints, *i.e.* power balance, spinning reserve and power generation limits. The approach proposed in this study incorporates a novel method to repair solutions that are infeasible, in order to render them feasible again, with minor modifications.

5.2.1 Objective Functions and Constraints

The hourly dispatch problem, which is addressed in the first phase, is formulated as follows:

Minimize $F_{0t},\ E_t,\ P_{loss,t}$

where,

$$F_{0t} = \sum_{i=1}^{NG}[FC_{it} + STC_{it} + SDC_{it}] \quad (5.1)$$

$$E_t = \sum_{i=1}^{NG}\{[\alpha_i + \beta_i P_{it} + \gamma_i {P_{it}}^2 + \varphi_i \, sin(\tau_i P_{it})]U_{it}\} \quad (5.2)$$

$$P_{loss,t} = \sum_{i=1}^{NG}\sum_{j=1}^{NG} P_{it} B_{ij} P_{jt} + \sum_{i=1}^{NG} B_{0i} P_{it} + B_{00} \quad (5.3)$$

Subject to power balance (4.11) or (4.12), spinning reserve (4.13) and power generation limits (4.14).

5.2.2 Encoding Scheme

In this phase, the MOEA is applied separately *T* times, once for each hourly time interval *t*=1, 2, …, *T*. Although earlier genetic algorithm based approaches for unit commitment have typically used binary coding schemes (to denote the OFF or ON state of each unit), our method explicitly determines the power output of each unit. Therefore we use real valued representation instead. Each solution in this phase is a row vector of length *NG*, whose *i*th entry corresponds to the output of unit *i* during the time interval *t* under consideration, as shown in figure 5.1. As there will be *NP* such solutions in the population at any given time, the population consisting of *NP* solutions, is a matrix of *NP*×*NG*, in which the *NP* solutions correspond to the rows of the matrix.

P_{1t}	P_{2t}	...	P_{NGt}

Figure 5.1 Solution encoding for hourly dispatch schedule

5.2.3 Initialization

The output of each unit *i* is generated from randomly generated numbers following the uniform distribution from 0 to P_i^{max}, which is not always feasible because of the generation limits and load balance constraints. However we have the following repair scheme so that the two constraints are always satisfied.

5.2.4 Feasibility Restoration Scheme

Not only do the initial randomly generated solutions, but also the solutions generated after crossover and mutation, sometimes violate the generation limits or make the system

unbalanced. The repair procedure has been devised to guarantee feasibility. The details of this scheme are explained below.

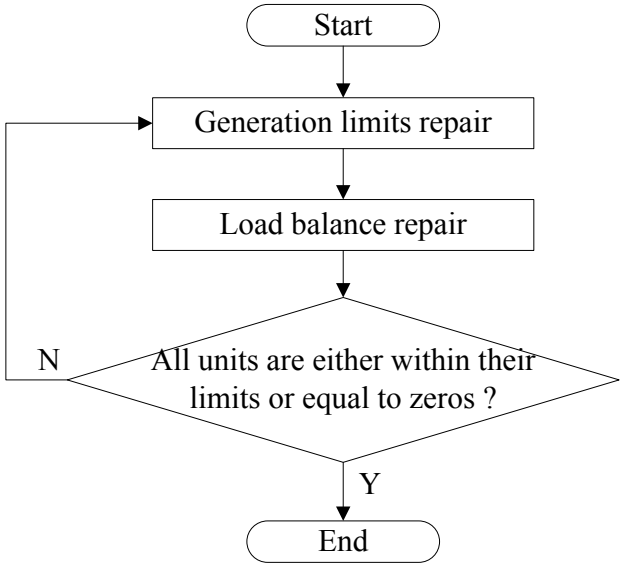

Figure 5.2 Feasibility restoration procedure

As shown in figure 5.2, the feasibility restoration procedure includes two major schemes: generation limits repair scheme and load balance repair scheme.

5.2.4.1 Generation Limits Repair Scheme

In the generation limits repair scheme, three possible situations, where generation limits are violated, can occur. As shown in figure 5.3, these violations are repaired in the following manner. A unit with its power output beyond the maximum limit $P_i^{max}$is kept at P_i^{max}. A parameter θ on interval (0, 1) is used as the threshold to rectify the infeasible unit outputs which are below minimum limits. A unit whose power output exceeds a threshold, θP_i^{min}, is increased to the minimum allowable value, P_i^{min} (the constant θ in this paper is set to 0.5). On the other hand, if the solution allocates a power output below θP_i^{min} to the unit, then this output is simply reset to zero. After this change, if each unit's output is zero, *i.e.* every unit is shut off, the output of each unit i is reset to a random number, uniformly distributed within the range $[P_i^{min}, P_i^{max}]$.

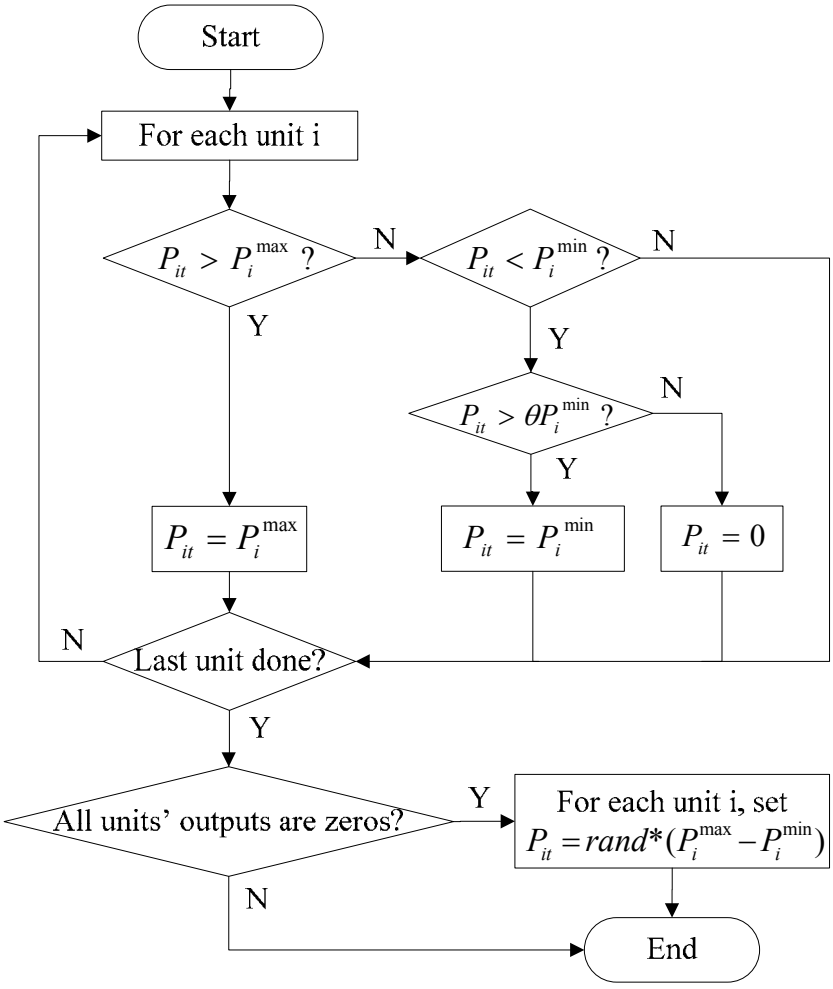

Figure 5.3 Generation limits repair scheme

5.2.4.2 Load Balance Repair Scheme without Transmission Losses

Figure 5.4 shows the load balance repair scheme when transmission losses are not under consideration. In this case, if the total generation of all units is greater than the load demand, the outputs of on-line units are decreased to keep load balance; On the other hand, if the total generation of all units is less than the load demand, two possible cases arise. When the total sum of the maximum output limits of all the on-line units is greater than the load demand, increase outputs of these on-line units to keep load balance. Even if all the on-line units reach their maximum output limits there are still an insufficiency of generation, some of those off-line units have to be turned on and their outputs will be increased in order to balance the load.

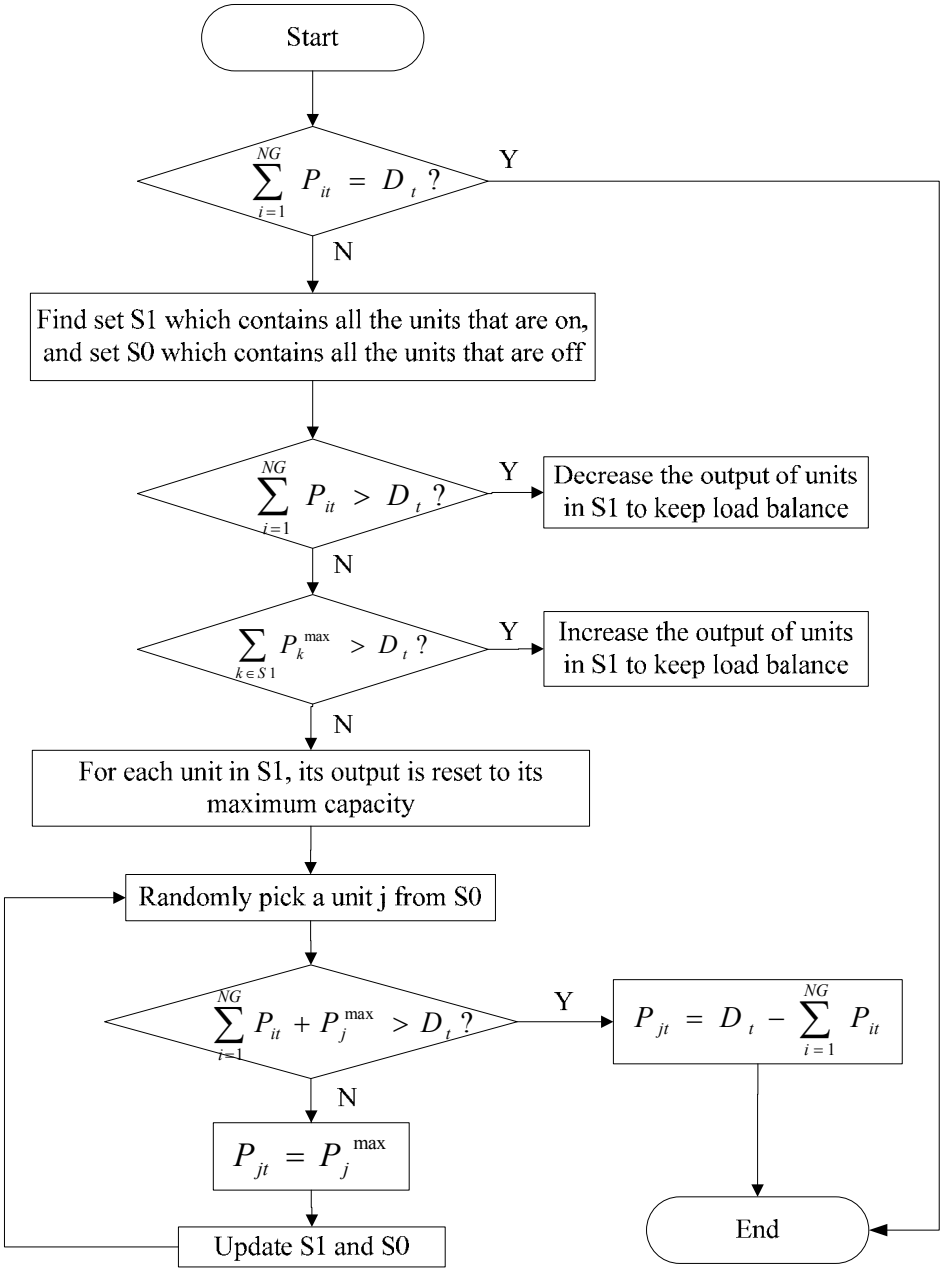

Figure 5.4 Load balance repair scheme without transmission losses

5.2.4.3 Load Balance Repair Scheme with Transmission Losses

The transmission losses can be rewritten as [KC93]:

$$P_{loss,t} = \mathbf{P}'B\mathbf{P} + \mathbf{P}'B_0 + B_{00} \tag{5.4}$$

where $\mathbf{P}'$ is the transpose of vector $\mathbf{P}$, which is a column vector of all generators' outputs at hour *t*. *B* is a *NG*×*NG* matrix, and B_0 is a *NG* column vector.

$$\mathbf{P} = \begin{bmatrix} P_{1t} \\ P_{2t} \\ \vdots \\ P_{NGt} \end{bmatrix} \tag{5.5}$$

$$B = \begin{bmatrix} B_{11} & \cdots & B_{1NG} \\ \vdots & \ddots & \vdots \\ B_{NG1} & \cdots & B_{NGNG} \end{bmatrix} \tag{5.6}$$

$$B_0 = \begin{bmatrix} B_{01} \\ B_{02} \\ \vdots \\ B_{0NG} \end{bmatrix} \tag{5.7}$$

Rearrangement of equation (5.4) gives:

$$P_{loss,t} = [\mathbf{P}_{\boldsymbol{a}}'|P_{rt}] \left[\frac{\boldsymbol{B_{aa}}|B_{ar}}{B_{ra}|B_{rr}}\right] \left[\frac{\mathbf{P_a}}{P_{rt}}\right] + [\mathbf{P}_{\boldsymbol{a}}'|P_{rt}] \left[\frac{B_{0a}}{B_{0r}}\right] + B_{00} \tag{5.8}$$

where $\mathbf{P}_{\boldsymbol{a}}'$ is the transpose of the vector $\mathbf{P_a}$, which is a column vector of the (NG-1) generators' outputs at hour t, except for the unit *r*. P_{rt} is a scalar value representing the generation output of unit *r* at hour *t*. $\boldsymbol{B_{aa}}$ is a (*NG*-1)×(*NG*-1) matrix. B_{ar} and B_{0a} are column vectors with size of (*NG*-1). B_{ra} is a row vector with size of (*NG*-1). B_{rr}, B_{0r} and B_{00} are scalars.

Equation (5.8) can be expressed by a quadratic function in the form of equation (5.9):

$$P_{loss,t} = k_2 P_{rt}^2 + k_1 P_{rt} + k_0 \tag{5.9}$$

where

$$k_2 = B_{rr} \tag{5.10}$$

$$k_1 = B_{ra}\mathbf{P_a} + \mathbf{P}_{\boldsymbol{a}}' B_{0r} + B_{ar} \tag{5.11}$$

$$k_0 = \mathbf{P}_{\boldsymbol{a}}' \boldsymbol{B_{aa}} \mathbf{P_a} + \mathbf{P}_{\boldsymbol{a}}' B_{0a} + B_{00} \tag{5.12}$$

Moreover, we also know that

$$P_{rt} = D_t - \sum_{\substack{i=1 \\ i \neq r}}^{NG} P_{it} + P_{loss,t} \tag{5.13}$$

After all the generators' outputs are determined by using load balance repair scheme without considering transmission losses as depicted in the previous section, an online generator *r* is randomly chosen from those online generators to pick up the transmission losses. From equation (5.9) and (5.13), the new output of generator *r* is calculated by solving the equation below:

$$k_2 P_{rt}^2 + (k_1 - 1)P_{rt} + \left(k_0 + D_t - \sum_{\substack{i=1 \\ i \neq r}}^{NG} P_{it}\right) = 0 \tag{5.14}$$

The above equation can also be written as

$$aP_{rt}^2 + bP_{rt} + c = 0 \tag{5.15}$$

where

$$a = k_2 \tag{5.16}$$

$$b = k_1 - 1 \tag{5.17}$$

$$c = k_0 + D_t - \sum_{\substack{i=1 \\ i \neq r}}^{NG} P_{it} \tag{5.18}$$

The two roots of the equation are $P_{rt,1} = \frac{-b+\sqrt{b^2-4ac}}{2a}$ and $P_{rt,2} = \frac{-b-\sqrt{b^2-4ac}}{2a}$. If both roots are within generation limits, one of them is randomly chosen to be the new generation output. If only one is within the generation limits, then the feasible one is chosen. On the other hand, if neither is within the limit, the one having a smaller violation is selected. This violation is calculated as the absolute value of the difference between the root and its closest boundary limit.

The load balance repair scheme considering transmission losses is shown in figure 5.5. In case the new generation output of generator *r* still exceeds its generation limits, the generation limit repair scheme will again take care of this situation.

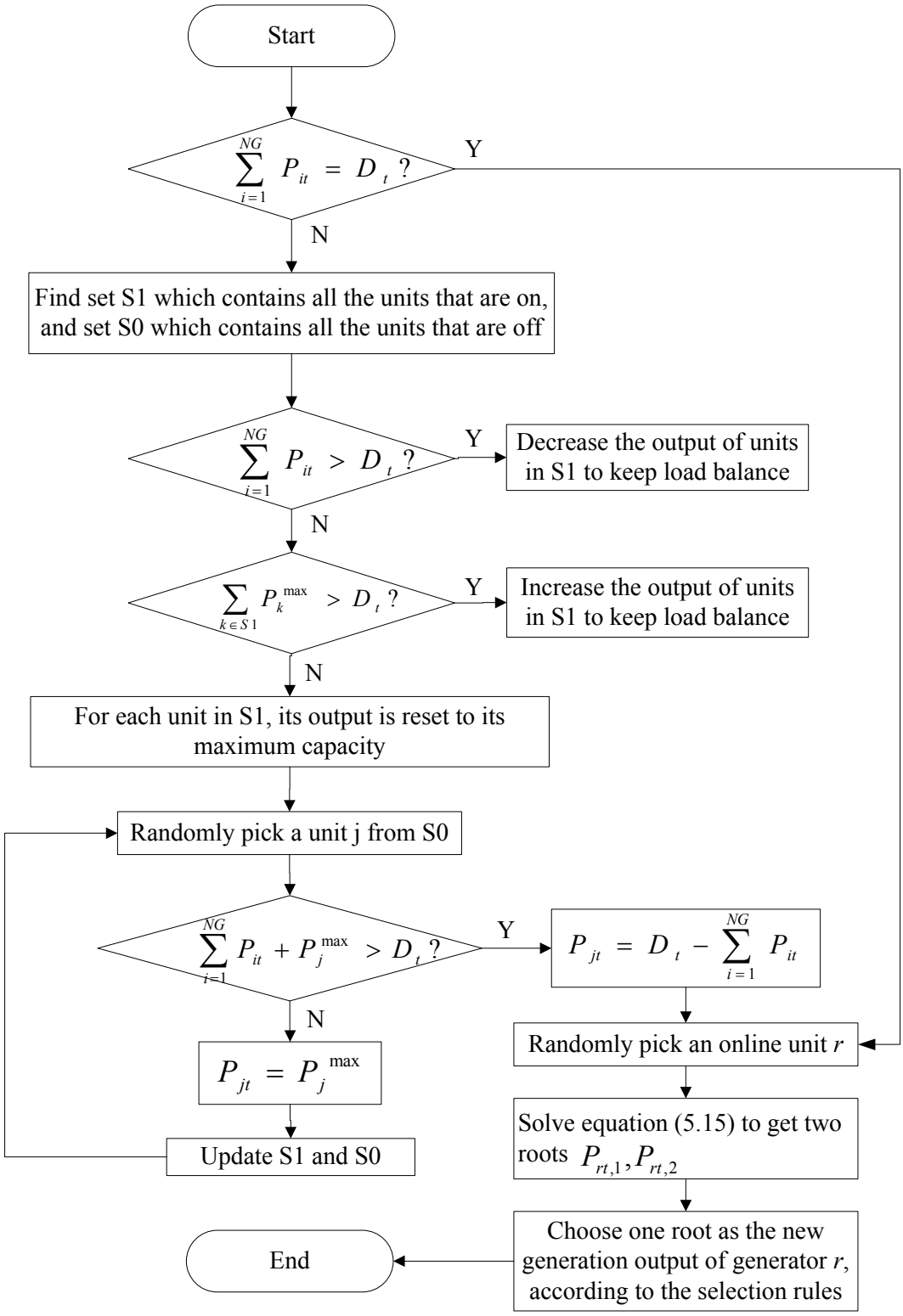

Figure 5.5 Load balance repair scheme with transmission losses

5.2.5 Crossover and Mutation

SBX [76] and polynomial mutation [90] are used in modified NSGA-II and SPEA-2. Polynomial mutation is also adopted in AMOSA. It should be noted that the lower bounds of the variables used for SBX and polynomial mutation are both set to 0 as negative values of generator outputs are clearly inadmissible.

5.2.6 Modified NSGA-II in the First Phase

The flowchart of modified NSGA-II in the first phase is provided in figure 5.6, illustrating how feasibility restoration is incorporated as a single stage within the overall scheme.

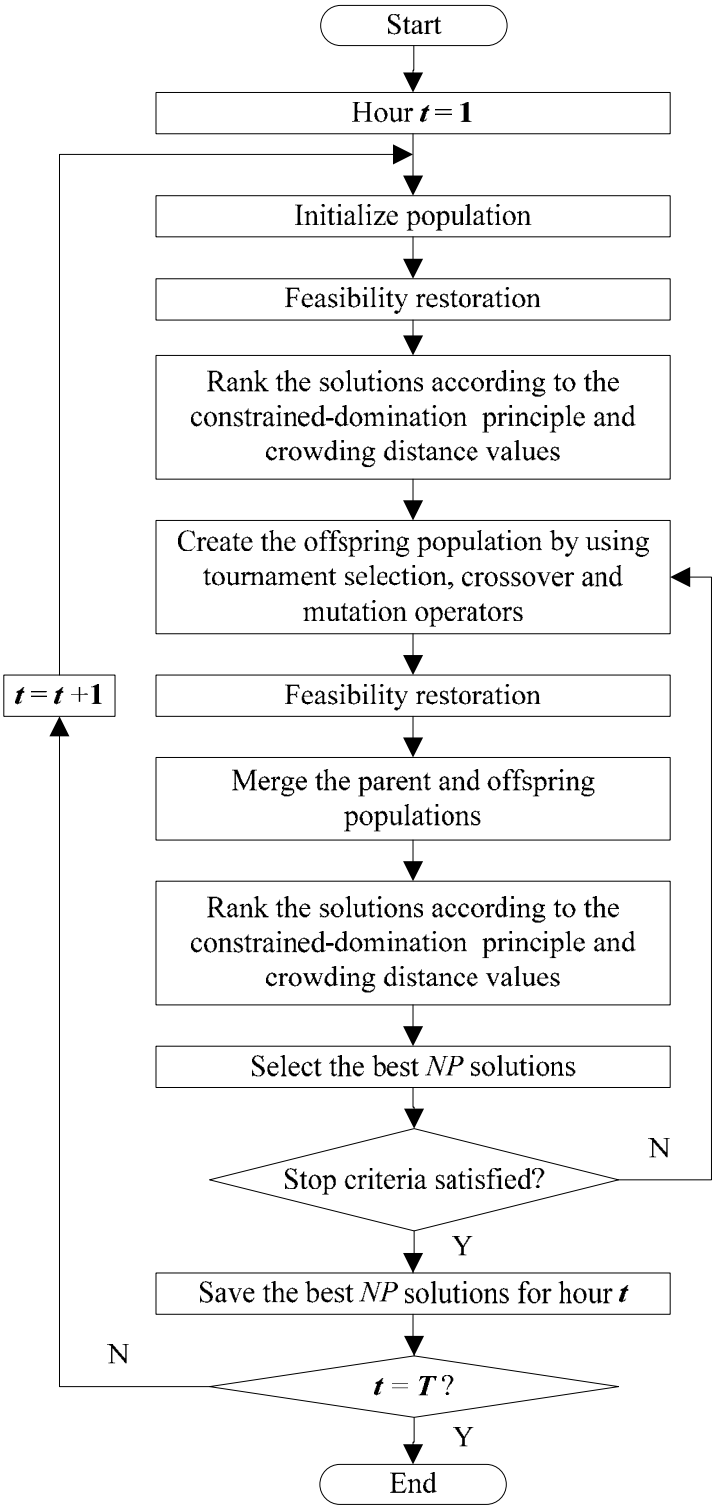

Figure 5.6 Flowchart of modified NSGA-II in the first phase

5.3 Second Phase (*T*-period Schedules)

In the second phase, the overall optimal schedule consisting of T separate periods is obtained by assembling all the hourly-optimal solutions from the first phase. The mathematical formulation of the overall dispatch problem is given below.

5.3.1 Objective Functions and Constraints

Minimize operation cost (4.7), emission (4.8) and transmission losses (4.10)

Subject to minimum up/down time (4.15), (4.16), ramp up/down rate (4.17), (4.18) and unit initial status constraints.

It should be noted that $\lambda=0$ indicates that the emission allowance trading is not considered in this phase.

5.3.2 Encoding Scheme

The generation schedule for the entire period T is represented by a vector of size T. The hth element ($1 \leq h \leq T$) in this vector, lying between 1 and NP, is the index of a solution in the hth hourly Pareto front obtained from the first phase. For example, if the vector [12 31 … 77] were to represent the generation schedule for the entire T periods, it would include the 12^{th} solution obtained during the first phase for the first hour, the 31^{th} solution for the second hour, and the 77^{th} solution for the last hour.

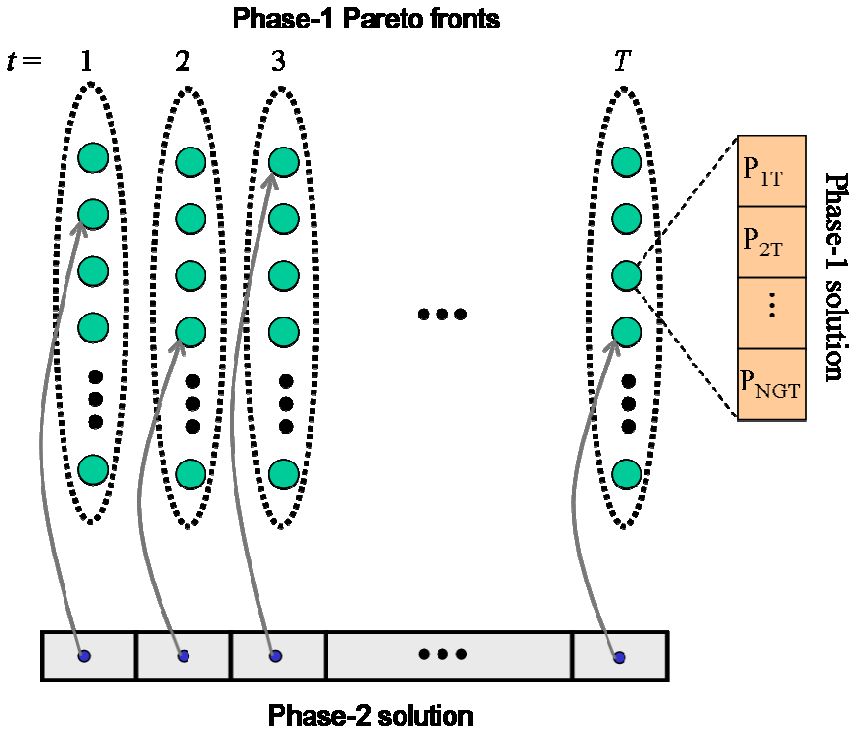

Figure 5.7 Solution encoding scheme in the second phase

Figure 5.7 illustrates this representation. Here, hourly solutions of the form [P_{1h} P_{2h} … P_{NGh}] are shown as circles. Pareto fronts of each of the T separate periods are grouped together using dotted lines. The second phase solution is made up of indexes of the hourly solutions. Initial solution vectors are generated randomly by picking an index between 1 and NP for each hour.

5.3.3 Crossover and Mutation

In this phase, two-point crossover is adopted in the modified NSGA-II and SPEA-2. Gaussian mutation is used for all the three algorithms, NSGA-II, SPEA-2 and AMOSA. The standard two-point crossover discussed earlier is applied to two parent vectors to yield two offspring vectors. Gaussian mutation is applied element-wise to each vector, the probability of mutating each element being equal to p_m, the mutation rate. As mutation is applied sparingly, p_m is a very small quantity. A random number that follows Gaussian distribution with zero mean and standard deviation σ is added to each such element, which is then rounded off to the nearest integer value. A correction is applied to elements that are below 1 or above NP, following

mutation, by replacing them with 1 and *NP* respectively. In this manner, each mutated element is now associated with another solution from the phase-1 Pareto front. Since best results were obtained when the level of mutation was higher during the initial stages of the algorithm, the standard deviation σ of the Gaussian mutation was set to $\sigma = \max(NP \times r^{-g}, 30)$, where r is a number slightly greater than 1. For our experiments, r was chosen to be 1.007. This way the extent of mutation reduces with increasing iterations, leading to a good convergence performance of the algorithm.

In the following argument, those solutions in the Pareto front, which are minimum along any one objective are called as *extreme* solutions. For bi-objective optimization problem, the Pareto front contains only two extreme solutions (indexed as 1 and *NP*). As neither the minimum up/down times nor the ramp up/down rates are considered when obtaining the hourly solutions in the first phase, attempting to produce extreme solutions for the T=24 hour period by simply concatenating the extreme solutions for each hour might be invalid in terms of any of these constraints. Thus, the extreme solutions of the Pareto front in the second phase might include as indexes, non-extreme, first phase solutions.

The second phase includes a separate scheme to increase the spread by making further improvements to the extreme solutions. The extreme solutions of the second phase are examined to see if they contain hourly solutions that are far away from their own hourly Pareto fronts. When the distance between any such hourly solution and the extreme of its own front exceeds a certain threshold, MOEAs of the first phase are re-invoked to generate a few additional solutions, while simultaneously imposing the minimum up/down time as well as the ramp up/down rate constraints. Simulation results reported in Chapter 6 shows that this improvement, although invoked rarely, helped in enhancing the spread of the resulting Pareto front.

CHAPTER 6 - Case Studies

In order to investigate the performance of the proposed two-phase approach, NSGA-II, SPEA2 and AMOSA were implemented on 4 different test systems. The two-objective model, which optimizes operation cost and emission, is tested on a benchmark 10-unit system first. Then the IEEE 118-bus system which has 54 units, is used to test the approach's applicability to large systems, while also taking into account emission trading. Thereafter, the three-objective model, which includes the operation cost, emission and transmission losses, is tested on a 15-unit system and a 60-unit system.

6.1 Two-Objective System Models

The two-objective model optimizes the operation cost (5.1) and emission (5.2) simultaneously, subject to the constraints of power balance (4.11), spinning reserve (4.13) and power generation limits (4.14).

6.1.1 Strategy of Increasing the Diversity

Any schedule of T periods that is obtained by optimizing each hourly schedule separately, is bound to violate either the minimum up/down time or the ramp up/down rate constraints. In other words, the best generation schedule consisting of T periods is not necessary optimal for each hour. Similarly, it is likely that extreme solutions for the entire T periods with the smallest and the largest values for one objective function consist of some 'inferior' hourly-solutions that are dominated by the hourly-optimal solutions on the Pareto fronts obtained from the first phase. In this case, to obtain the extreme solutions, determining the hourly-solutions on the boundary of the hourly-optimal fronts in each hour is required. Next, those hours in which the hourly-solutions on the boundary of the hourly-optimal fronts are not included in the boundary of T-period solutions of the second phase's Pareto front is identified. Finally, for each of those hours, the minimum up/down time constraints based on the on/off duration information of the boundary hourly-solutions in the previous and subsequent periods in enforced, and the first-phase' MOEAs are rerun to get another set of hourly-optimal solutions. These sets of hourly-solutions will be involved in the second phase' MOEAs to get the solutions around the boundaries of the T-period Pareto fronts. For example, let's consider a three-unit system for 24

hours, for which each unit has a minimum up/down time of 5 hours. If only the 7th and 8th hours' hourly-optimal solutions with minimum operation costs on the boundary of hourly Pareto fronts are not included in the final 24-hour-optimal solution on the boundary of the 24-hour Pareto front, in which the 6th and 9th hours' status are [1 0 0] and [1 1 0] respectively, then it is concluded that the status of the three units in the 7th and 8th hours both are [1 x 0], where x is 1 or 0, depending on the second unit's on/off status before the 6th hour and after the 9th hour. Hence it is reasonable to enforce the first unit to be on and the third unit to be off during the 7th and 8th hours to get two new sets of hourly-optimal solutions for each hour, in order to help get the boundary 24-hour-optimal solutions in the second phase.

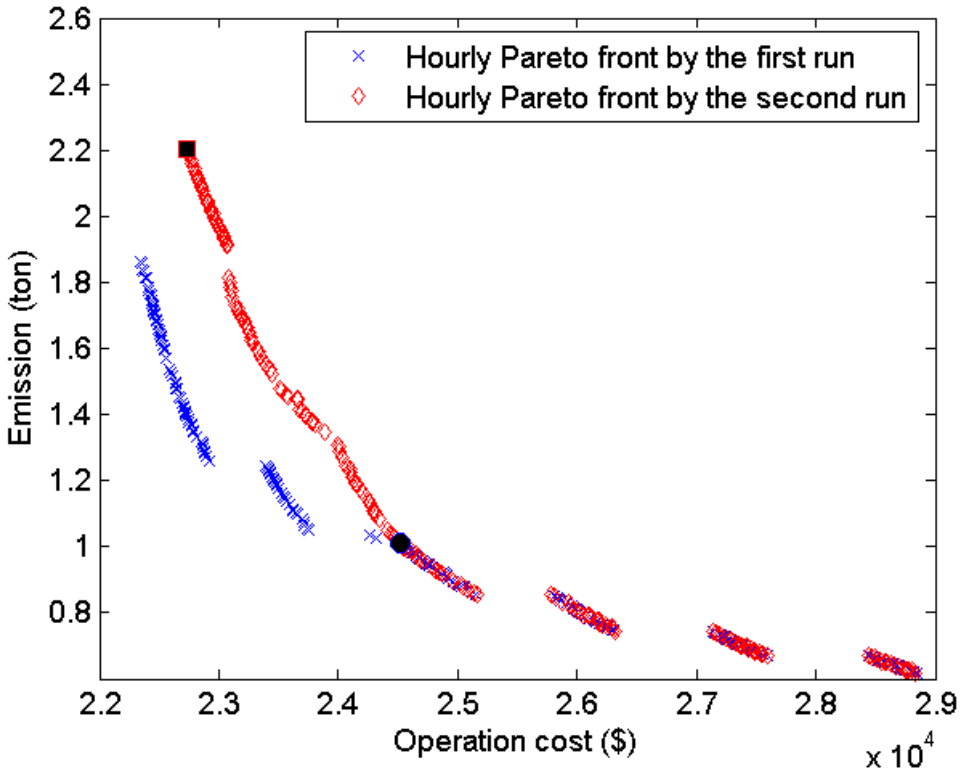

Figure 6.1 Hourly Pareto fronts obtained with/without the strategy to increase the diversity in hour 22

Figure 6.1 shows two hourly Pareto fronts obtained with and without the strategy to increase the diversity in hour 22 in the first phase for the 10-unit system. The black dot represents the corresponding boundary hourly-solutions on the hourly-optimal fronts included in the extreme boundary 24-hour-optimal solution in the second phase with the minimum operation

cost, without the minimum on/off constraints of unit 1, 2, 6, 7, in the hours immediately before and after the current one. It is clear that the extreme solution of the second phase contains the hourly solution that is far away from the boundary of its own hourly Pareto front. When the distance between any such hourly solution and the extreme of its own front exceeds a certain threshold, MOEAs of the first phase are rerun while enforcing the minimum on time constraints of unit 1, 2, 6, 7. In this case, the threshold is set as the 5% of difference between the maximum and minimum objective values. It can be seen that the final boundary hourly solution represented by the black square is exactly on the boundary of the new Pareto front.

6.1.2 The Improvement of AMOSA

The original AMOSA was tested on a 10-unit system, and it was found not to be efficient in dealing with short-term thermal generation scheduling. Therefore, the AMOSA has been improved by adopting several strategies as follows.

6.1.2.1 Improvement of Diversity Preservation

During our experiments of the original AMOSA, it was found not to be robust. First, in its original perturbation, AMOSA uses the m as the number of total genes to be perturbed. During short-term generation scheduling, m is the total number of generators whose outputs should be changed during the annealing process. With the perturbation as the only method to get the new solution, the performance of the original AMOSA is highly affected by the total amount of load demand. This is because when the load is low, there are several combinations of generators that can be online, making a large value of m necessary. For instance, if the maximum capacity in a 7-unit system of each unit is 100 MW, when the load demand is low, say 150 MW, only two or three units are adequate to match the load, requiring the value of m to be large, *i.e.* 4, to ensure that the perturbation results in different units to be on or off, using the generation limits repair and load balance repair strategies. On the other hand, when the load is high, at say 500 MW, the value of m should be small enough, *i.e.* 1 or 2, to ensure that only a few units are shut down, as several units are needed to satisfy the load. Figure 6.2 and 6.3 show the Pareto fronts obtained for the 10-unit system by using different values for m in the original AMOSA, under different load conditions. From figure 6.2, it is seen that when the load is low, the Pareto-front obtained with m=5 is better than that with m=1, in terms of the diversity as well as convergence.

Conversely, under high load conditions, the Pareto-front obtained with *m*=5 was worse than the one with *m*=1, which is shown in figure 6.3.

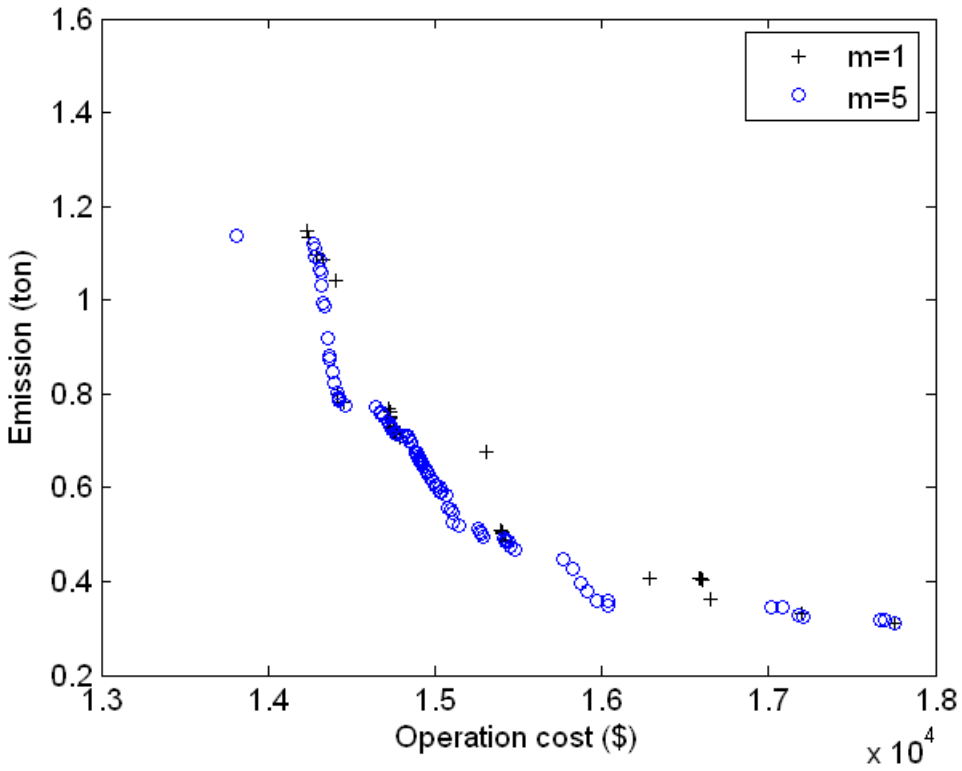

Figure 6.2 Hourly Pareto front obtained by original AMOSA with different *m* in hour 1 (load=700MW)

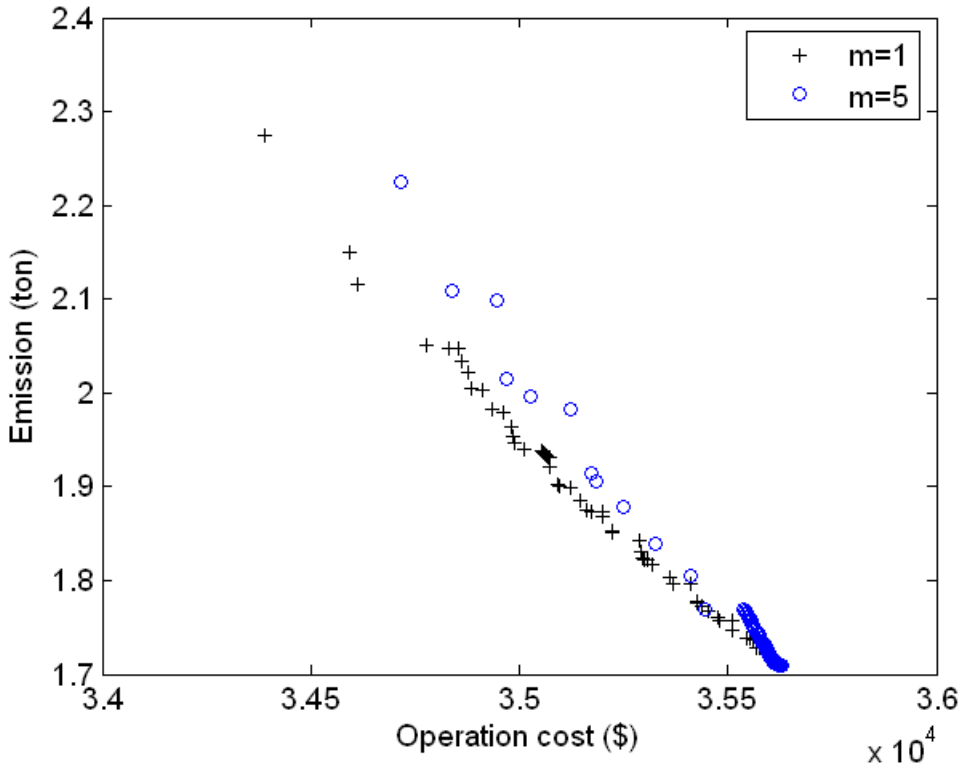

Figure 6.3 Hourly Pareto front obtained by original AMOSA with different *m* in hour 12 (load=1500MW)

6.1.2.2 Improvement of Perturbation to Produce New Solutions

To circumvent the lack of robustness of the original AMOSA, the crossover and mutation operators are incorporated to produce new solutions from current ones in the archive. This is illustrated in figure 6.4.

In the original AMOSA, a solution $\mathbf{x}_{cur}$ is randomly selected from the archive that undergoes perturbation to obtain a new solution $\mathbf{x}_{new}$. To determine the probability of acceptance of $\mathbf{x}_{new}$, the domination status of the latter is checked with $\mathbf{x}_{cur}$ and the other archived solutions, Here, instead of randomly selecting a solution from the archive for perturbation, n ($n \leq HL$) solutions are randomly selected from the archive, and then the one with the worst diversity is picked as $\mathbf{x}_{cur}$, to explore the possibility of obtaining $\mathbf{x}_{new}$ within the neighborhood of $\mathbf{x}_{cur}$ to fill out the gap around $\mathbf{x}_{cur}$, and therefore to improve the diversity of the Pareto-front. In addition, a solution $\mathbf{x}_{tmp}$ is randomly selected from the archive. Then crossover and mutation operators are

performed on the two parent $\mathbf{x}_{cur}$ and $\mathbf{x}_{tmp}$, to produce two children $\mathbf{x}_{c1}$ and $\mathbf{x}_{c2}$, which could violate the generation limits and load balance constraints. Therefore the feasibility restoration procedure is applied to render such solutions feasible. Subsequently, the domination relationship between $\mathbf{x}_{c1}$ and $\mathbf{x}_{c2}$ is checked. There are two different cases that may arise. If one dominates the other, then the former one is chosen as $\mathbf{x}_{new}$. If the two do not dominate each other, then the one that is dominated by less number of solutions in the archive is chosen as $\mathbf{x}_{new}$. It can be seen from figure 6.4 that the new perturbation method has dramatically improved the performance of the algorithm, resulting in the Pareto front with better diversity and convergence. Figure 6.5 shows the detailed procedure of improved perturbation method.

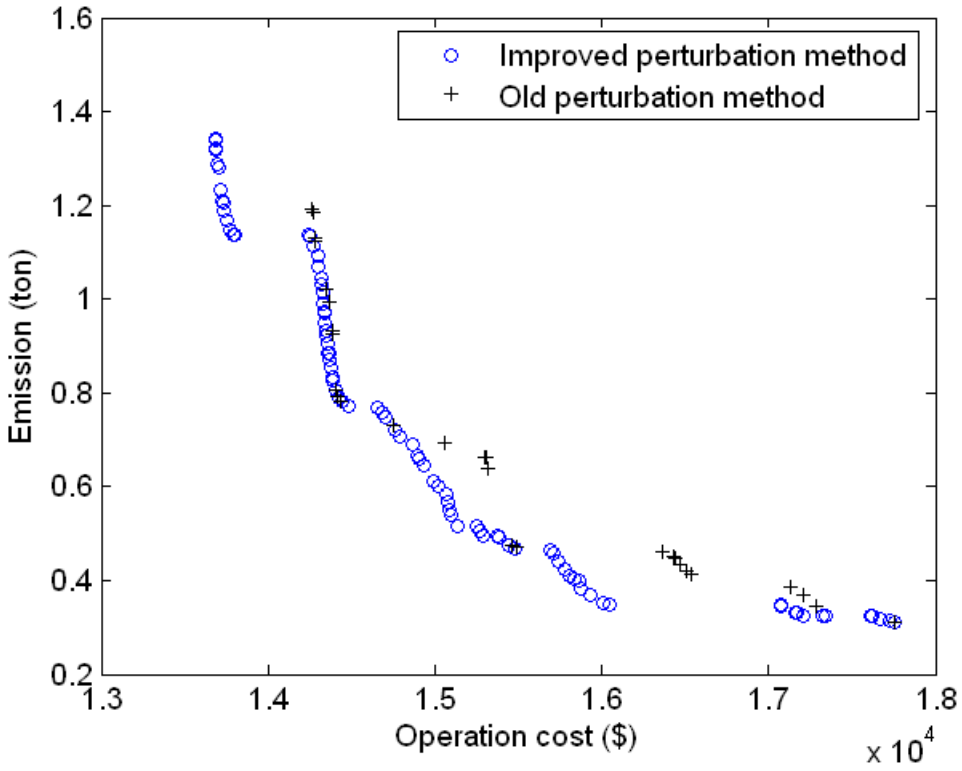

Figure 6.4 Hourly Pareto fronts obtained by AMOSA with the improved perturbation method and the old perturbation method for the 10-unit system in hour 1

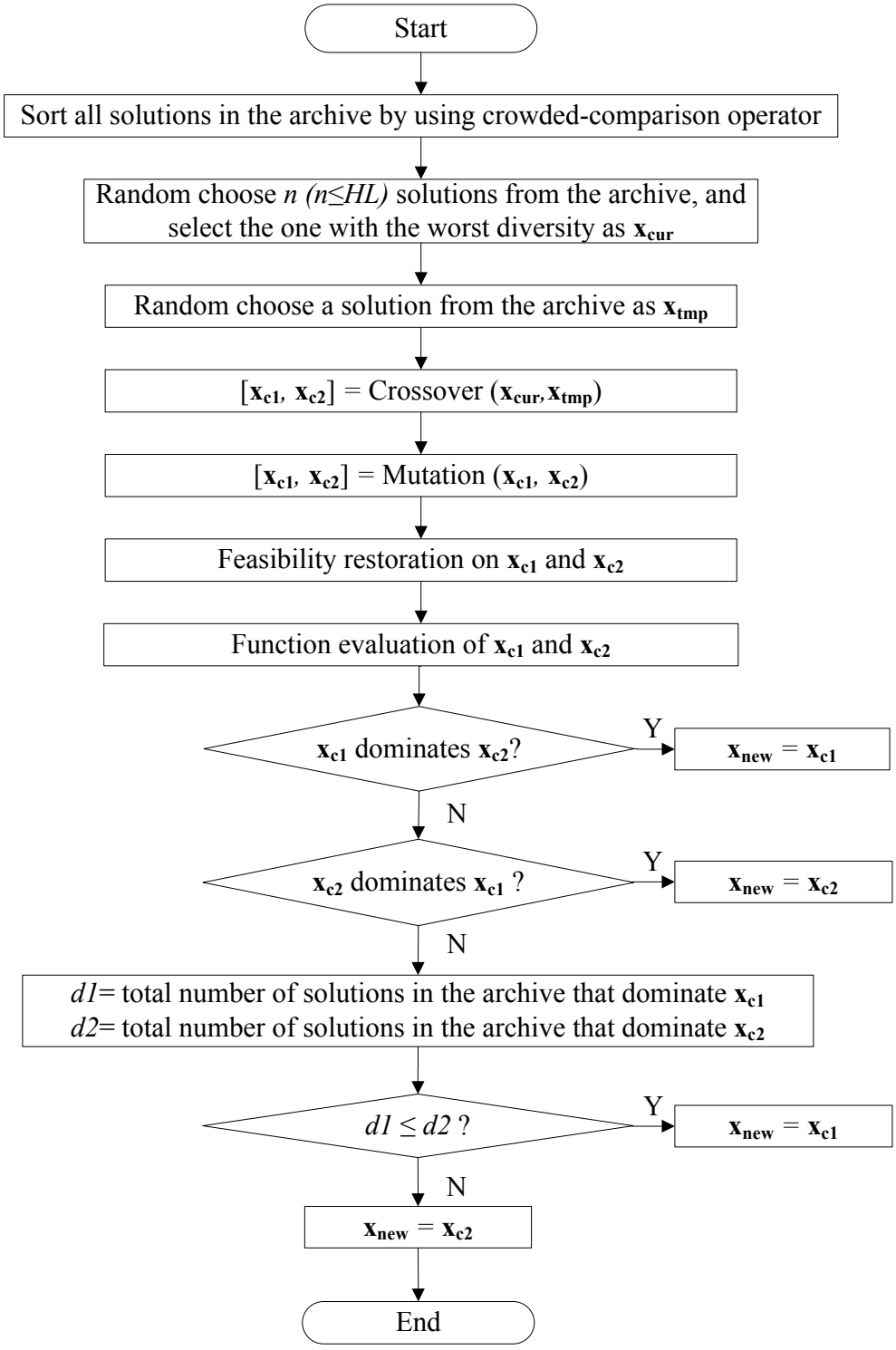

Figure 6.5 Improvement of the procedure to generate new solutions

AMOSA applies a clustering method to the non-dominated solutions in the archive in order to enhance the diversity of solutions. There are two parameters related to the size of the archive, *HL*, which is the maximum size of the archive on termination, and *SL*, the maximum size to which the archive can be filled before clustering is invoked to reduce the size to *HL*. The original AMOSA uses the single linkage algorithm [91] as the clustering method, where the distance between two clusters is calculated as the shortest distance between a pair of elements, one from each cluster. However experiments show that due to the lack of normalization of objective values and the strategy of always keeping boundary solutions, original AMOSA does not perform as well as using the crowded distance estimation procedure, with respect to diversity preservation. Figure 6.6 shows that the Pareto fronts obtained by using these two methods with *SL*=200 and *HL*=100 for the 10-unit system in hour 1.

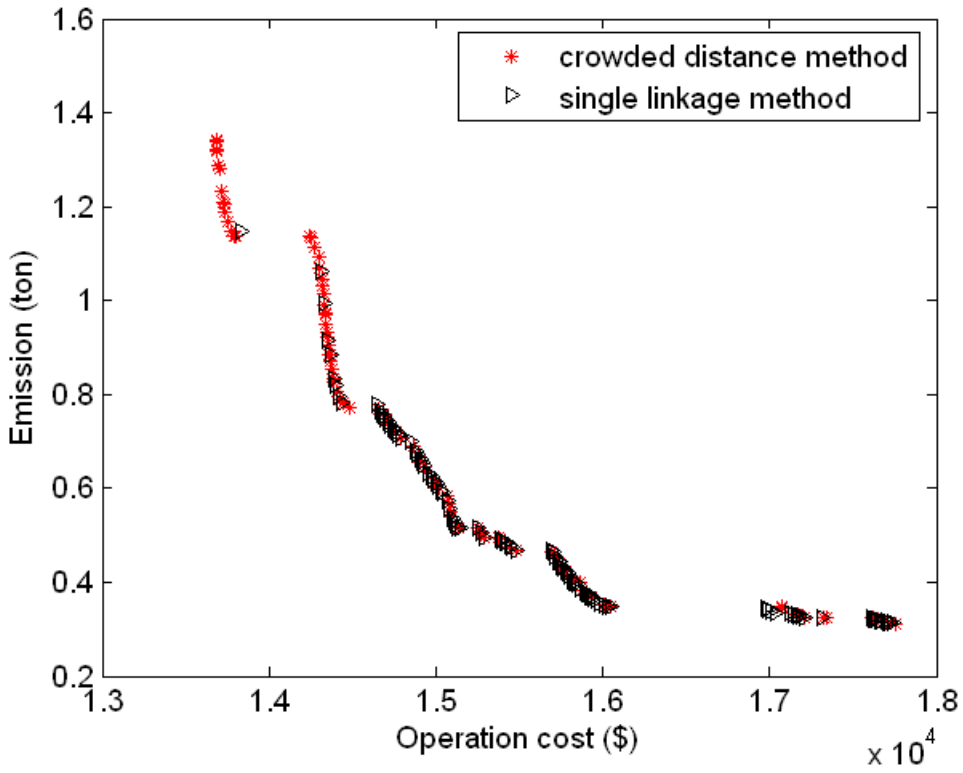

Figure 6.6 Hourly Pareto fronts obtained by AMOSA with different diversity preservation methods

6.1.3 10-Unit System

In order to investigate the performance of the proposed method, without considering transmission losses and the emission allowance trading (λ=0), the 10-unit system is studied. The system data are based on [92]. For comparison, the spinning reserve at each hour was kept at 10% of the load demand and the shutdown cost for each unit was neglected as in [92]. A total of 20 independent runs were carried out to compare the performance of the proposed method using NSGA-II, SPEA-2 and AMOSA.

During the first phase, the population size (*NP*) was kept at 200. NSGA-II was executed for a total of 200 iterations. The percentage of solutions in the population that were subject to crossover was 90%. The probability of mutation of each entry of the solution vectors was 10%. The distribution indexes for crossover and mutation were 10 and 20 (see [76], [90] for details).

In SPEA-2 the number of iterations and the population and archive sizes were kept at the same values as NSGA-II. Additionally, the crossover and mutation operators were identical to the latter. Due to the poor performance of the original AMOSA, the improved version of AMOSA is used which incorporates the crossover, polynomial mutation, crowded distance ranking, and the new method to produce new solutions. The lower bound on the archive size was equal to NSGA-II's population size, while the upper bound, adjusted for best performance, was 350. It was run for an equal number of function evaluations as NSGA-II.

Theoretically there are $(2^{10}\text{-}1)^{24} \approx 1.7259\times10^{72}$ solutions (including infeasible ones) to be explored, and employing a genetic algorithm helps curtail this search by a substantial amount. Due to the stochastic nature of the proposed approach, a total of 20 independent runs, comprising of both phases, were carried out. Figure 6.7 shows 24 hourly non-dominated fronts obtained by the three algorithms in the first phase, based on the results from one sample run. It is obvious that the non-dominated front more closely resemble a convex front with increase in load from hour 1 to hour 12. The reason is that increasing load needs more units to be on to meet the load balance, resulting in more plausible combinations of these units, which produces a more even distribution of solutions on the front.

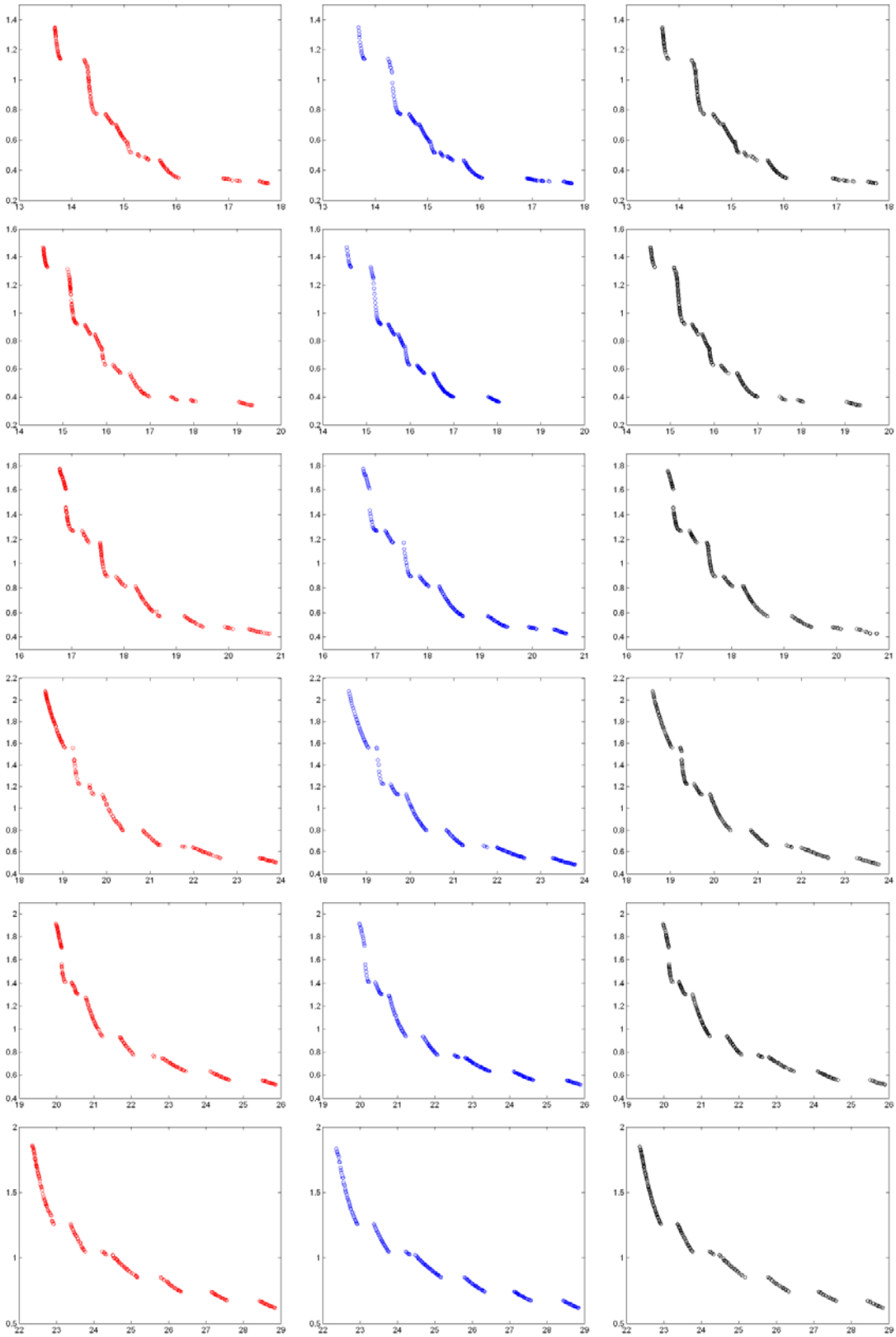

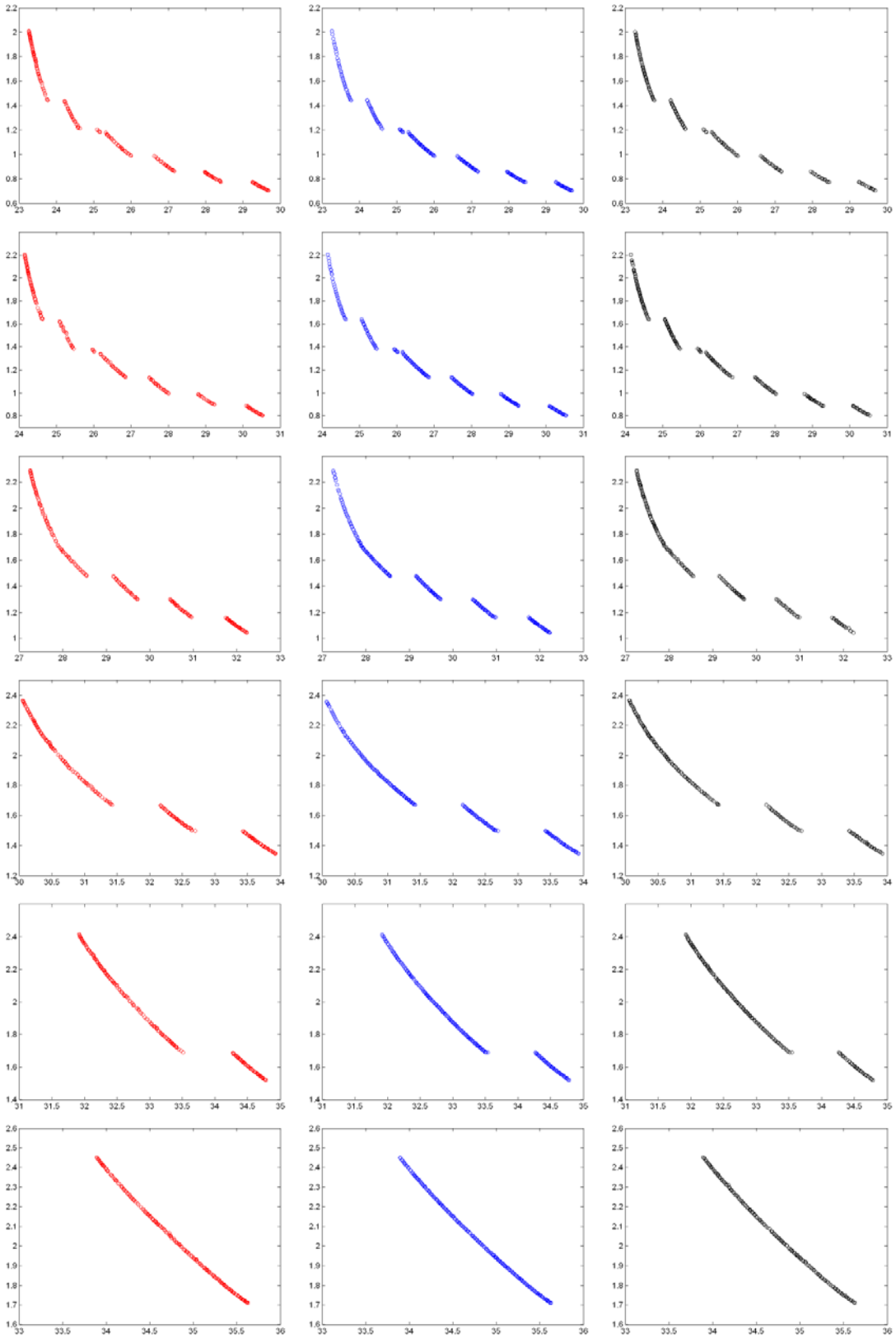

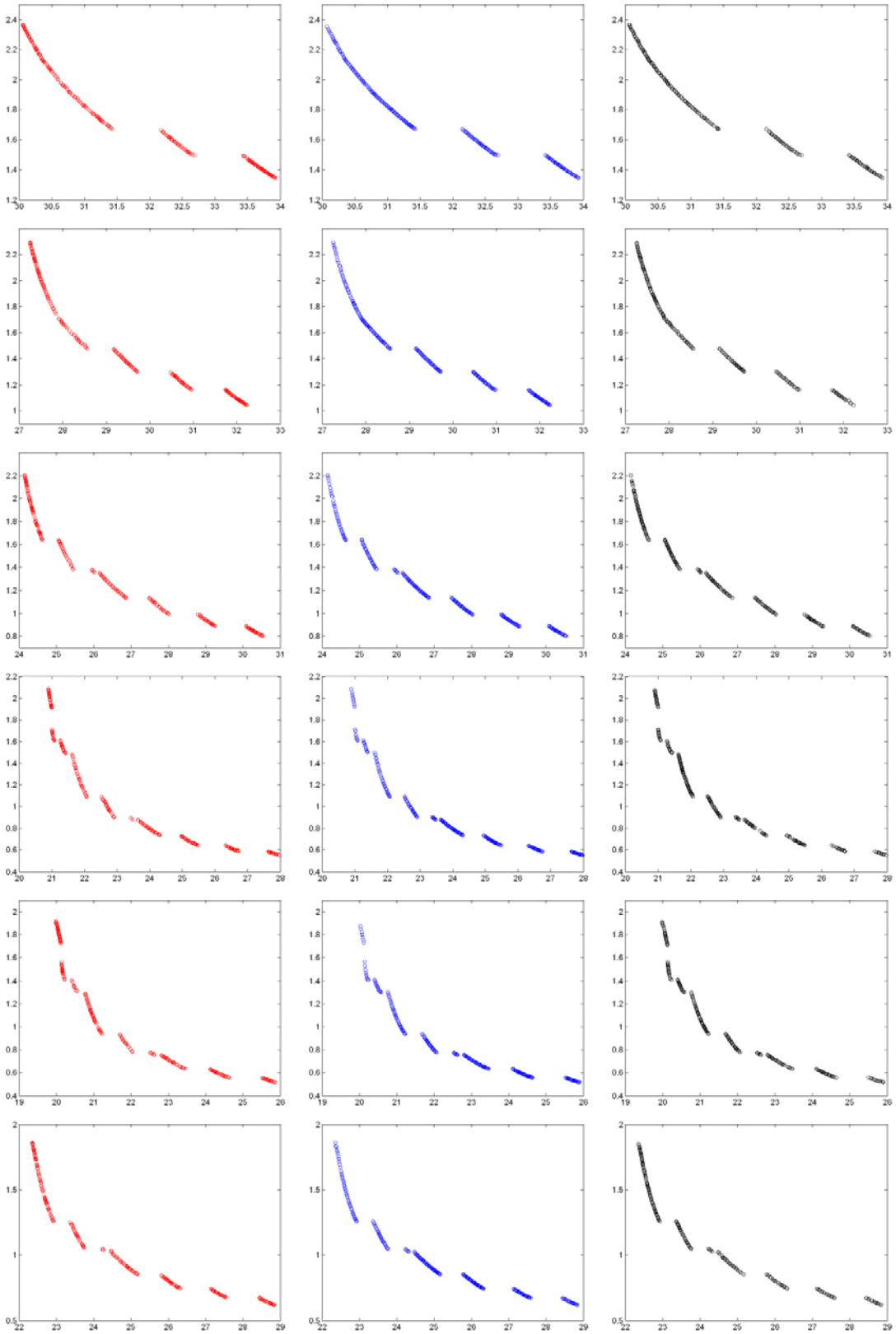

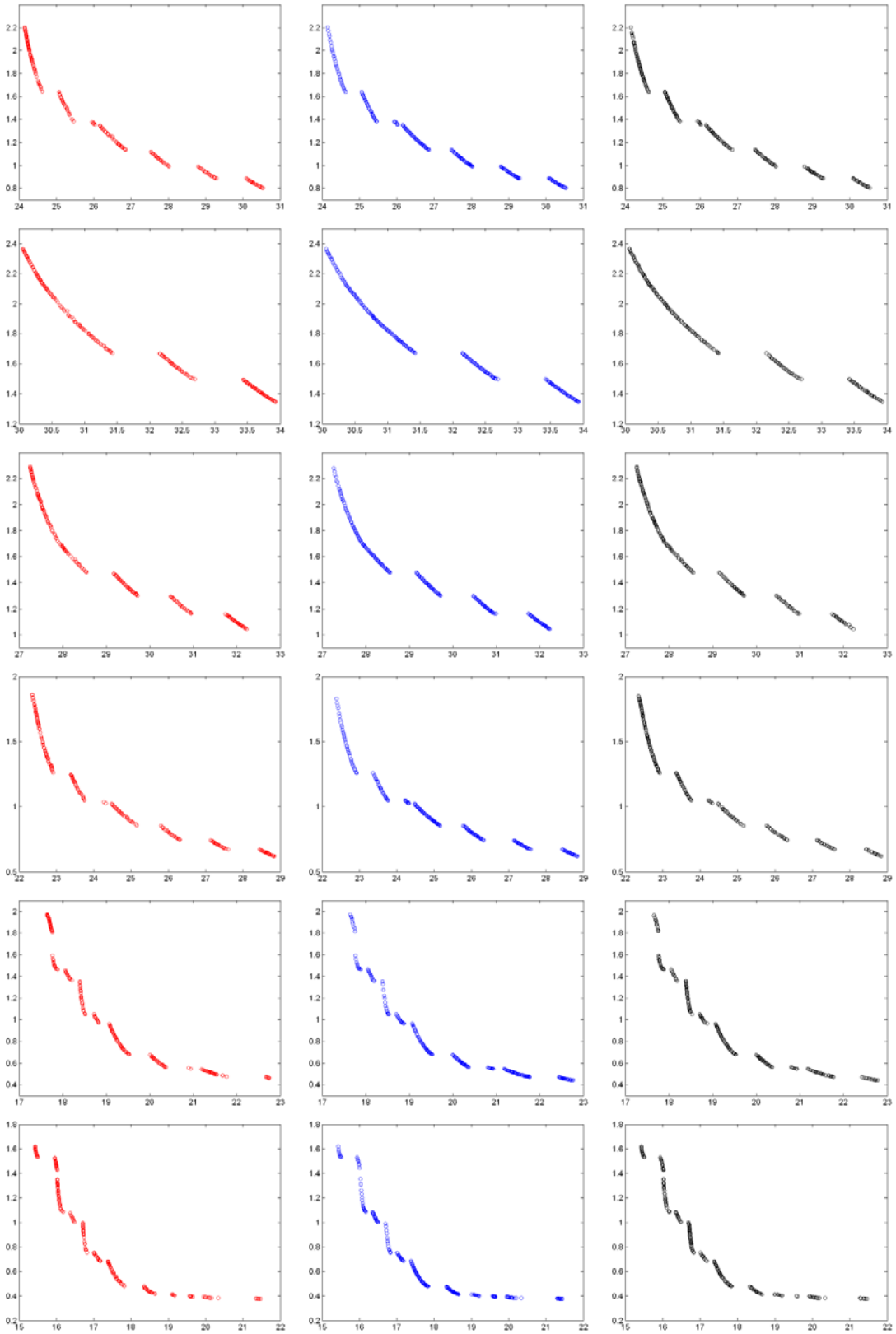

Figure 6.7 Hourly Pareto fronts for the 10-unit system obtained by NSGA-II (left), SPEA-2 (middle) and AMOSA (right) from hour 1(top) to hour 24 (bottom) in the first phase.

The population size in the second phase was kept at 300 and 500 iterations of both NSGA-II and SPEA-2 were allowed. In AMOSA, the lower bound on the archive size was equal to NSGA-II's population size, while the upper bound, adjusted for best performance, was 450. It was run for an equal number of function evaluations as NSGA-II. The mutation rate was lowered slightly to 5%, while the crossover rate was kept at 80%.

A sample Pareto front containing 300 solutions associated with 24-hour generation scheduling, which were obtained from the second phase of a sample run, is shown in figure 6.8. It can be seen that for NSGA-II, the total operation cost of 24 hours has a range from $563,943 to $660,813, corresponding to the emission's range from 48.61 to 22.19 ton; for SPEA-2, the total operation cost of 24 hours has a range from $565,278 to $648,779, corresponding to the emission's range from 46.45 to 26.16 ton; for AMOSA, the total operation cost of 24 hours has a range from $572,285 to $639,471, corresponding to the emission's range from 39.93 to 23.74 ton.

These wide spread solutions give the plant operator more operating feasibility according to the realistic system conditions. It is clear that the NSGA-II performs better than both SPEA-2 and AMOSA. While, AMOSA gives more spread non-dominated solutions close to the Pareto-front than SPEA-2, but SPEA-2 finds the better operation cost than the one by AMOSA.

The best boundary solution obtained by the proposed two-phase multi-objective evolutionary approach using NSGA-II in the second phase with minimum operation cost of $563,943 from this front is shown in table 6.1. The average emission rate is 1.7936 kg/MWh based on this solution, which is a litter higher than the national NOx average emission rate of 1.66 kg/MWh in USA and lower than 1.83 kg/MWh in Mexico in 2002 [88]. By comparison, the rate decreases to 0.8188 kg/MWh according to the other boundary solution with maximum operation cost of $660,813.

Table 6.1 Boundary solution with minimum operation cost on the 24-hour Pareto front for the 10-unit system obtained by NSGA-II in the second phase

Hour	Fuel Cost ($)	Startup Cost ($)	Emission (ton)	Emission Rate (kg/MWh)	Generation Schedule (MW)									
1	13683	0	1.3481	1.9258	455	245	0	0	0	0	0	0	0	0
2	14554	0	1.4694	1.9592	455	295	0	0	0	0	0	0	0	0
3	16809	900	1.738	2.0447	455	370	0	0	25	0	0	0	0	0
4	18598	0	2.0792	2.1886	455	455	0	0	40	0	0	0	0	0
5	20020	560	1.8772	1.8772	455	390	0	130	25	0	0	0	0	0
6	22387	1100	1.8246	1.6587	455	360	130	130	25	0	0	0	0	0
7	23262	0	2.0121	1.7497	455	410	130	130	25	0	0	0	0	0
8	24154	0	2.1961	1.83	455	453.56	129.99	130	31.451	0	0	0	0	0
9	27253	860	2.2898	1.7614	455	454.5	130	130	85.409	20.088	25	0	0	0
10	30058	60	2.3659	1.6899	455	455	130	130	162	33	25	10	0	0
11	31916	60	2.4138	1.6647	455	455	130	130	161.99	73.014	25	10	10	0
12	33890	60	2.4511	1.6341	455	455	130	130	162	80	25	43.001	10	10
13	30058	0	2.3659	1.6899	455	455	130	130	162	33	25	10	0	0
14	27251	0	2.2919	1.763	455	455	130	130	85	20	25	0	0	0
15	24150	0	2.2029	1.8357	455	455	130	130	30	0	0	0	0	0
16	21514	0	1.6658	1.5865	455	310	130	130	25	0	0	0	0	0
17	20642	0	1.5361	1.5361	455	260	130	130	25	0	0	0	0	0
18	22387	0	1.8246	1.6587	455	360	130	130	25	0	0	0	0	0
19	24150	0	2.2029	1.8357	455	455	130	130	30	0	0	0	0	0
20	30058	490	2.3659	1.6899	455	455	130	130	162	33.002	25	10	0	0
21	27251	0	2.2915	1.7627	455	454.91	130	130	85.095	20.001	25.005	0	0	0
22	22736	0	2.2028	2.0026	455	455	0	0	145	20	25	0	0	0
23	17645	0	1.9714	2.1905	455	425	0	0	0	20	0	0	0	0
24	15427	0	1.6193	2.0241	455	345	0	0	0	0	0	0	0	0
Total/ Average	559853+4090 =563943		48.6061	1.7936										

Table 6.2 Minimum operation cost comparison of different techniques for the 10-unit system

Technique	SPL [93]	EP [20]	EPL [94]	PLEA [95]	PSO [96]	IPSO [96]	HPSO [97]	LRGA [98]	ELR [99]	GA [92]	LR [92]	ICGA [100]
Operation Cost ($)	564950	565352	563977	563977	564212	563954	563942	564800	563977	565825	565825	566404
Technique	UCCGA [101]	ACSA [102]	DP [92]	DPLR [99]	TS-RP [103]	TS-IRP [103]	MA [104]	MRCGA [105]	SF [106]	Our approach (NSGA-II)	Our approach (SPEA-2)	Our approach (AMOSA)
Operation Cost ($)	563977	564049	565825	564049	564551	563937	565827	564244	563977	563943	565278	572285

Table 6.3 Performance of the proposed approach for the 10-unit system (20 run average)

Two-phase Multi-objective Evolutionary Approach		Operation Cost ($)			Emission (ton)		
		Min	Median	Max	Min	Median	Max
NSGA-II	Best Operation Cost	563943	563949	563952	48.59	48.6	48.61
	Best Emission	658374	659345	660813	22.19	22.28	22.32
SPEA-2	Best Operation Cost	565278	565363	565507	46.24	46.30	46.45
	Best Emission	645692	645737	648778	26.16	26.30	26.32
AMOSA	Best Operation Cost	572285	572536	572810	39.63	39.89	39.93
	Best Emission	638026	639050	639471	23.74	23.95	23.96

In table 6.2, the boundary solutions with the minimum operation cost achieved by the proposed two-phase multi-objective evolutionary approach are compared with other solutions by different unit commitment solving techniques that have appeared in recent literature. It is clear that our approach with NSGA-II produces almost the best one with the cost of $563,943, which is only $1 more than the best outcome of $563,942 [97]. It should be noted that in [106], the best operation cost calculated by the unit output power provided in the paper is $563,977 instead of $563,865 as reported by the author. Table 6.3 shows the minimum, maximum and the median values of each objective that were found by merging the Pareto-optimal solutions of all 20 runs, based on the experiment results by the proposed two-phase multi-objective evolutionary approach. The small variation between the values of the best and worst boundary solutions proves the robustness of the proposed approach.

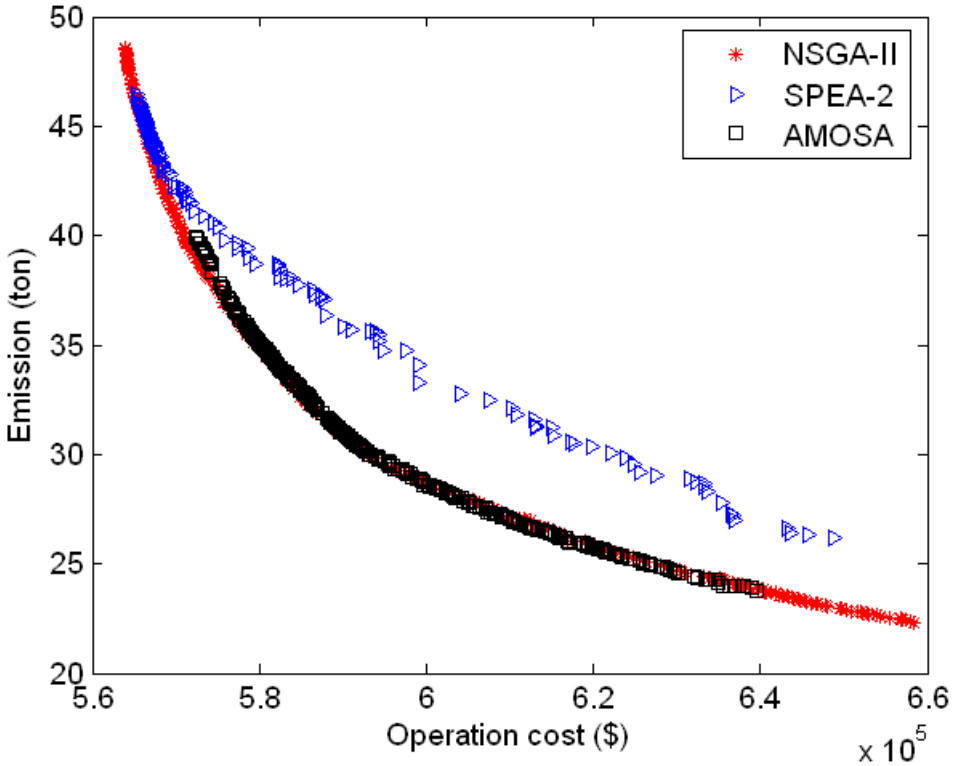

Figure 6.8 24-hour Pareto fronts for the 10-unit system obtained in the second phase

6.1.4 IEEE 118-Bus System

To study the effect of the emission allowance trading, standard IEEE 118-bus 54-unit system is tested in this case. The system data are provided in [106].

Parameters of the two-phase approach with NSGA-II, SPEA-2 used here are the same as in the case of 10-unit system, except for the population size of 500 and iterations of 600 in the first phase, and 800 and 1500 in the second phase. In the improved AMOSA, both crossover and mutation operators were used. The lower bound on the archive size was equal to the population size of NSGA-II in both phases, while the upper bound, adjusted for best performance, was 750 in the first phase and 1100 in the second phase. It was run for an equal number of function evaluations as NSGA-II.

Figure 6.9 shows 24 hourly non-dominated fronts obtained by the three algorithms, based on the results from one sample run. From the figure, NSGA-II outperform both and SPEA-2 and AMOSA for most hours in the first phase. Additionally, from visual inspection,

NSGA-II's solutions were more uniformly distributed over the front in all cases than those of SPEA-2 and AMOSA. A comparison between the performances of these three algorithms in the second phase is provided as follows.

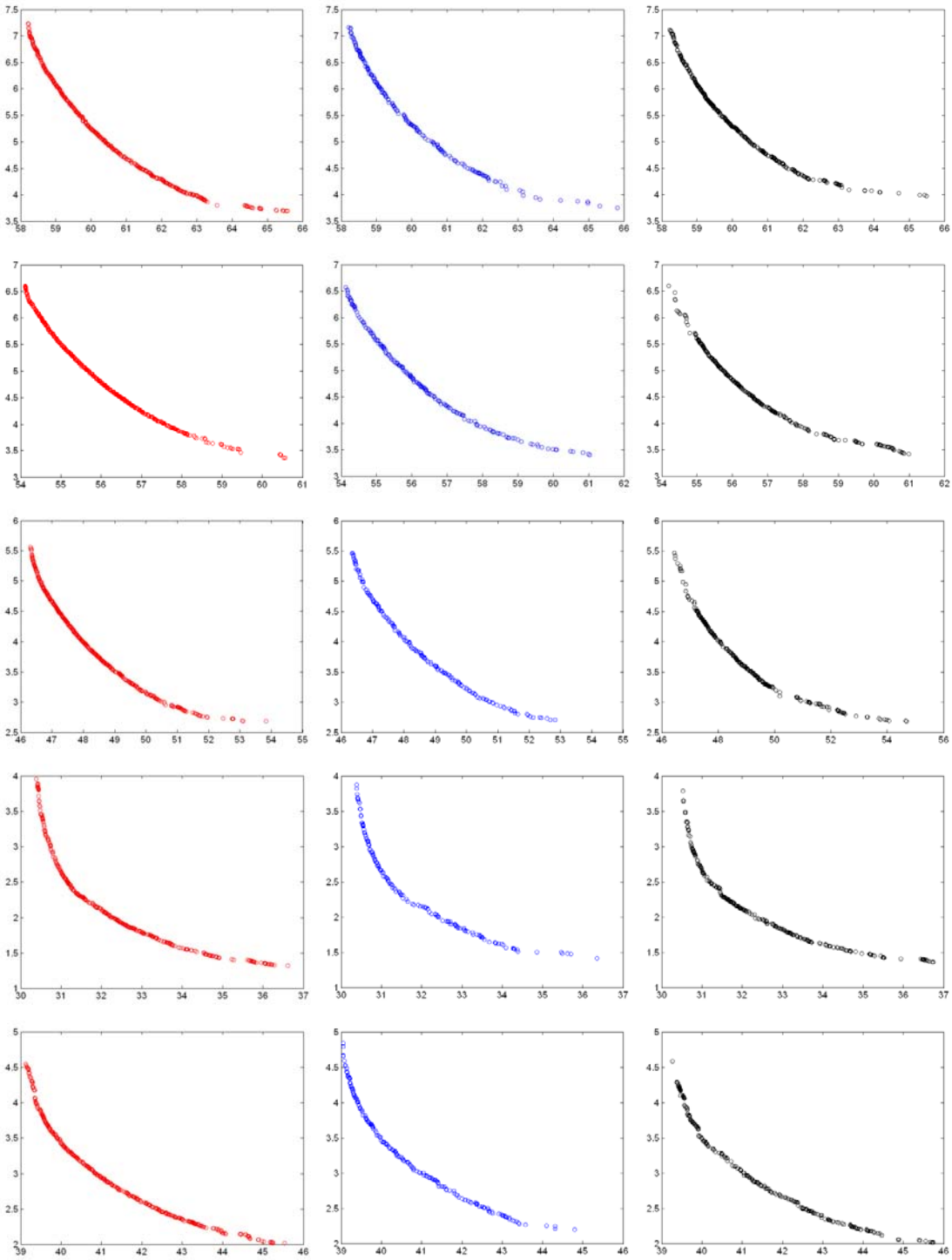

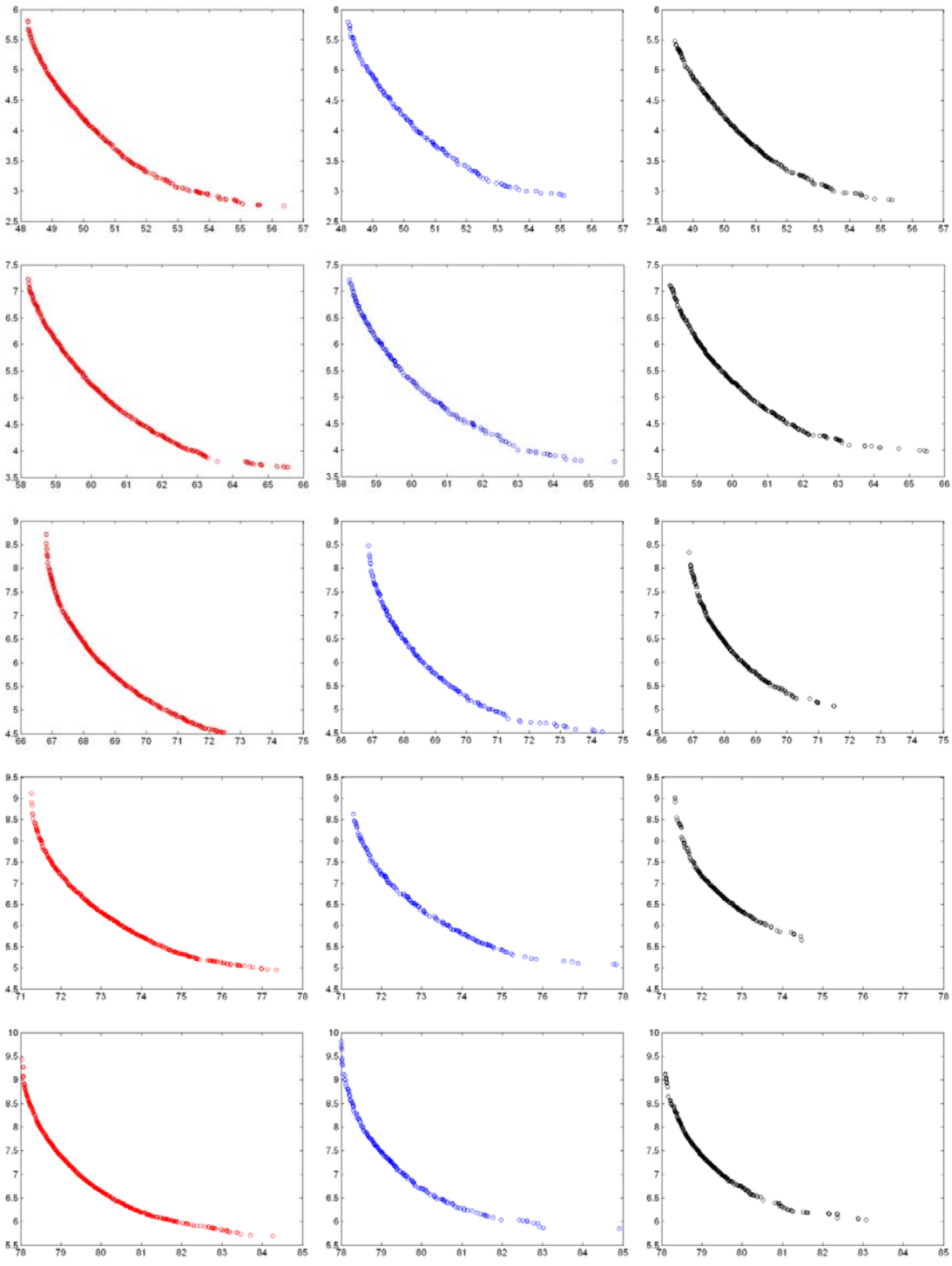

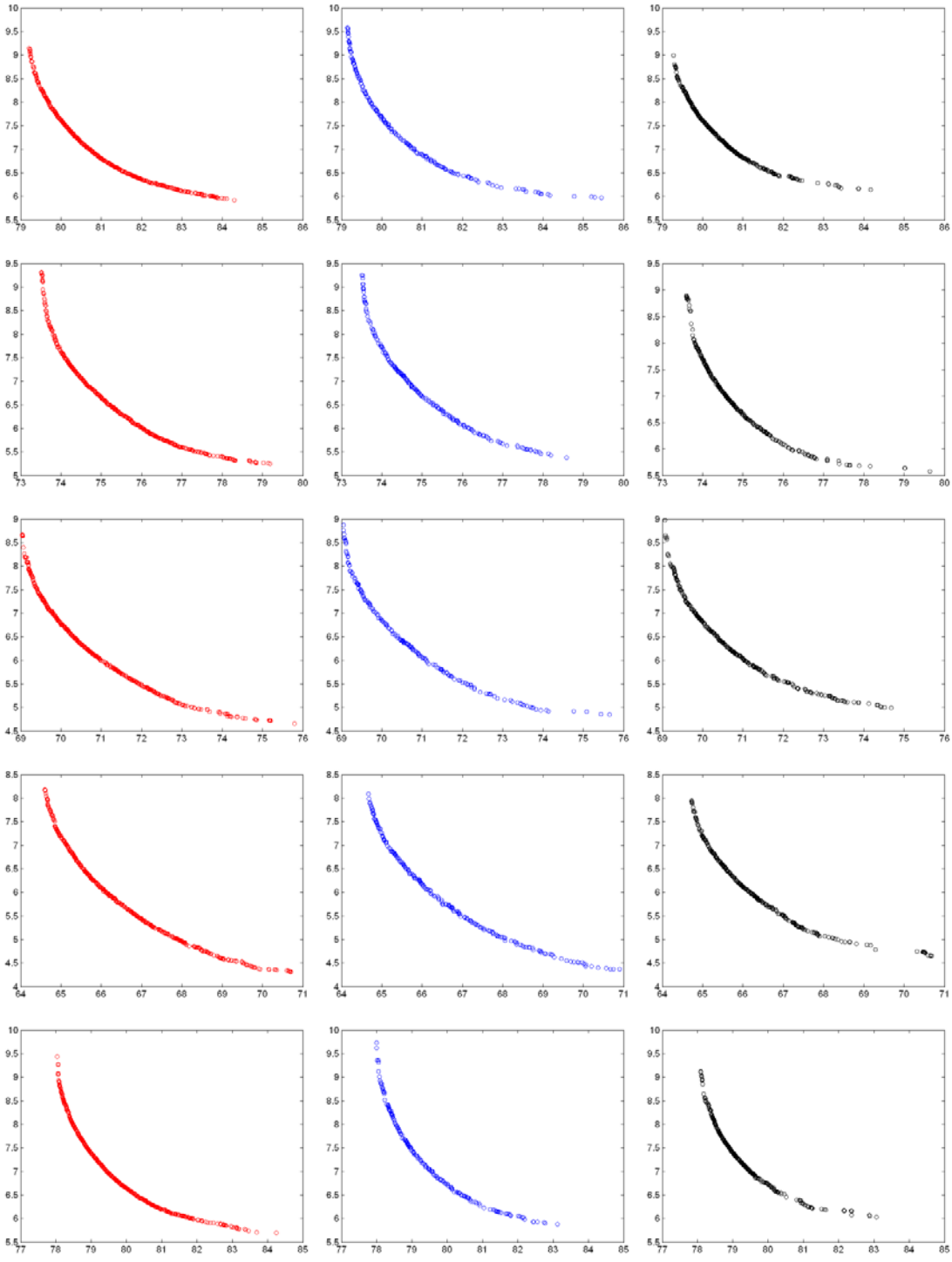

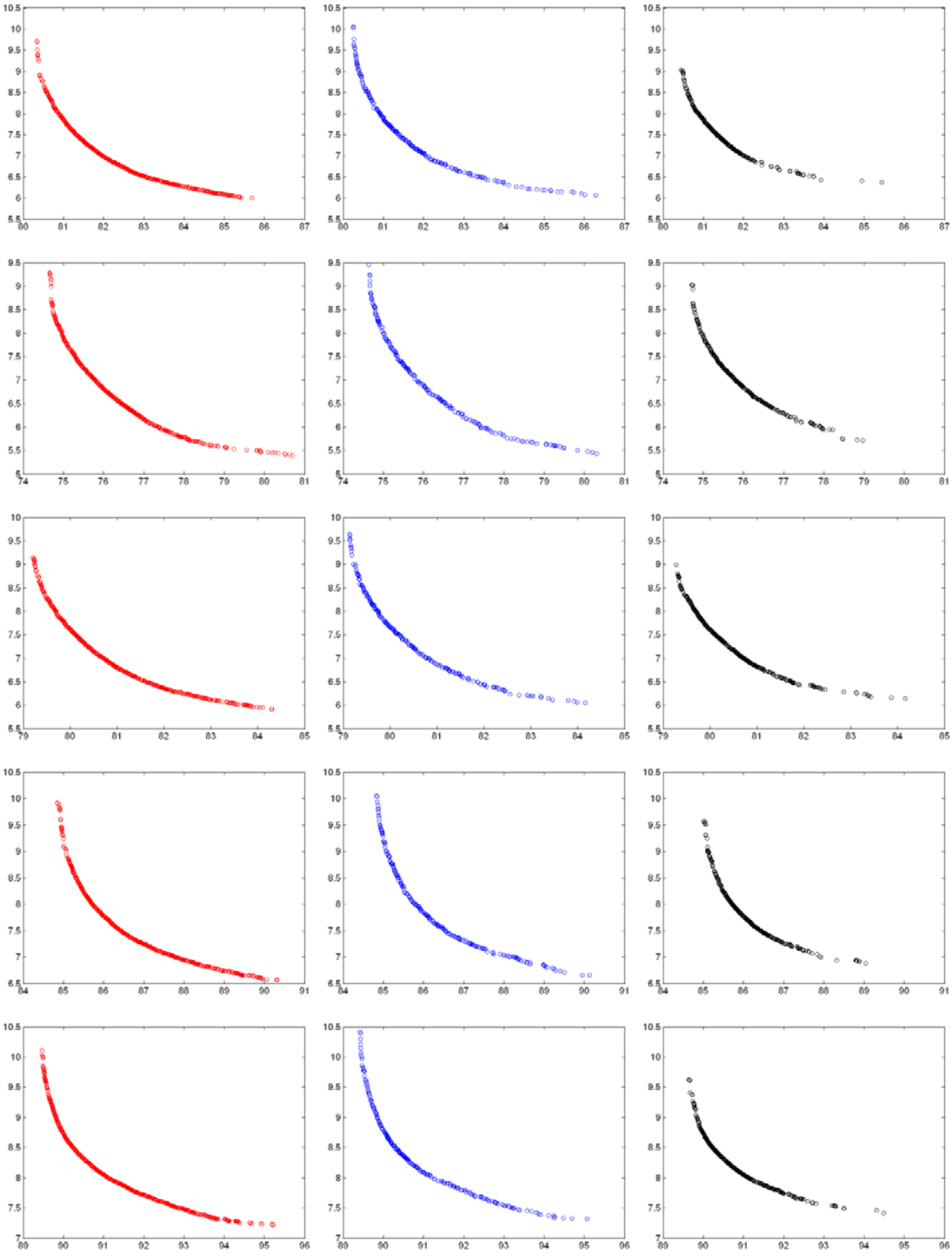

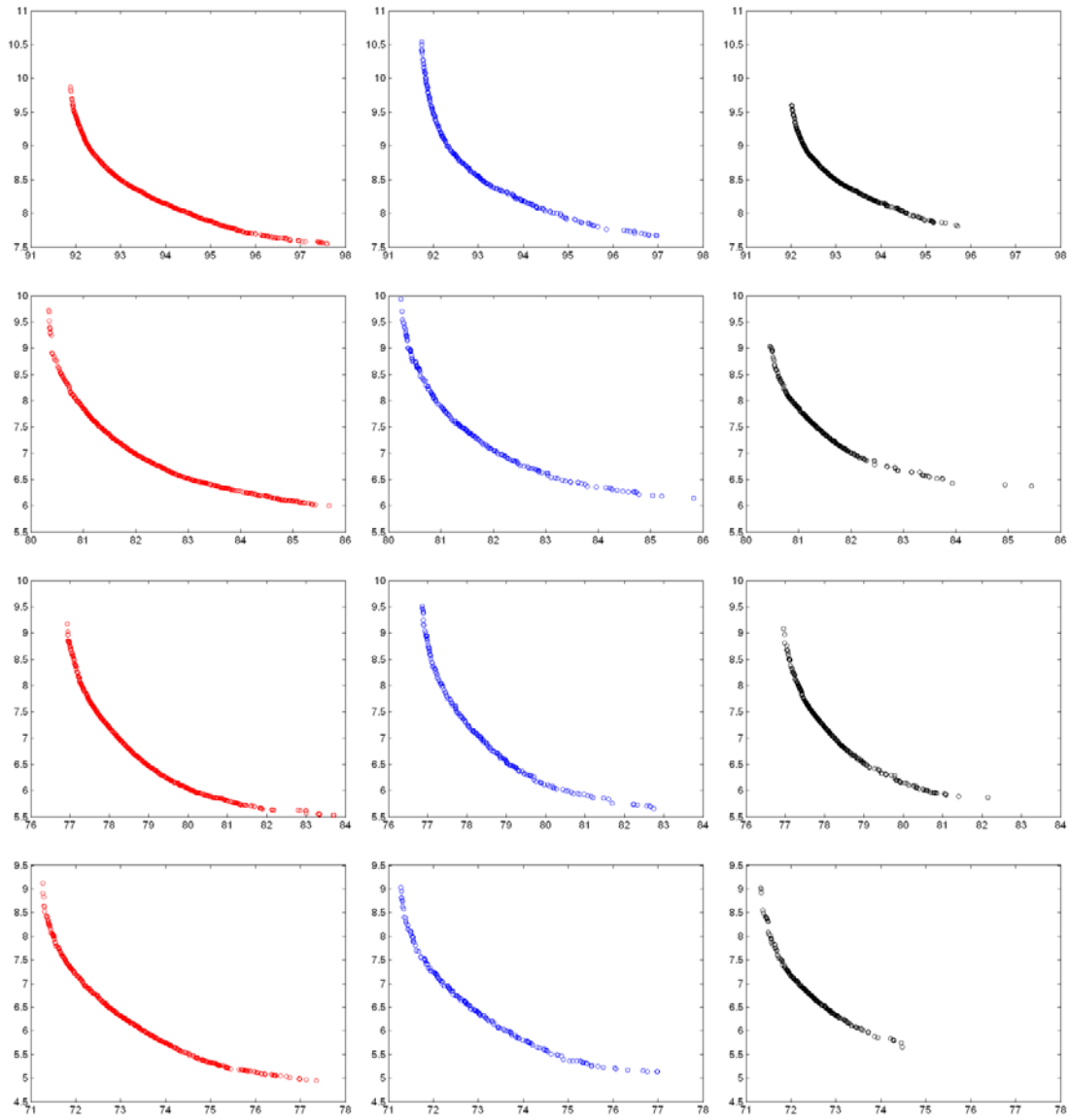

Figure 6.9 Hourly Pareto fronts for the IEEE 118-bus system obtained by NSGA-II (left), SPEA-2 (middle) and AMOSA (right) from hour 1(top) to hour 24 (bottom) in the first phase

In the second phase, the base study without considering the allowance trading by using NSGA-II shows the boundary solutions with maximum emission *Emax* of 205.8 tons (corresponding to the minimum cost of $1,645,374) and minimum emission *Emin* of 147.93 tons (corresponding to the maximum cost of $1,701,868), as shown in figure 6.10. While SPEA-2

achieves *Emax* of 174.34 tons (corresponding to the minimum cost of $1,658,071) and *Emin* of 146.59 tons (corresponding to the maximum cost of $1,700,249), and AMOSA achieves *Emax* of 178.97 tons (corresponding to the minimum cost of $1,654,853) and *Emin* of 144.03 tons (corresponding to the maximum cost of $1,712,598). It can be seen that although the best operation cost was achieved by NSGA-II, the least emission was obtained by AMOSA. In addition, the Pareto front obtained by NSGA-II has a better diversity than SPEA-2. NSGA-II and AMOSA both have better convergence compared with SPEA-2. Next the allowance trading is considered. The emission cap is set as $Emin+\rho(Emax-Emin)$, where ρ is equal to 0.5.

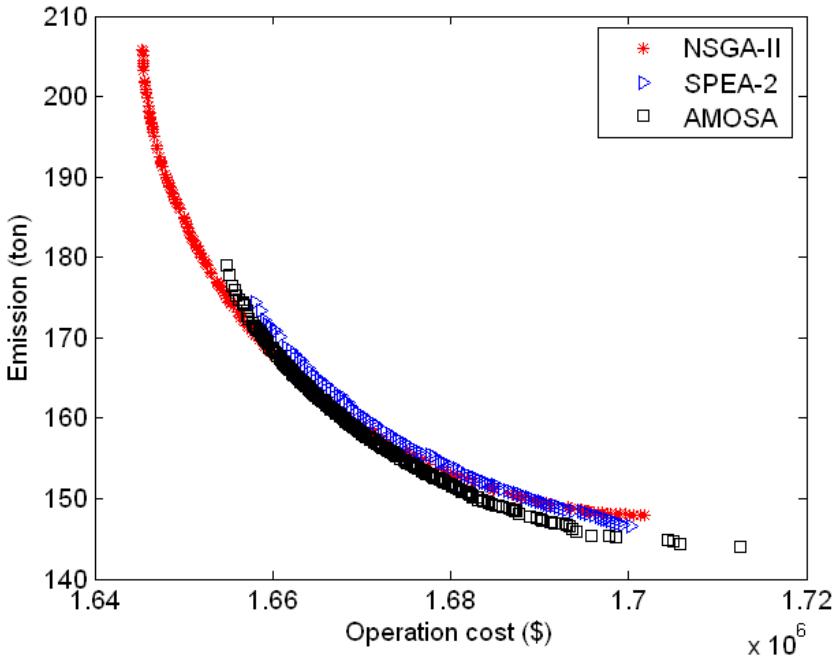

Figure 6.10 24-hour Pareto fronts for the IEEE 118-bus system obtained in the second phase

In 2007, NOx allowance market spot price began the year around $900/ton, fluctuating between $500/ton and $1000/ton throughout the year, ended up to a year-end closing price of $825/ton [107], [108]. So in our simulation, the market price for emission allowance is set to λ=500, 600, 700, 800, 900 and 1000 $/ton respectively. Then for each λ, each of the three MOEAs are run in the second phase to get the Pareto-optimal solutions, which are shown in

figures 6.11, 6.13, and 6.15. It is apparent that with the increasing of λ, the Pareto front converges to a narrower range of closely spaced solution set.

Figures 6.12, 6.14, and 6.16 show obtained Pareto fronts by each MOEA for different emission caps with ρ=0.1, 0.3, 0.5, 0.7, 0.9 when the allowance price is equal to 800 $/ton. It is found that although the emission caps are different, the obtained optimal emissions corresponding to the minimum operation costs are almost all around 170 ton. Meanwhile, the minimum emissions for each case of emission caps are also around *Emin* for each MOEA.

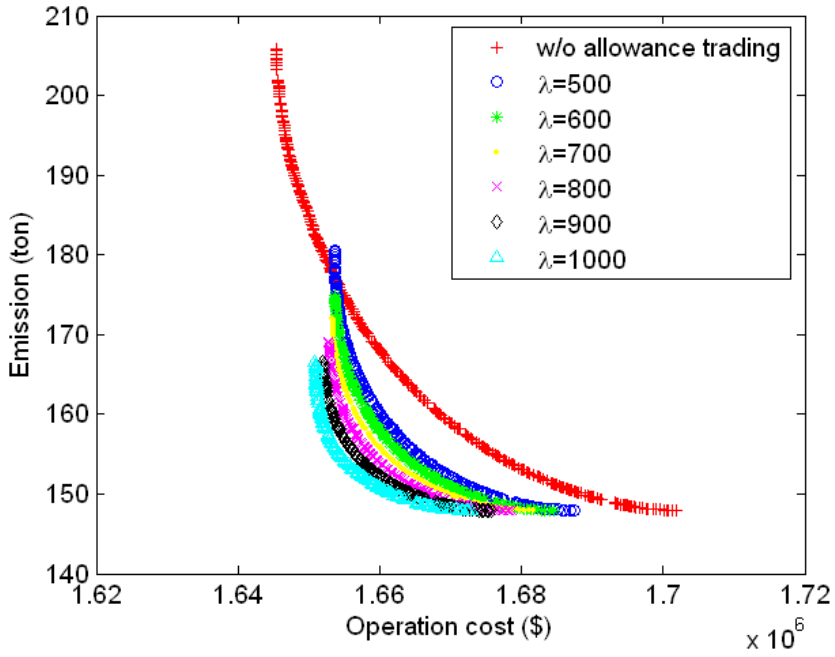

Figure 6.11 24-hour Pareto fronts for the IEEE 118-bus system for different emission allowance prices with ρ=0.5 obtained by NSGA-II in the second phase

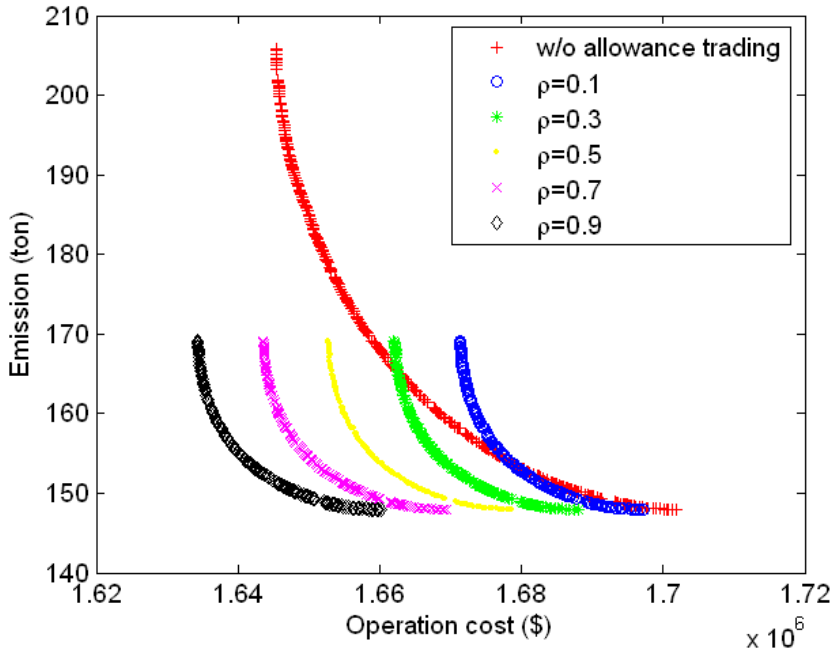

Figure 6.12 24-hour Pareto fronts for the IEEE 118-bus system for different emission caps with λ=800 obtained by NSGA-II in the second phase

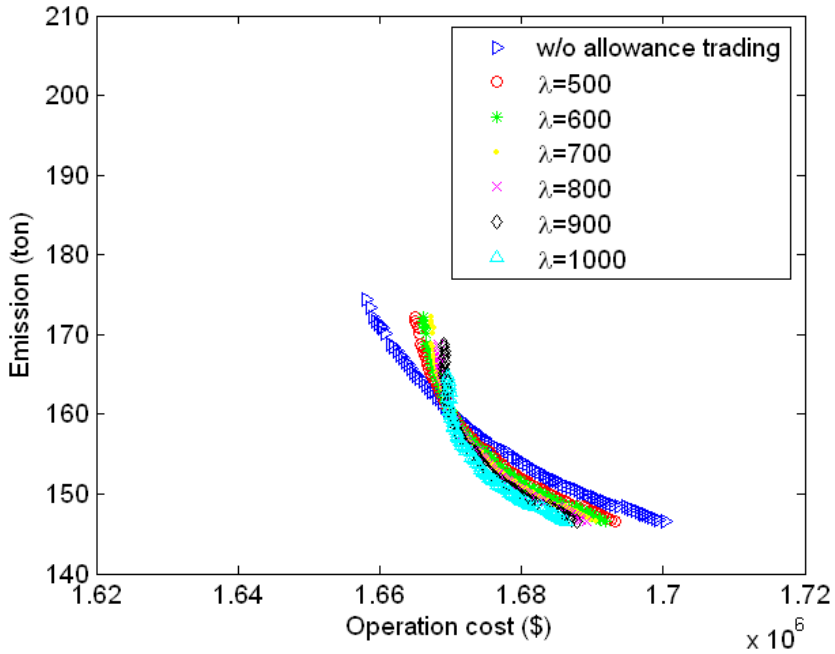

Figure 6.13 24-hour Pareto fronts for the IEEE 118-bus system for different emission allowance prices with ρ=0.5 obtained by SPEA-2 in the second phase

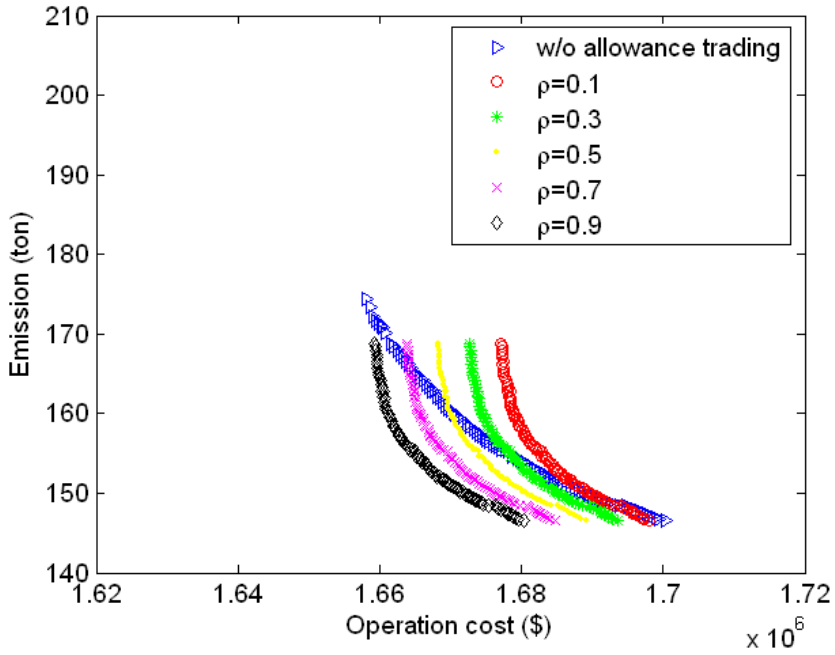

Figure 6.14 24-hour Pareto fronts for the IEEE 118-bus system for different emission caps with λ=800 obtained by SPEA-2 in the second phase

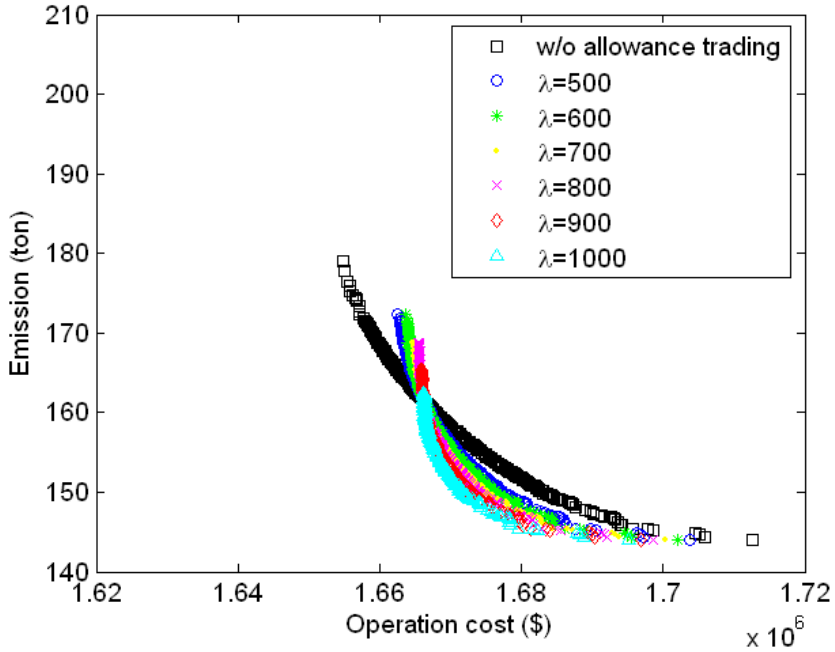

Figure 6.15 24-hour Pareto fronts for the IEEE 118-bus system for different emission allowance prices with ρ=0.5 obtained by AMOSA in the second phase

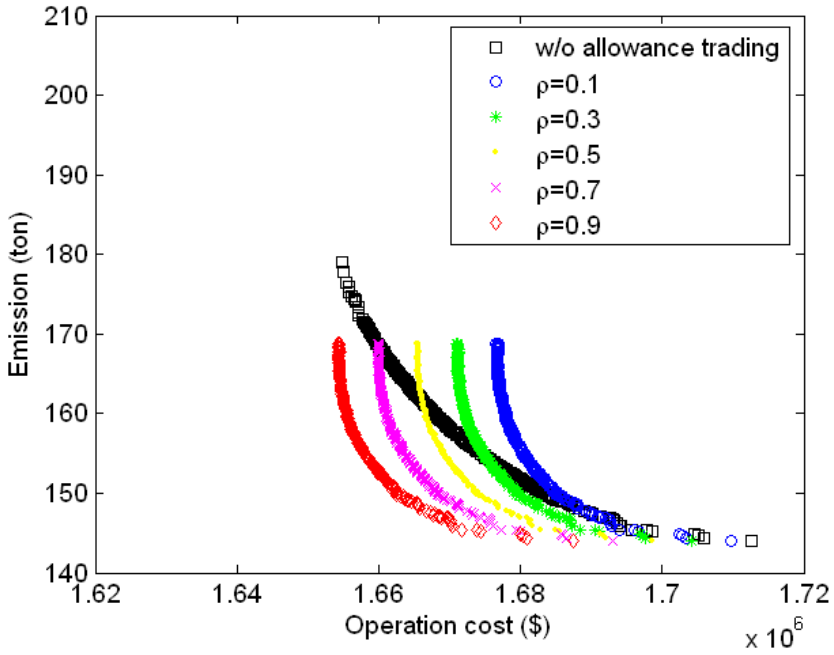

Figure 6.16 24-hour Pareto fronts for the IEEE 118-bus system for different emission caps with λ=800 obtained by AMOSA in the second phase

6.2 Three-Objective System Models

In order to investigate the performance of the proposed two-phase evolutionary approach while taking into account transmission losses, the three-objective model was studied on a 15-unit system and a 60-unit system. The third objective in formulation was the transmission losses.

6.2.1 15-Unit System

The system data is provided in [109]. The shutdown cost for each unit was neglected, and the emission allowance trading was not considered (λ=0). A total of 20 independent runs were carried out to compare the performance of the proposed method by using NSGA-II, SPEA-2 and AMOSA.

During the first phase, the population size was kept at 300. NSGA-II was executed for a total of 300 iterations. The percentage of solutions in the population that were subject to crossover was 90%. The probability of mutation of each entry of the solution vectors was 10%. The distribution indexes for crossover and mutation were 10 and 20.

In SPEA-2 the number of iterations and the population and archive sizes were kept at the same values as NSGA-II. Additionally, the crossover and mutation operators were identical to the latter. The improved version of AMOSA is used which incorporates the crossover, polynomial mutation, crowded distance ranking, and the new method to produce the new solutions. The lower bound on the archive size was equal to NSGA-II's population size, while the upper bound, adjusted for best performance, was 450. It was run for an equal number of function evaluations as NSGA-II.

Figure 6.17 shows 24 hourly non-dominated fronts obtained by the three algorithms, based on the results from one sample run.

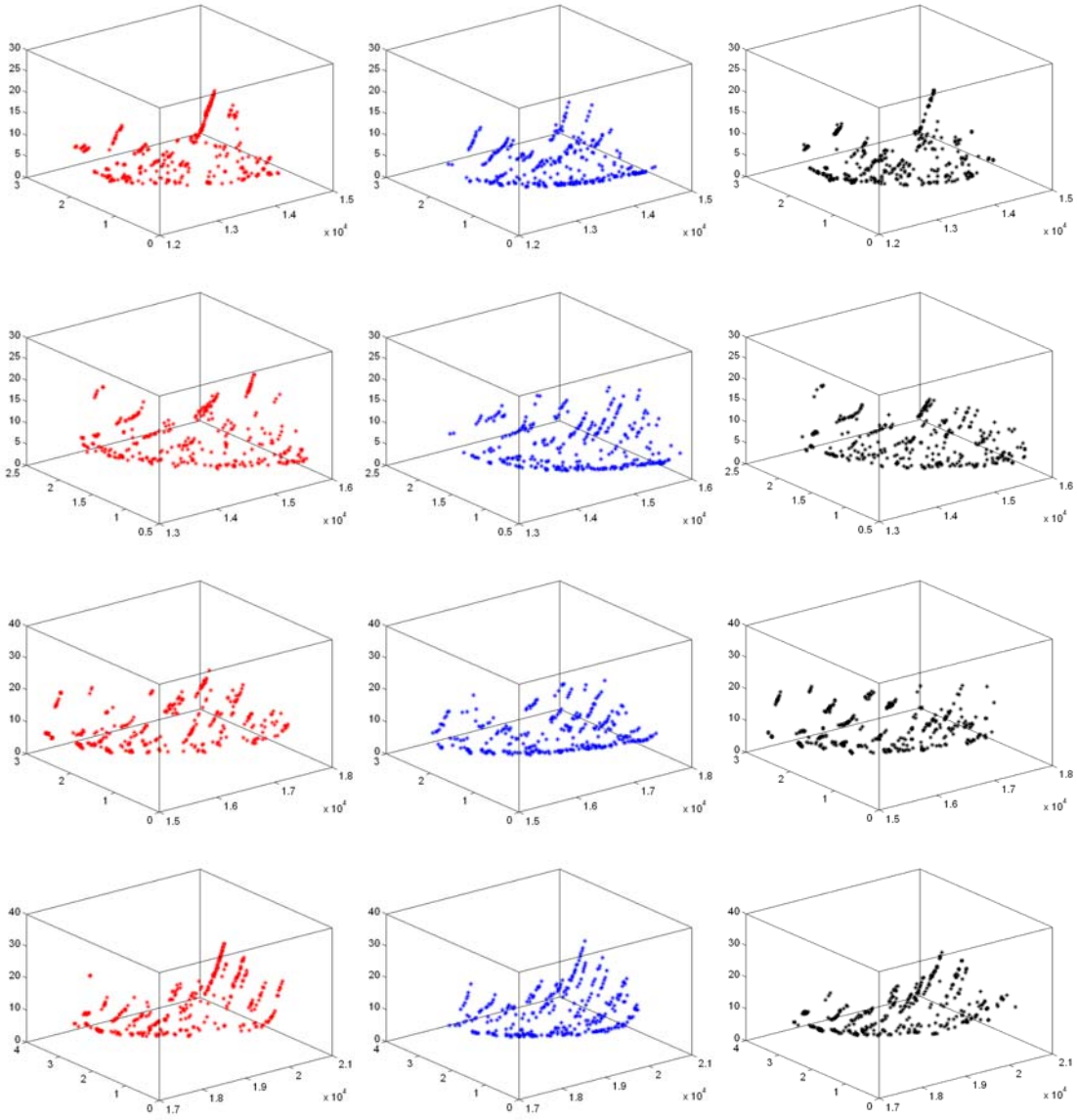

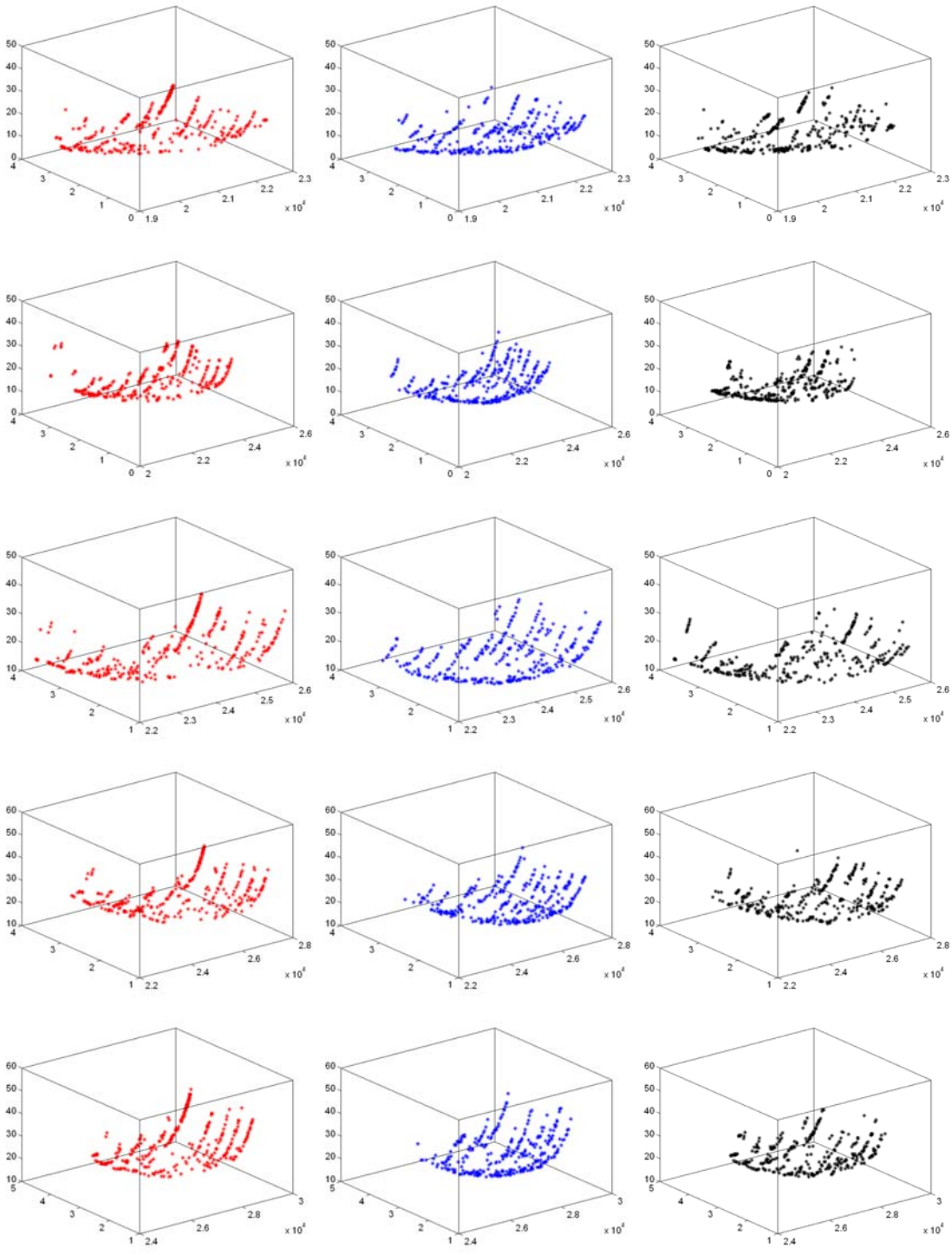

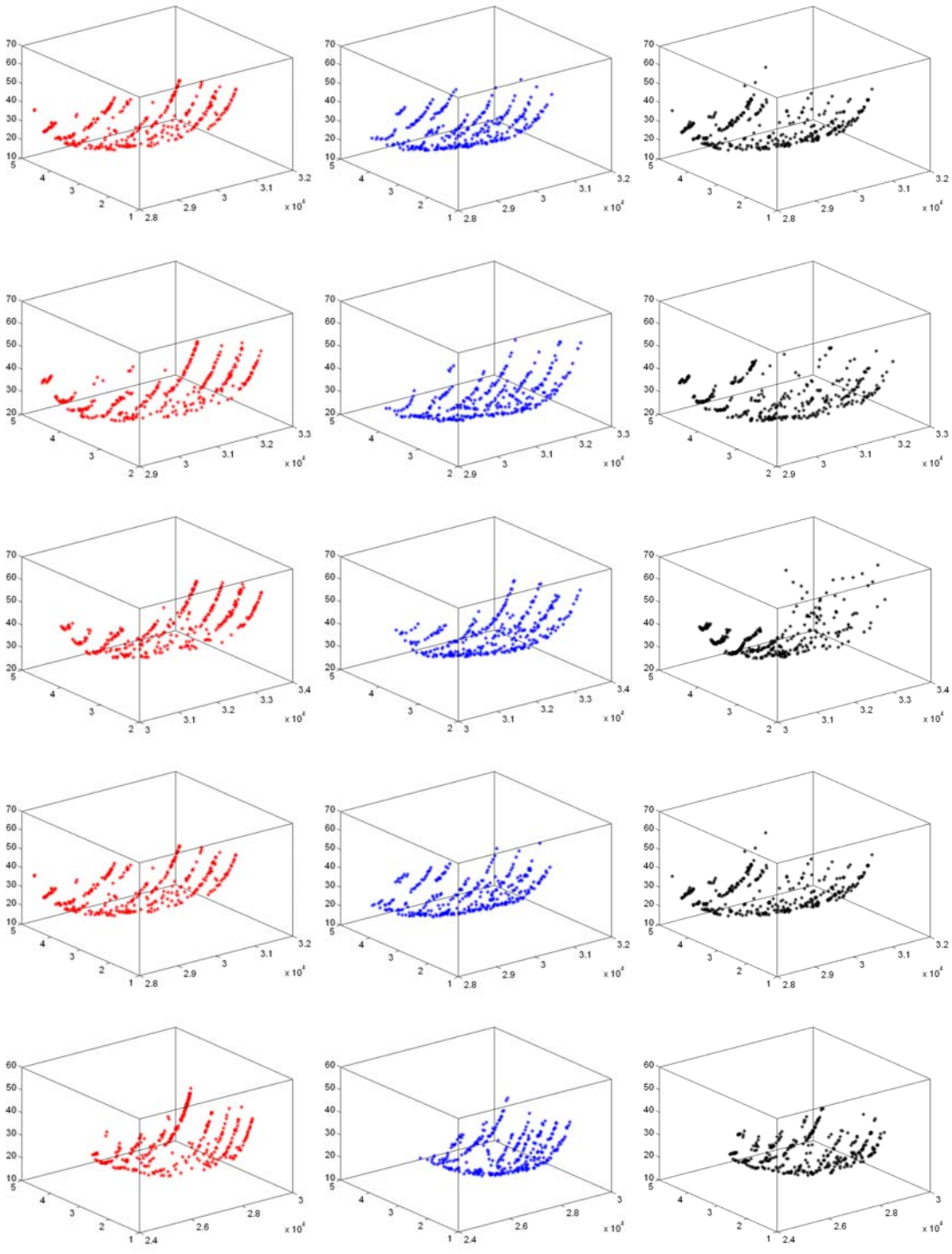

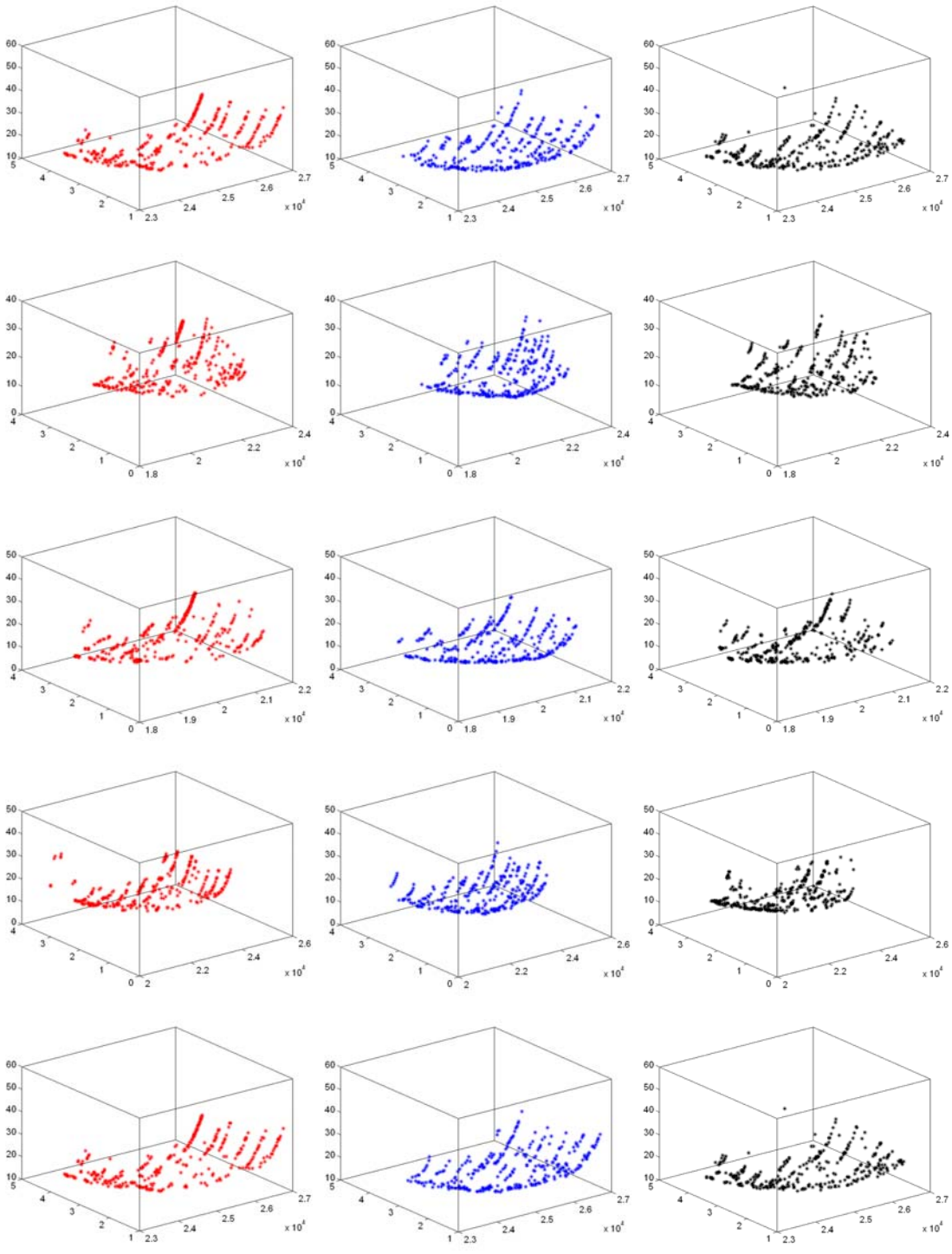

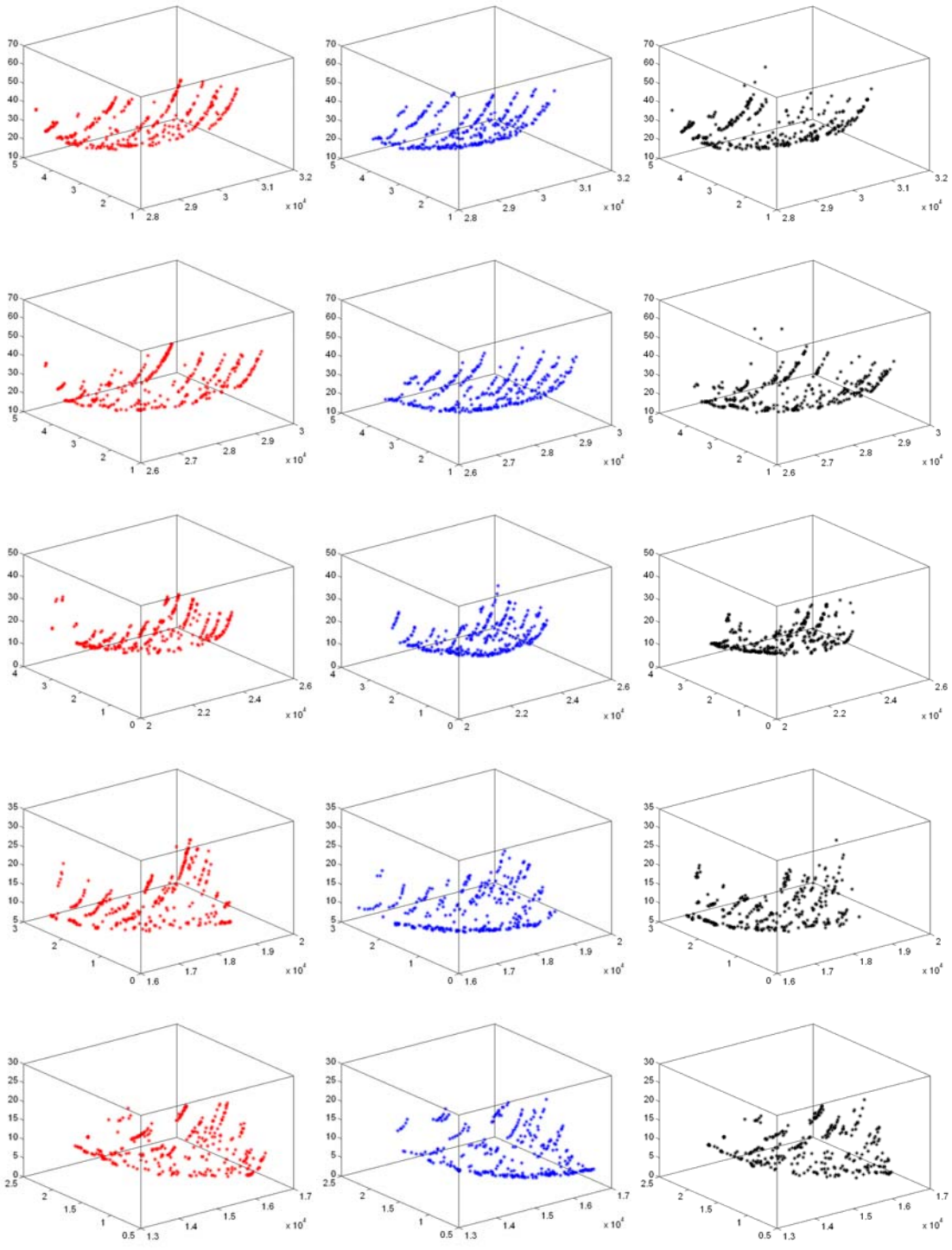

Figure 6.17 Hourly Pareto fronts for the 15-unit system obtained by NSGA-II (left), SPEA-2 (middle) and AMOSA (right) from hour 1(top) to hour 24 (bottom) in the first phase

The population size in the second phase was kept at 300 and 500 iterations of both NSGA-II and SPEA-2 were allowed. In AMOSA, the lower bound on the archive size was equal to NSGA-II's population size, while the upper bound, adjusted for best performance, was 450. It was run for an equal number of function evaluations as NSGA-II. The mutation rate was lowered slightly to 5%, while the crossover rate was kept at 80%.

Three sample 3-dimensional Pareto fronts associated with 24-hour generation scheduling, which are obtained from the second phase of a sample run by NSGA-II, SPEA-2 and AMOSA respectively, are shown in figure 6.18, 6.22 and 6.26 respectively. The scatter 2-dimensional plots of corresponding operation cost, emission and transmission losses are shown in figures 6.19, 6.20 and 6.21 for NSGA-II, figures 6.23, 6.24 and 6.25 for SPEA-2, and figures 6.27, 6.28 and 6.29 for AMOSA respectively. Tables 6.4, 6.5 and 6.6 show the minimum, maximum and the median values of each objective that were found by merging the Pareto-optimal solutions of all 20 runs, for NSGA-II, SPEA-2 and AMOSA respectively. The small variation between the values of the best and worst boundary solutions proves the robustness of the proposed approach.

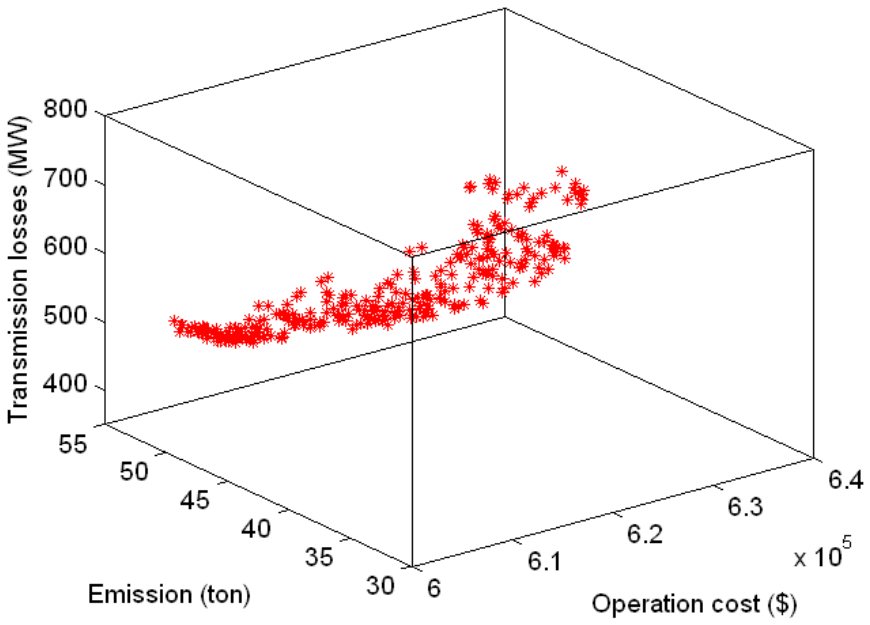

Figure 6.18 24-hour Pareto front for the 15-unit system obtained by NSGA-II in the second phase

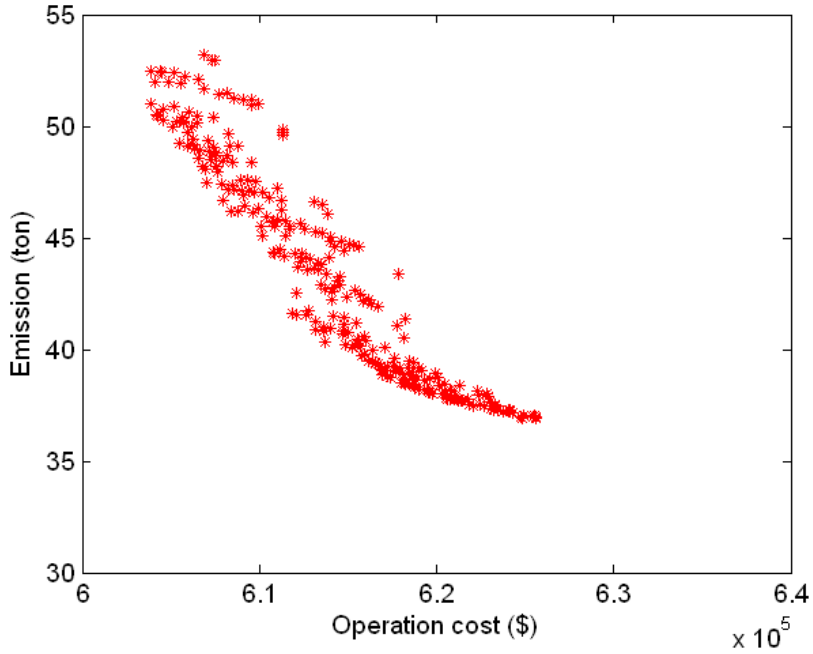

Figure 6.19 Operation cost vs. emission (based on the 24-hour Pareto front for the 15-unit system obtained by NSGA-II in the second phase)

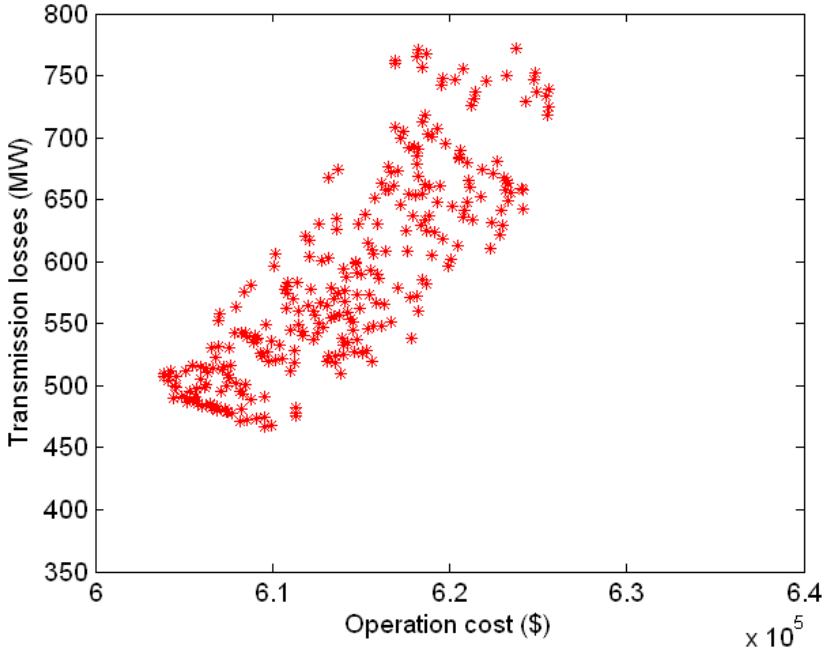

Figure 6.20 Operation cost vs. transmission losses (based on the 24-hour Pareto front for the 15-unit system obtained by NSGA-II in the second phase)

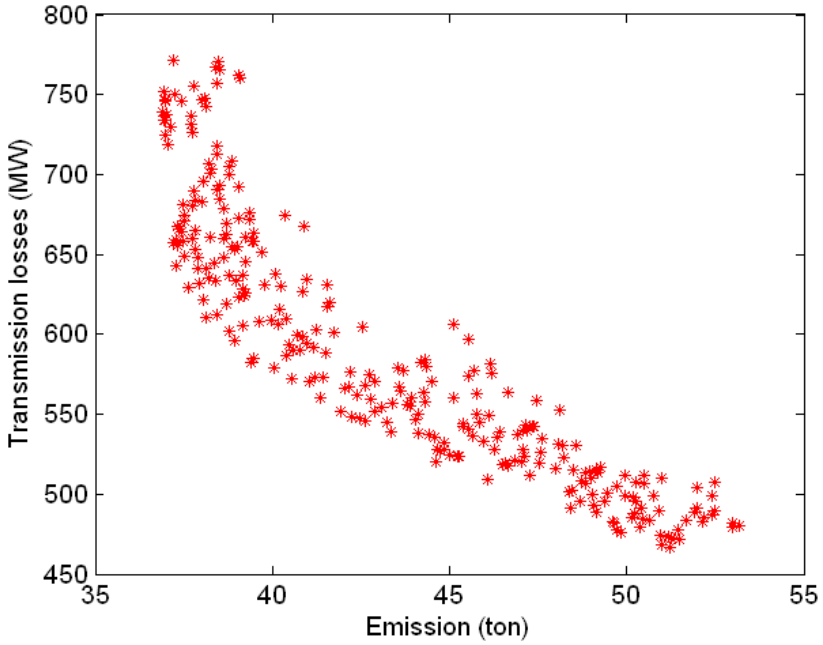

Figure 6.21 Emission vs. transmission losses (based on the 24-hour Pareto front for the 15-unit system obtained by NSGA-II in the second phase)

Table 6.4 Performance of the proposed approach with NSGA-II for the 15-unit System (20 run average)

	Operation Cost ($)			Emission (ton)			Transmission Losses (MW)		
	Min	Median	Max	Min	Median	Max	Min	Median	Max
Best Operation Cost	603844	603875	604133	50.98	52.00	52.49	503.92	507.15	510.22
Best Emission	624867	625477	625586	36.92	36.94	36.96	733.80	739.35	751.98
Best Transmission Losses	608143	609523	609956	50.98	51.20	51.48	467.00	467.91	471.43

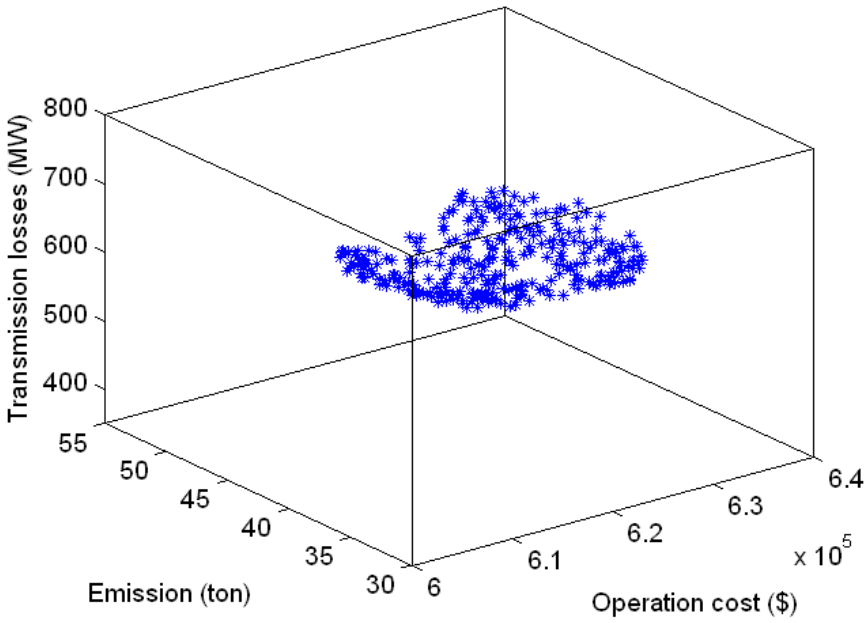

Figure 6.22 24-hour Pareto front for the 15-unit system obtained by SPEA-2 in the second phase

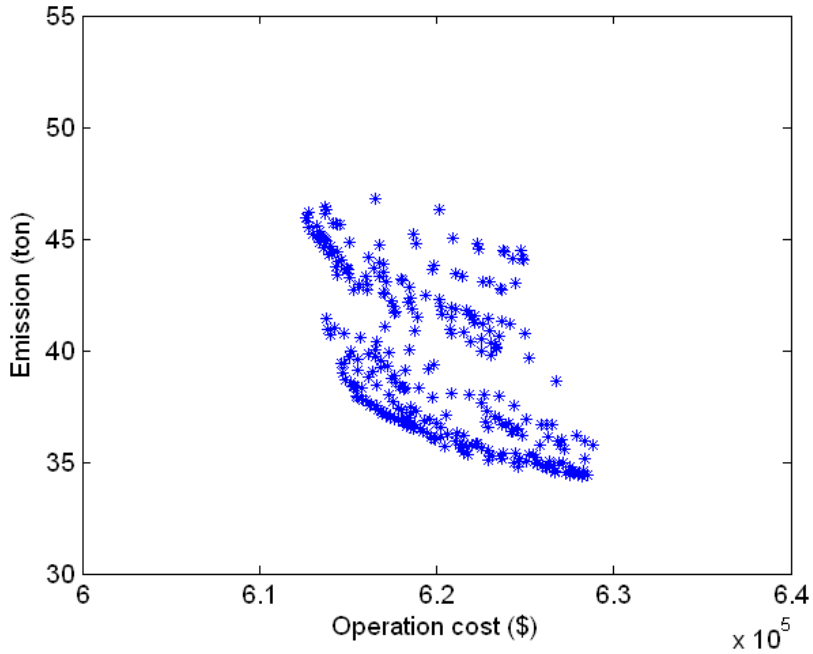

Figure 6.23 Operation cost vs. emission (based on the 24-hour Pareto front for the 15-unit system obtained by SPEA-2 in the second phase)

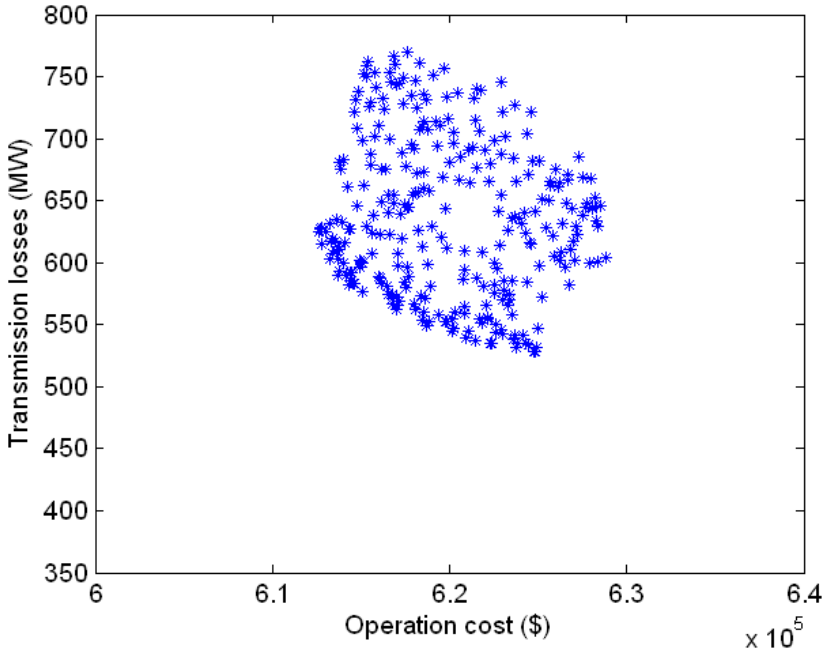

Figure 6.24 Operation cost vs. transmission losses (based on the 24-hour Pareto front for the 15-unit system obtained by SPEA-2 in the second phase)

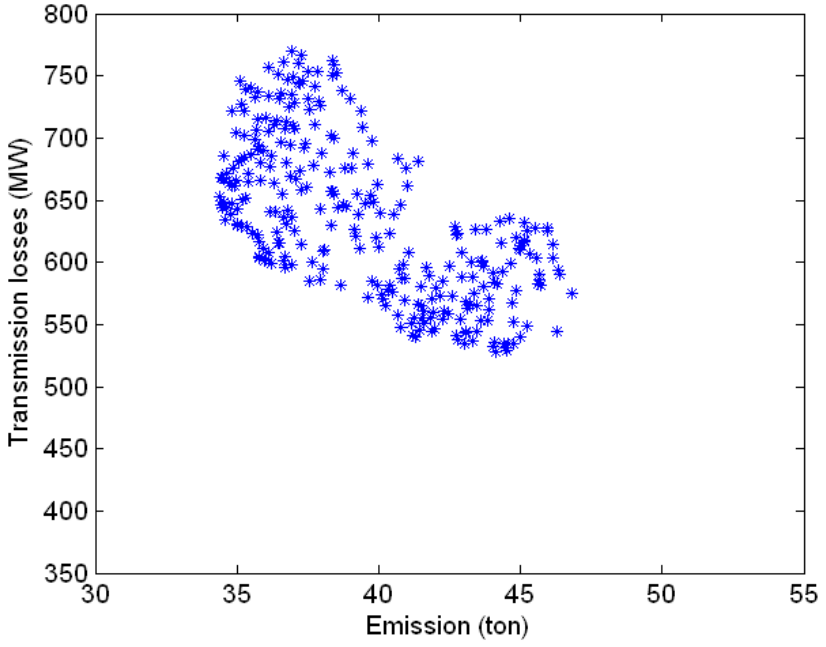

Figure 6.25 Emission vs. transmission losses (based on the 24-hour Pareto front for the 15-unit system obtained by SPEA-2 in the second phase)

Table 6.5 Performance of the proposed approach with SPEA-2 for the 15-unit System (20 run average)

	Operation Cost ($)			Emission (ton)			Transmission Losses (MW)		
	Min	Median	Max	Min	Median	Max	Min	Median	Max
Best Operation Cost	612628	612714	612749	45.93	45.95	46.16	614.76	625.03	627.63
Best Emission	627554	628217	628502	34.37	34.43	34.45	645.68	652.58	668.42
Best Transmission Losses	623772	624769	624835	44.13	44.48	44.50	528.25	528.63	531.12

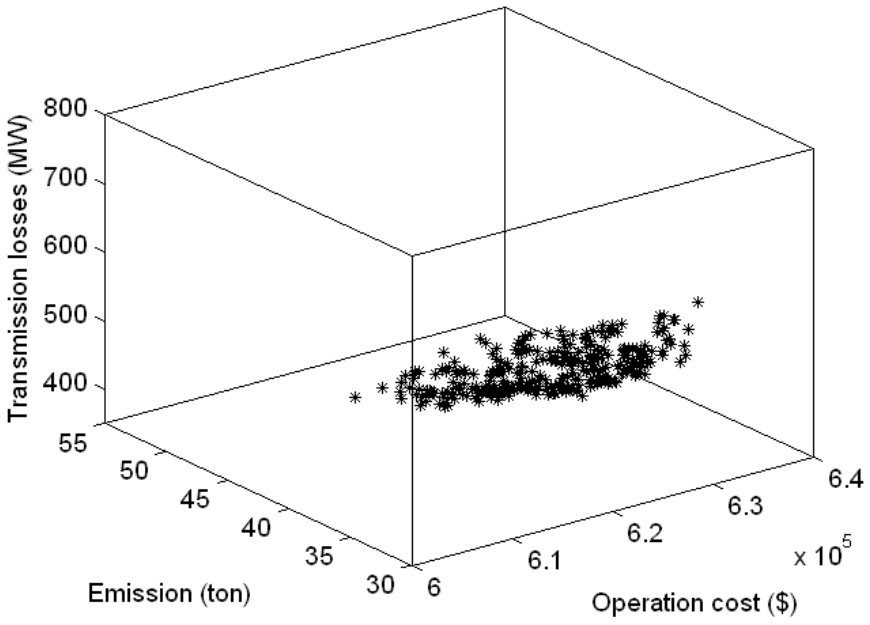

Figure 6.26 24-hour Pareto front for the 15-unit system obtained by AMOSA in the second phase

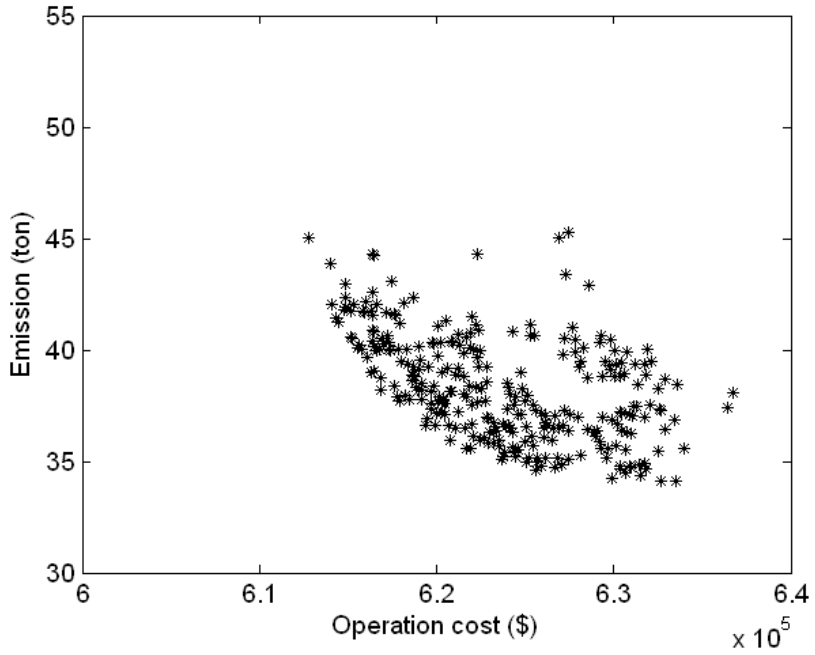

Figure 6.27 Operation cost vs. emission (based on the 24-hour Pareto front for the 15-unit system obtained by AMOSA in the second phase)

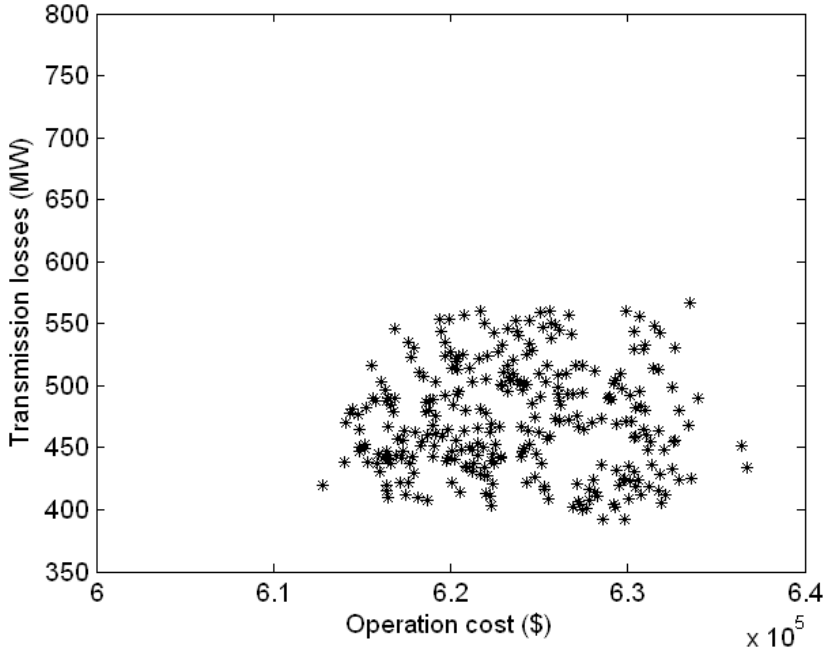

Figure 6.28 Operation cost vs. transmission losses (based on the 24-hour Pareto front for the 15-unit system obtained by AMOSA in the second phase)

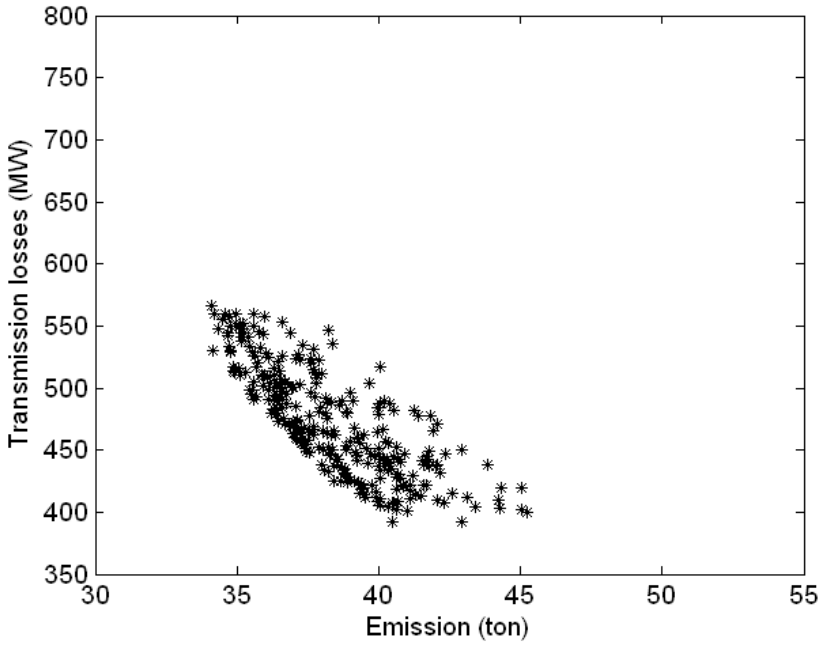

Figure 6.29 Emission vs. transmission losses (based on the 24-hour Pareto front for the 15-unit system obtained by AMOSA in the second phase)

Table 6.6 Performance of the proposed approach with AMOSA for the 15-unit System (20 run average)

	Operation Cost ($)			Emission (ton)			Transmission Losses (MW)		
	Min	Median	Max	Min	Median	Max	Min	Median	Max
Best Operation Cost	612791	614011	614108	42.06	43.86	45.03	419.37	438.5	470.71
Best Emission	629881	632704	633521	34.11	34.13	34.22	530.46	559.87	566.57
Best Transmission Losses	627426	628567	629806	40.48	42.92	45.25	391.82	392.08	400.11

From all runs, SPEA-2's solutions were dominated by 38.67% of those of NSGA-II, whereas NSGA-II's solutions were only dominated by 34.67% of those of SPEA-2 in the front. Solutions of NSGA-II and SPEA-2 were dominated by 44.33% and 70% of those of AMOSA respectively, while no solutions of AMOSA were dominated by either NSGA-II or SPEA-2. From table 6.4, 6.5 and 6.6, among the three algorithms, it is also shown that the best operation cost was $603844, which was obtained by NSGA-II, while the least emission (34.11 ton) and

transmission losses (391.82 MW) were both obtained by AMOSA. This demonstrates that the improved AMOSA outperformed both NSGA-II and SPEA-2.

6.2.2 60-Unit System

A 60-unit system was used to further investigate the performance of the proposed approach. The system data is based on the reference [14] with some modifications. Parameters of the two-phase approach with NSGA-II, SPEA-2 used here are the same as in the case of 15-unit system, except for the population size of 500 and iterations of 600 in the first phase, and 800 and 1500 in the second phase. In the improved AMOSA, both crossover and mutation operators were used. The lower bound on the archive size was equal to the population size of NSGA-II in both phases, while the upper bound, adjusted for best performance, was 750 in the first phase and 1100 in the second phase. It was run for an equal number of function evaluations as NSGA-II.

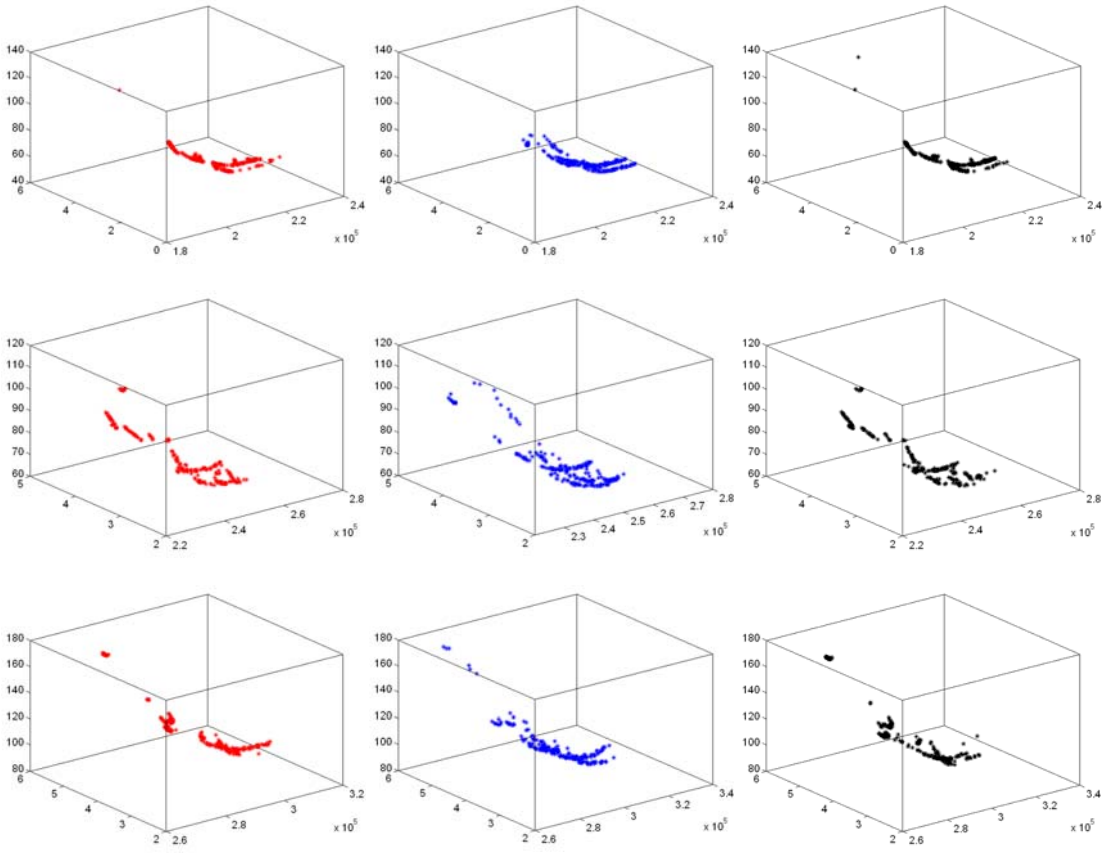

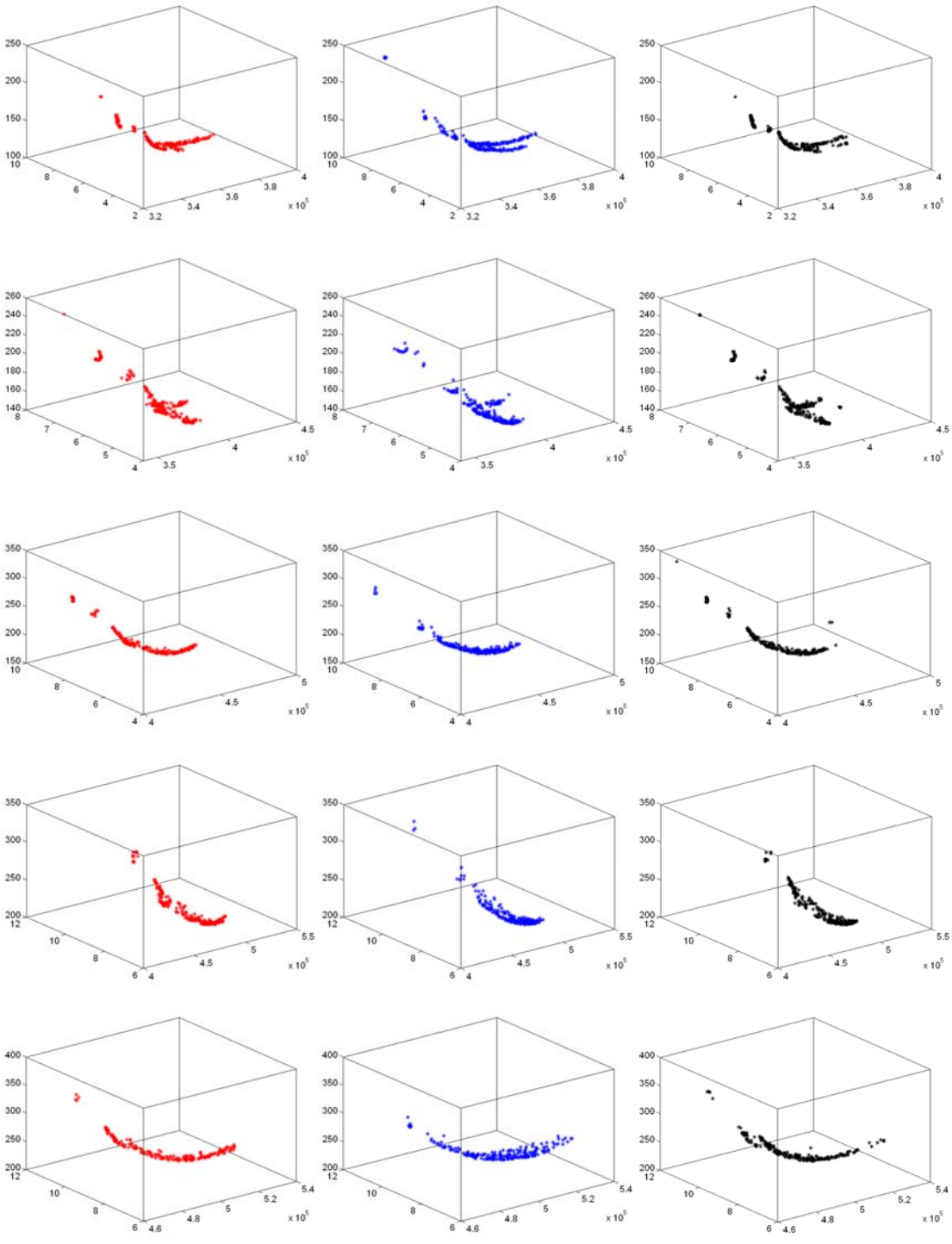

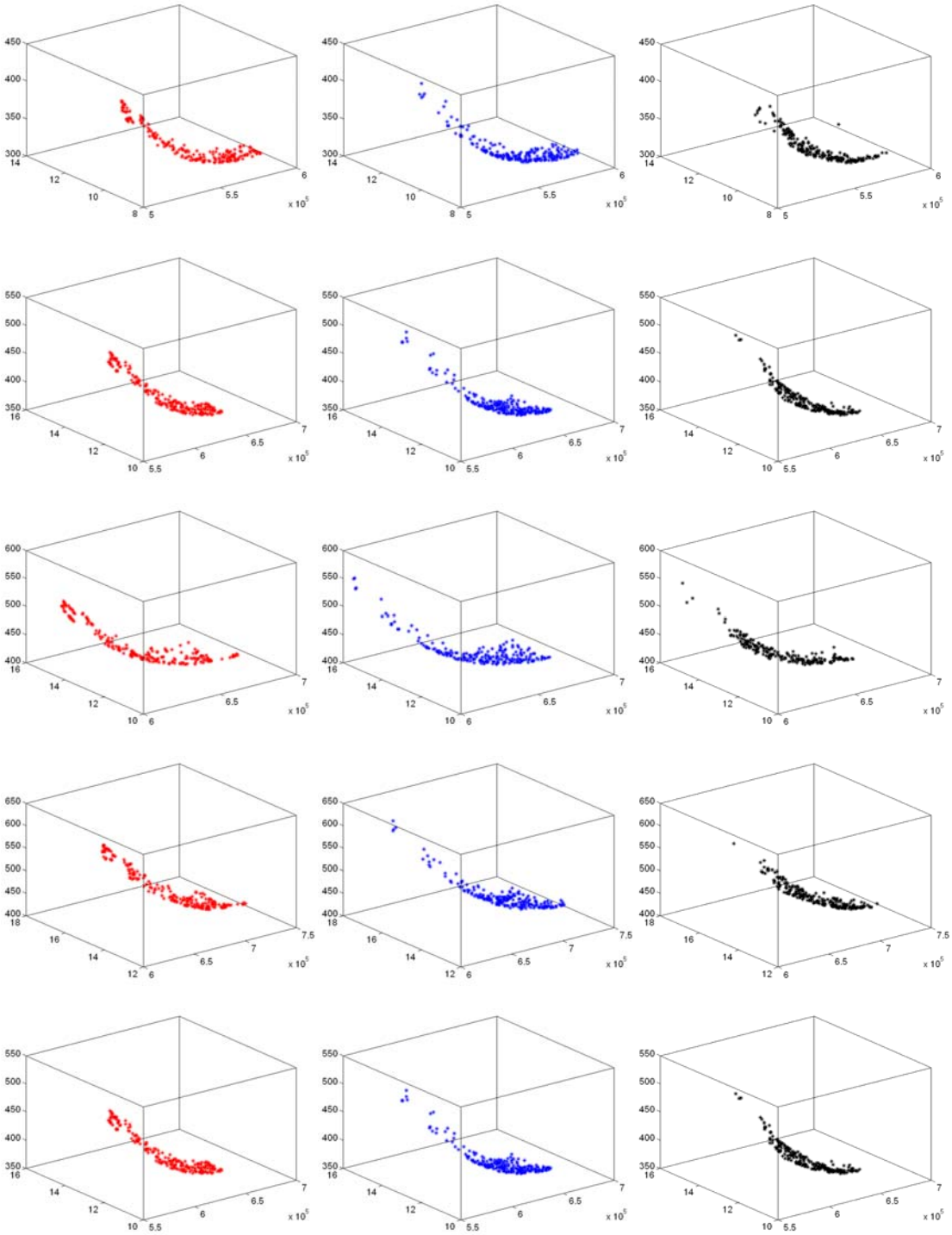

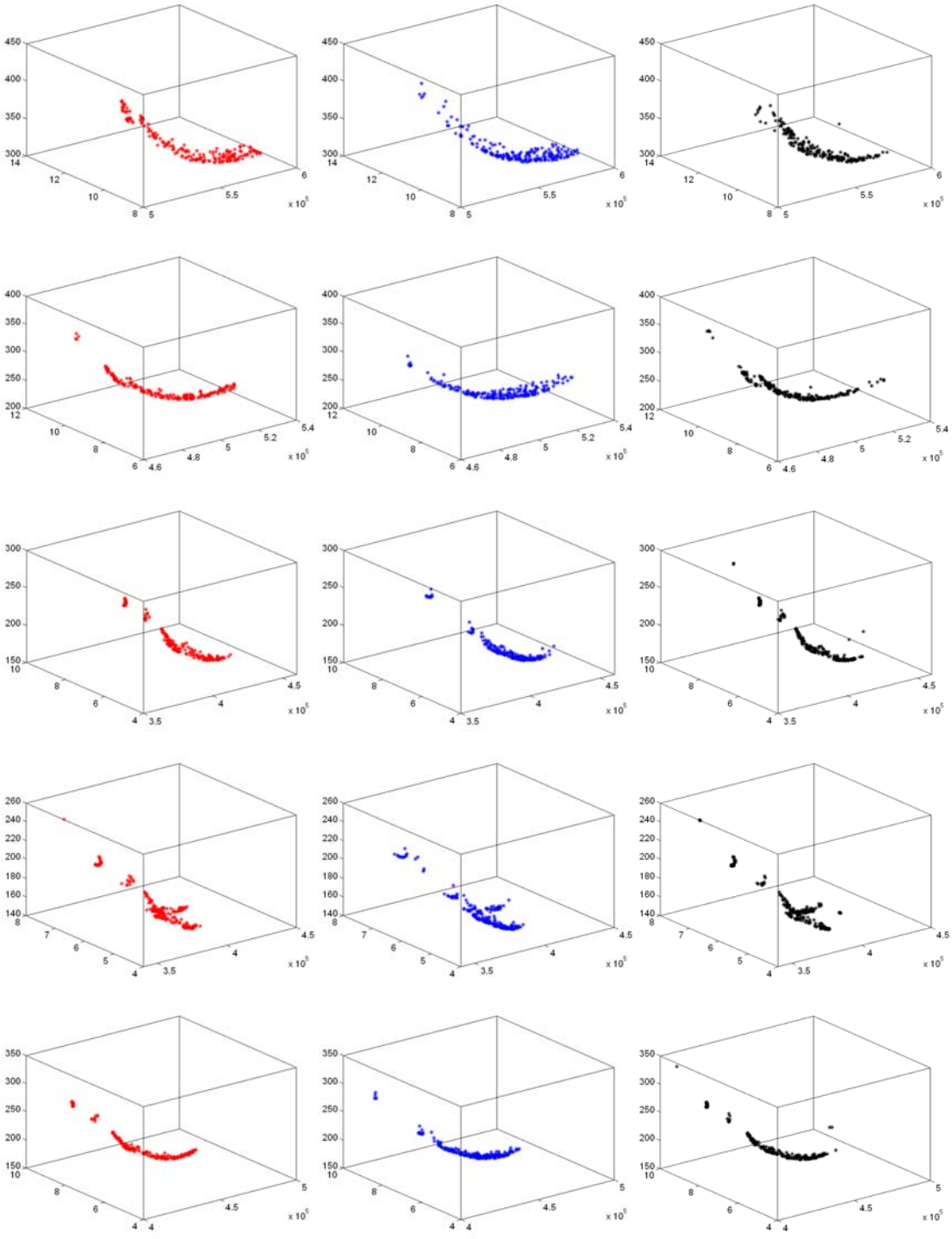

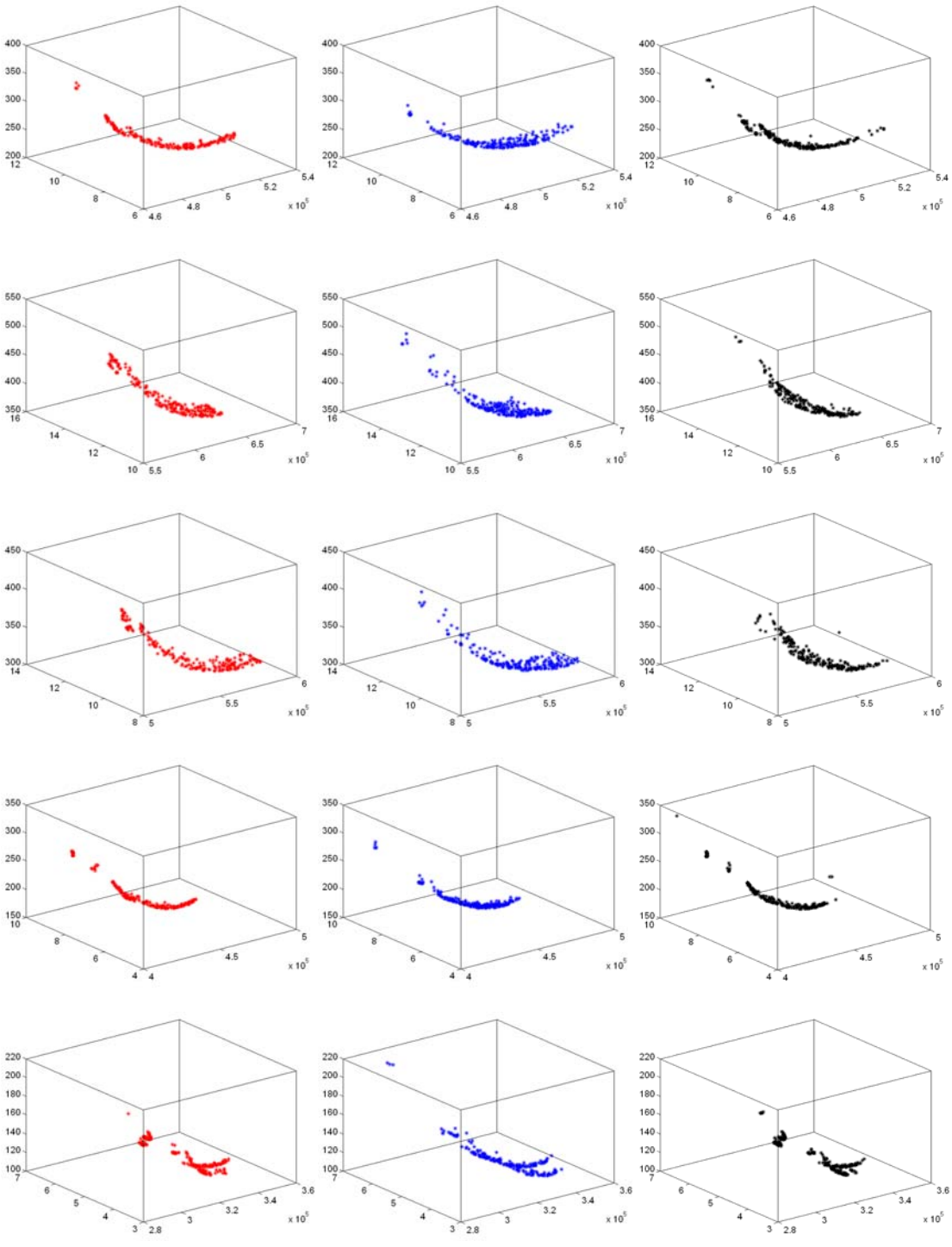

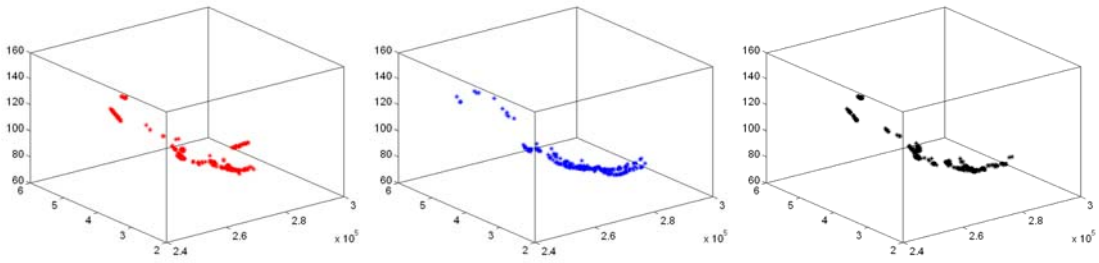

Figure 6.30 Hourly Pareto fronts for the 60-unit system obtained by NSGA-II (left), SPEA-2 (middle) and AMOSA (right) from hour 1(top) to hour 24 (bottom) in the first phase

Three sample 3-dimensional Pareto fronts associated with 24-hour generation scheduling, which are obtained from the second phase of a sample run by NSGA-II, SPEA-2 and AMOSA respectively, are shown in figure 6.31, 6.35 and 6.39 respectively. The scatter 2-dimensional plots of corresponding operation cost, emission and transmission losses are shown in figures 6.32, 6.33 and 6.34 for NSGA-II, figures 6.36, 6.37 and 6.38 for SPEA-2, and figures 6.40, 6.41 and 6.42 for AMOSA respectively. Tables 6.7, 6.8 and 6.9 show the minimum, maximum and the median values of each objective that were found by merging the Pareto-optimal solutions of all 20 runs, for NSGA-II, SPEA-2 and AMOSA respectively. The small variation between the values of the best and worst boundary solutions proves the robustness of the proposed approach.

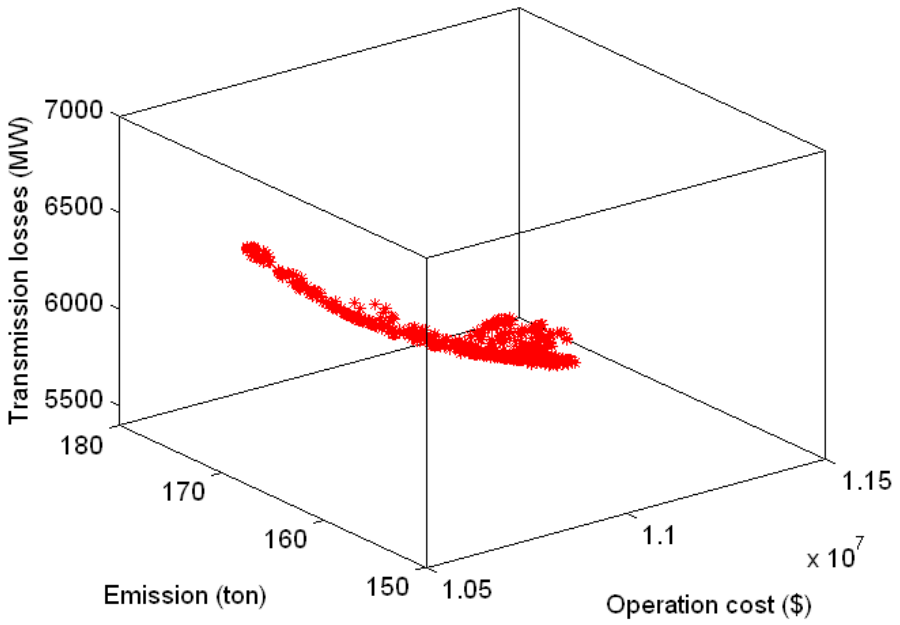

Figure 6.31 24-hour Pareto front for the 60-unit system obtained by NSGA-II in the second phase

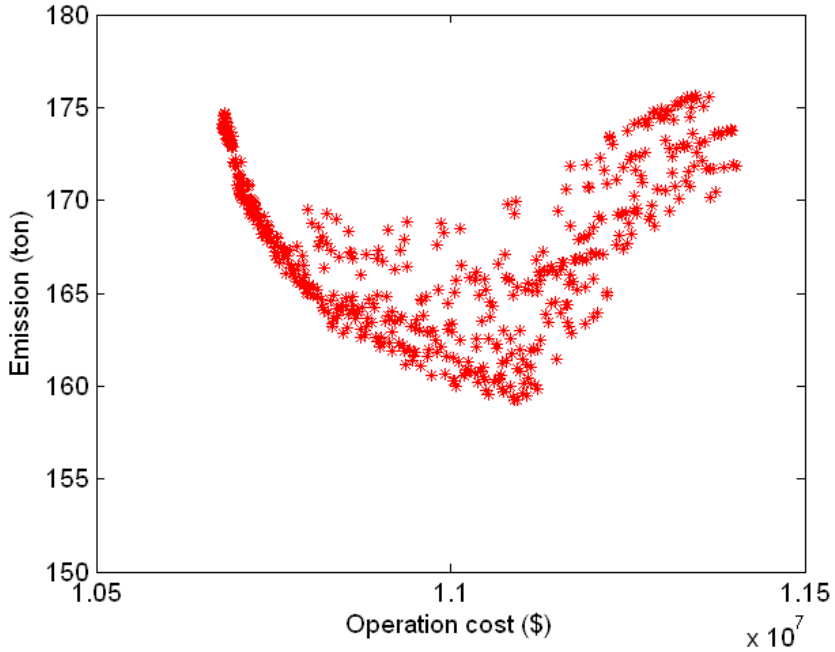

Figure 6.32 Operation cost vs. emission (based on the 24-hour Pareto front for the 60-unit system obtained by NSGA-II in the second phase)

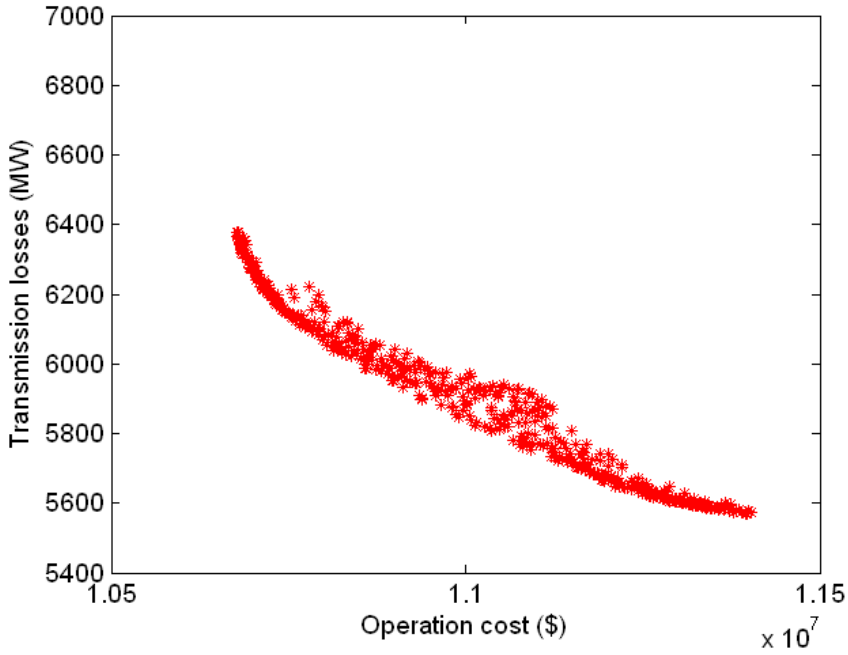

Figure 6.33 Operation cost vs. transmission losses (based on the 24-hour Pareto front for the 60-unit system obtained by NSGA-II in the second phase)

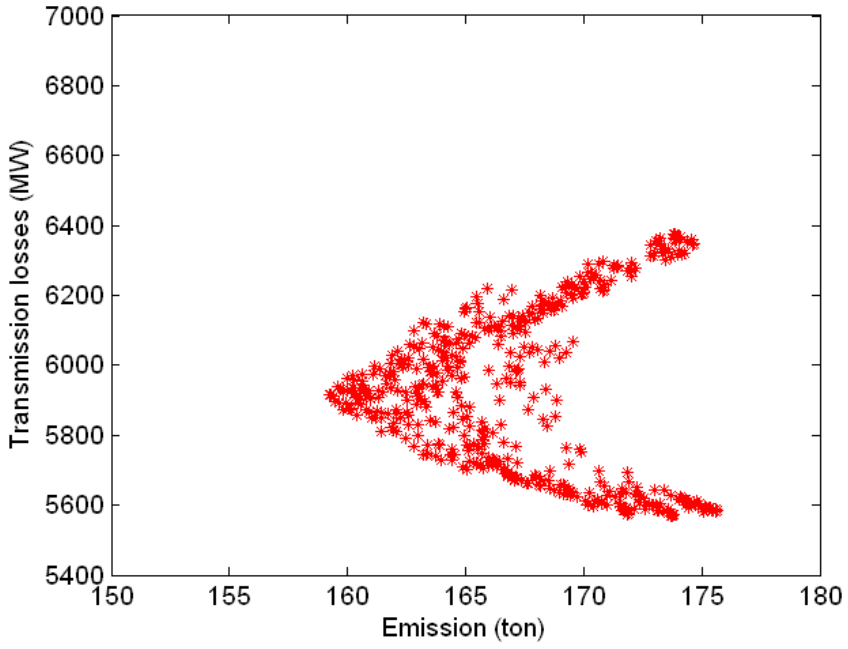

Figure 6.34 Emission vs. transmission losses (based on the 24-hour Pareto front for the 60-unit system obtained by NSGA-II in the second phase)

Table 6.7 Performance of the proposed approach with NSGA-II for the 60-unit System (20 run average)

	Operation Cost ($)			Emission (ton)			Transmission Losses (MW)		
	Min	Median	Max	Min	Median	Max	Min	Median	Max
Best Operation Cost	10677540	10677630	10678680	173.81	173.88	174.08	6367.67	6375.85	6376.92
Best Emission	11087980	11090640	11093900	159.23	159.28	159.43	5912.06	5914.21	5916.01
Best Transmission Losses	11394740	11395610	11398000	173.71	173.75	173.81	5570.11	5571.24	5571.91

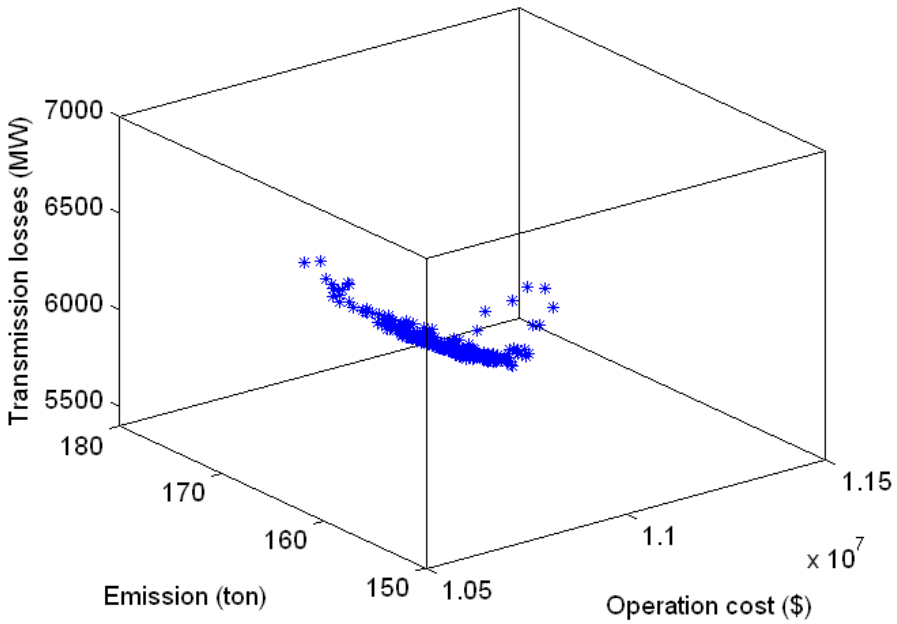

Figure 6.35 24-hour Pareto front for the 60-unit system obtained by SPEA-2 in the second phase

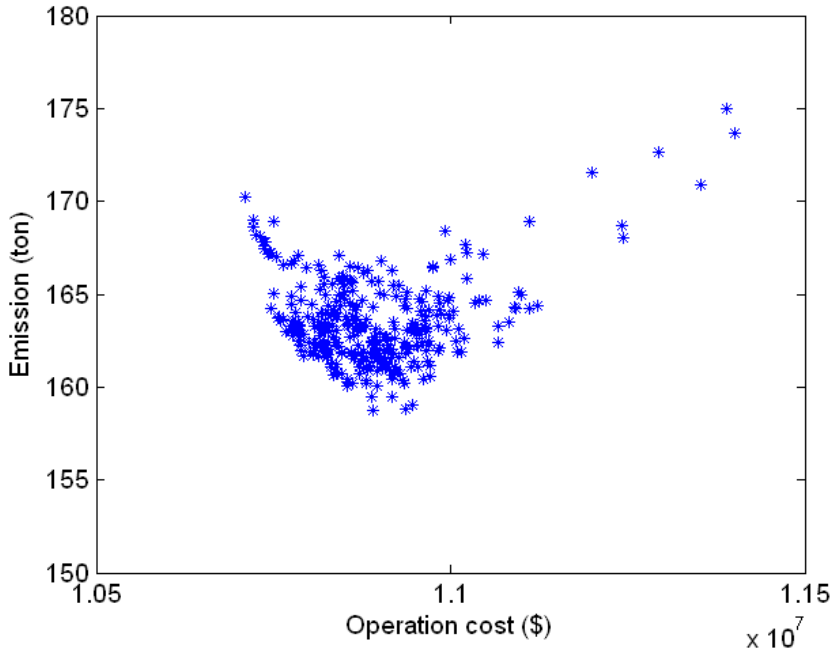

Figure 6.36 Operation cost vs. emission (based on the 24-hour Pareto front for the 6-unit system obtained by SPEA-2 in the second phase)

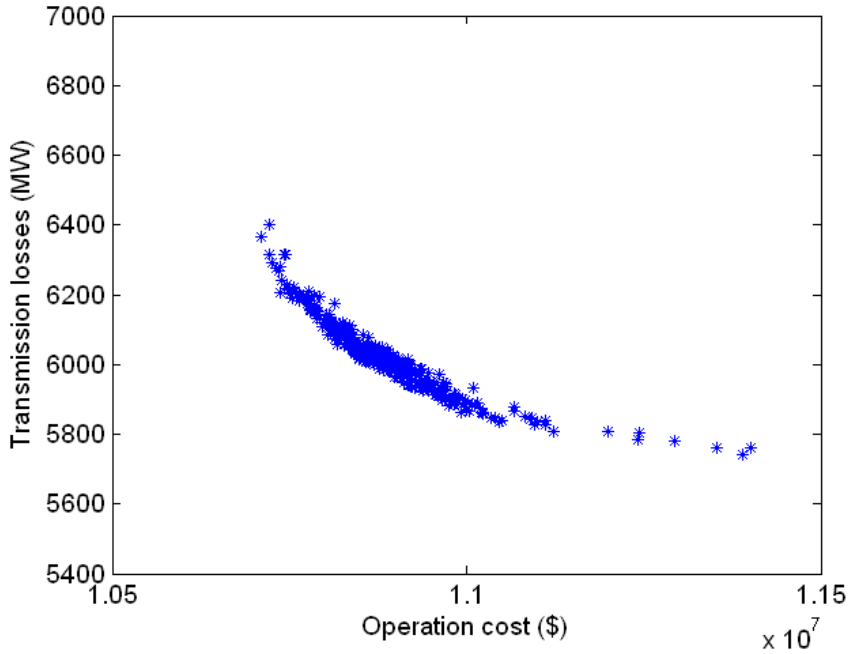

Figure 6.37 Operation cost vs. transmission losses (based on the 24-hour Pareto front for the 60-unit system obtained by SPEA-2 in the second phase)

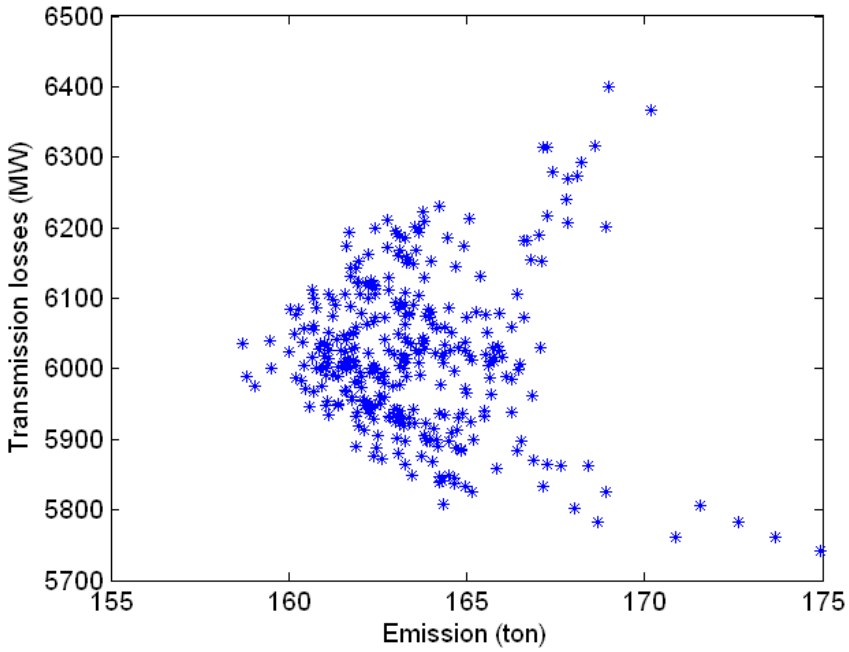

Figure 6.38 Emission vs. transmission losses (based on the 24-hour Pareto front for the 60-unit system obtained by SPEA-2 in the second phase)

Table 6.8 Performance of the proposed approach with SPEA-2 for the 60-unit System (20 run average)

	Operation Cost ($)			Emission (ton)			Transmission Losses (MW)		
	Min	Median	Max	Min	Median	Max	Min	Median	Max
Best Operation Cost	10710390	10721530	10722440	168.59	168.97	170.19	6315.28	6367.15	6400.34
Best Emission	10890880	10937040	10945660	158.71	158.81	159.03	5975.88	5988.72	6035.54
Best Transmission Losses	11292920	11352730	11401190	170.88	172.63	174.96	5741.92	5761.78	5781.93

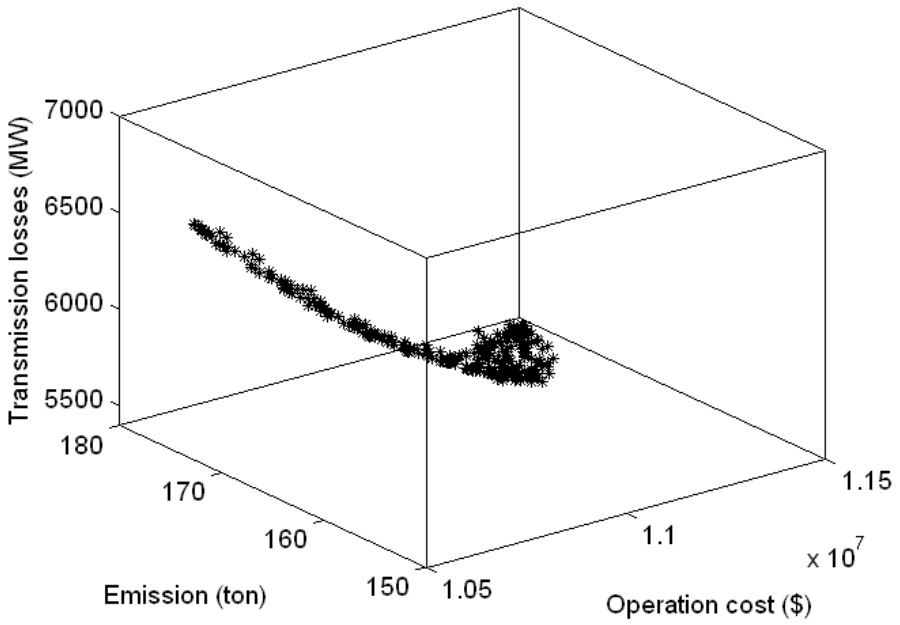

Figure 6.39 24-hour Pareto front for the 60-unit system obtained by AMOSA in the second phase

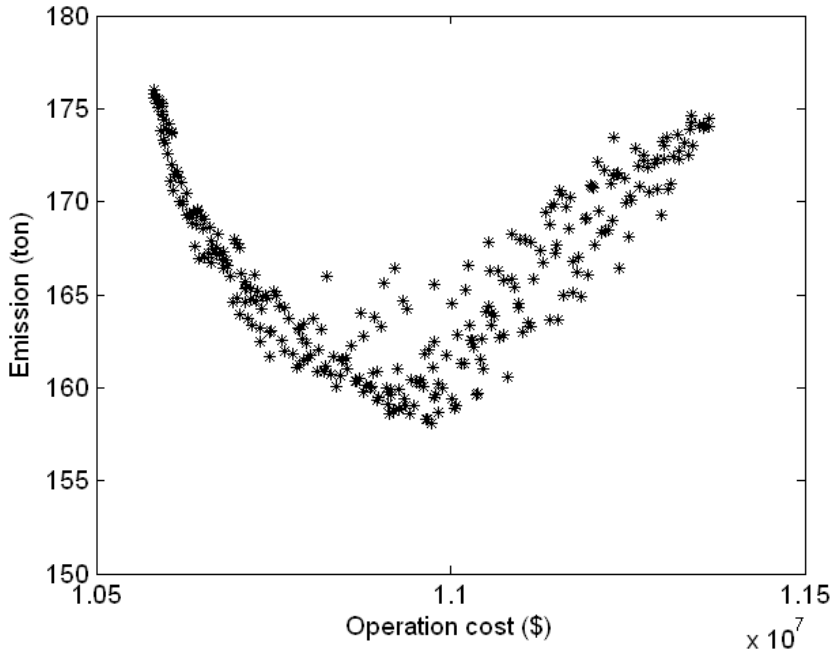

Figure 6.40 Operation cost vs. emission (based on the 24-hour Pareto front for the 60-unit system obtained by AMOSA in the second phase)

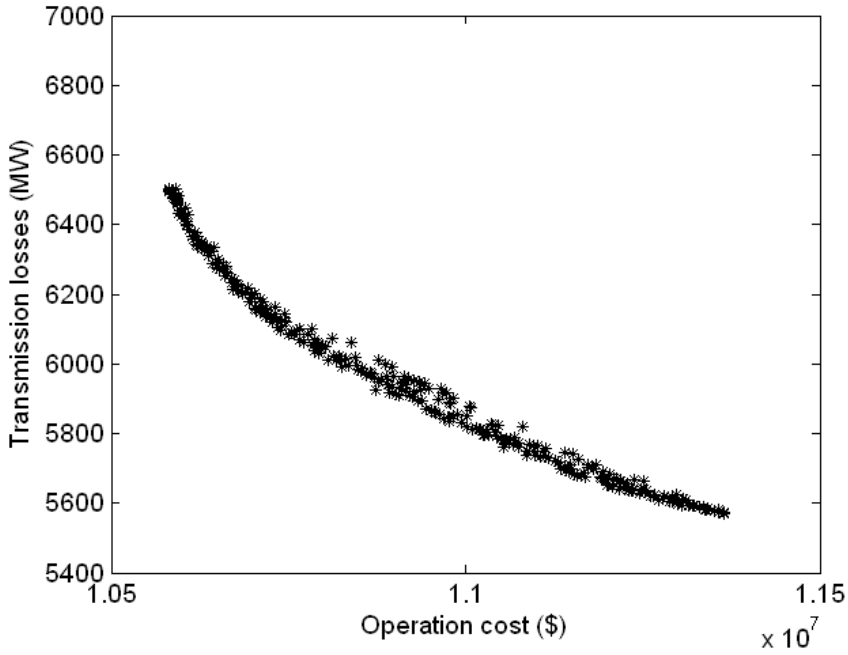

Figure 6.41 Operation cost vs. transmission losses (based on the 24-hour Pareto front for the 60-unit system obtained by AMOSA in the second phase)

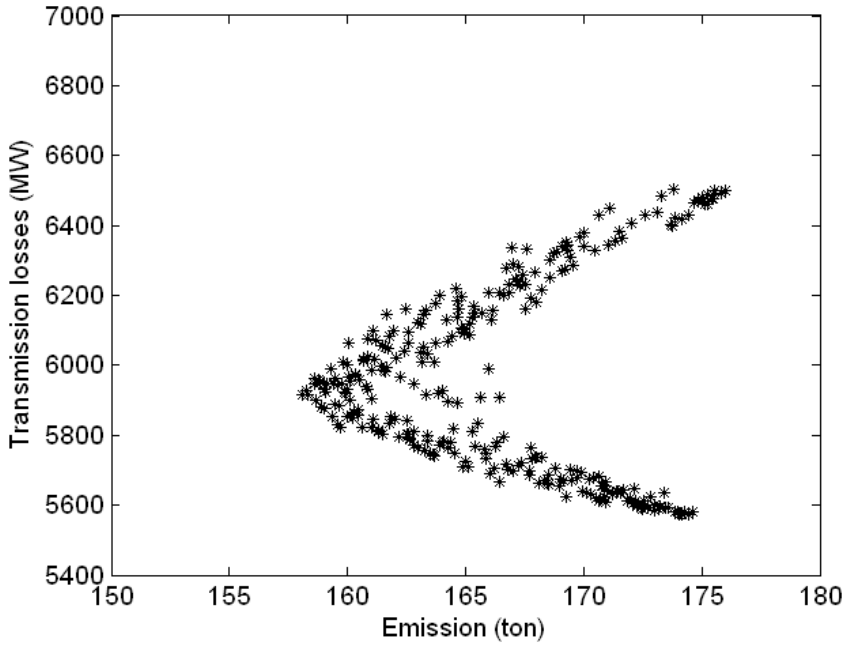

Figure 6.42 Emission vs. transmission losses (based on the 24-hour Pareto front for the 60-unit system obtained by AMOSA in the second phase)

Table 6.9 Performance of the proposed approach with AMOSA for the 60-unit System (20 run average)

	Operation Cost ($)			Emission (ton)			Transmission Losses (MW)		
	Min	Median	Max	Min	Median	Max	Min	Median	Max
Best Operation Cost	10581940	10582250	10582340	175.54	175.99	175.81	6493.68	6497.86	650.12
Best Emission	10965110	10973110	10973110	158.09	158.27	158.33	5916.23	5917.31	5928.00
Best Transmission Losses	11356160	11364140	11364450	174.01	174.14	174.45	5571.61	5574.42	5575.01

From all runs, SPEA-2's solutions were dominated by 74.33% of those of NSGA-II, whereas NSGA-II's solutions were dominated by 70.66% of those of SPEA-2 in the front. Solutions of NSGA-II and SPEA-2 were dominated by 79% and 89% of those of improved AMOSA respectively, while only 4% of solutions of AMOSA were dominated by NSGA-II, and no solutions of improved AMOSA were dominated by SPEA-2. Moreover, from table 6.7, 6.8 and 6.9, among the three algorithms, it is shown that the best operation cost ($10581940) and the least emission (158.09 ton) were both obtained by improved AMOSA, while the least transmission losses (5570.11 MW) was obtained by NSGA-II. It can be concluded that the improved AMOSA outperformed both NSGA-II and SPEA-2.

CHAPTER 7 - Conclusions and Future Work

This dissertation presents a novel, two-phase multi-objective evolutionary approach to address the optimal thermal generation scheduling problem, while considering the environmental issue of emission as well as transmission losses, in addition to the economic issue of operation cost. A number of new techniques have been proposed during the research work of development of this two-phase approach, which are outlined below:

- In the first phase, this approach formulates the hourly-optimal scheduling problem as a three-objective optimization problem, which simultaneously minimizes operation cost, emission and transmission losses, while satisfying constraints such as power balance, spinning reserve and power generation limits.
- Improved versions of three well known MOEAs- NSGA-II, SPEA-2 and AMOSA are proposed. These new algorithms incorporate several additional features for faster convergence and to guarantee feasibility.
- Real-coded chromosome is used to represent the power output, also to indicate the on/off status.
- The first phase also includes a repair method that is used to meet the constraint requirements of power generation limits for each unit as well as balancing load with generation.
- A new scheme to keep load balance with consideration of transmission losses is proposed.
- The three MOEAs are applied to get the optimal solutions for each hourly time interval.
- In the second phase, the chromosome is encoded as the indexes of the solutions on the Pareto front obtained in the first phase.
- With the minimum up/down time and ramp up/down rate enforced, using the three modified MOEAs with or without considering emission allowance trading, the 24-hour dispatch schedules are acquired by picking out all the hourly solutions for each hour achieved from the first phase.

- A special scheme is proposed to increase the diversity of Pareto front in the second phase, in which the hourly-optimal solution on the boundary of Pareto front in the first phase is checked with the obtained best solutions obtained in the second phase.
- Several new features are included to improve the original AMOSA, including the new diversity preservation method and the new perturbation method to produce new solutions, which has improved the performance of AMOSA significantly.
- The proposed two-phase approach is tested on four systems. The two-objective model, which optimizes the operation cost and emission simultaneously, is tested on the 10-unit system and the IEEE 118-bus system. Simulation results demonstrate that NSGA-II outperforms SPEA-2 and is comparable to the improved AMOSA. The three-objective model, which optimizes the operation cost, emission and transmission losses simultaneously, is tested on the 15-unit system and 60-unit system. It is shown that the improved AMOSA, with new features of crossover, mutation and diversity preservation, outperforms NSGA-II and SPEA-2.
- Numerical results demonstrate that the proposed approach is effective in addressing the multi-objective generation scheduling problem, obtaining a set of optimal solutions that account for trade-offs between multiple objectives. This feature allows much greater flexibility in decision-making. Since all the solutions are non-dominated, the choice of a final 24-hour schedule depends on the plant operator's preference and practical operating conditions.
- The proposed two-phase multi-objective evolutionary approach gives a general frame work of solving optimal thermal generation scheduling problem.
- This work can also be extended to include additional objectives as well as constraints for analyzing different operational scenarios.
- Moreover, since only three major MOEAs are studied in the two-phase multi-objective approach in this dissertation, future work may focus on employing some other latest MOEAs in the two-phase approach to solve the multi-objective generation scheduling problem.
- In addition, this two-phase approach has a good perspective on other mixed-integer programming problem as long as the model can be fitted into this general framework.

References

[1] H. Saadat, *Power System Analysis*. McGraw Hill, 2002, pp. 257–258.

[2] A. J. Wood and B. F. Wollenberg, *Power Generation, Operation and Control*. New York: Wiley, 1996.

[3] C. K. Pang and H. C. Chen, "Optimal short-term thermal unit commitment," *IEEE Trans. Power App. Syst.*, vol. PAS-95, pp. 1336–1346, July/Aug. 1976.

[4] N. P. Padhy, "Unit Commitment-A Bibliographical Survey," *IEEE Trans. Power Syst.*, vol. 19, pp 1196–1205, May 2004.

[5] X. Guan, P. B. Luh, and H. Yan, "An optimization based method for unit commitment," *Int. J. Elect. Power Energy Syst.*, vol. 14, no. 1, pp. 9–17, Feb. 1992.

[6] C. Li, R. B. Johnson, and A. F. Svaboda, "A new unit commitment method," *IEEE Trans. Power Syst.*, vol. 12, pp. 113–119, Feb. 1997.

[7] A. A. El-Keib. H. Ma. and J. L. Hart. "Economic dispatch in view of the clean air act of 1990," *IEEE Trans. Power Syst.*, vol. 9, no. 2, pp. 972–978,1994.

[8] I. H. Talaq, F. El-Hawary, and M. E. El-Hawary. "A summary of environmental/economic dispatch algorithms," *IEEE Trans. Power Syst.*, vol. 9, no. 3, pp. 1508–1516, 1994.

[9] H.W. Whittington and I.A. Robson, "Hydroelectric power in emissions-constrained Electricity generation," *Engineering Science and Education Journal*, 3, 4, pp.185–191, 1994.

[10] J. H. Talaq, F. El-Hawary, and M. E. El-Hawary, "Minimum emission power flow," *IEEE Trans. Power Syst.*, vol. 9, pp. 429–435, Feb. 1994.

[11] R. Ramanathan, "Emission constrained economic dispatch," *IEEE Trans. Power Syst.*, vol. 9, pp. 1994–2000, Nov. 1994.

[12] M. A. Abido, "Environmental/Economic power dispatch using multi-objective evolutionary algorithms," *IEEE Trans. Power Syst.*, vol. 18, no.4, pp. 1529–1537, 2003.

[13] L. Wang and C. Singh, "Stochastic economic emission load dispatch through a modified particle swarm optimization algorithm," *Elect. Power Syst. Res.*, vol. 78, pp. 1466–1476, 2008.

[14] X. Liu, "Study of multi-objective optimization and multi-attribute decision-making for economic and environmental power dispatch," *Elect. Power Syst. Res.*, vol. 79, pp. 789–795, 2009.

[15] Technology Options 2003. (2003). US Climate Change Technology Program.

[16] "Question: Where can I find data on electricity transmission and distribution losses?" Frequently Asked Questions – Electricity. U.S. Energy Information Administration. 2009-11-19.

[17] R.H. Kerr, J.L. Scheidt, A.J. Fontana and J.K. Wiley, "Unit commitment," *IEEE Trans. Power Apparatus Syst.,* PAS-85 (5) (1966) 417–421.

[18] F.N. Lee, "Application of commitment utilization factor (CUF) to thermal unit commitment," *IEEE Trans. Power Syst.,* vol. 6, no. 2, pp. 691–698, 1991.

[19] Y. Al-Kalaani, F.E. Villaseca, F. Renovich, "Storage and delivery constrained unit commitment," *IEEE Trans. Power Syst.*, vol. 11, no. 2, pp. 1059–1066, 1996.

[20] K.A. Juste, H. Kita, E. Tanaka and J. Hasegawa, "An evolutionary programming solution to the unit commitment problem," *IEEE Trans. Power Syst.*, vol. 14, pp. 1452–1459, 1999.

[21] J.A. Muchkstadt and R.C. Wilson, “An application of mixed-integer programming duality to scheduling thermal generating systems,” *IEEE Trans. Power Syst.* (1968) 1968–1978.
[22] S. Takriti and J.R. Birge, “Using integer programming to Lagrangian-based unit commitment solutions,” *IEEE Trans. Power Syst.*, vol. 15, pp. 151–156, 2000.
[23] S. Salam, “Unit Commitment Solution Methods,” *Proceedings of World Academy of Science, Engineering and Technology,* vol. 26, December 2007, ISSN 2070–3740.
[24] A. I. Cohen and M. Yoshimura, “A branch-and-bound algorithm for unit commitment,” *IEEE Trans. Power App. Syst.*, vol. PAS-102, pp. 444–451, Feb. 1983.
[25] C.L. Chen, S.C. Wang, “Branch-and-bound scheduling for thermal generating units,” *IEEE Trans. Energy Convers.*, vol. 8, no. 2, pp. 184–189, 1993.
[26] H.Y. Yamin , “Review on methods of generation scheduling in electric power systems,” *Elect. Power Syst. Res.*, 69 (2004) 227–248
[27] A. I. Cohen and V. R. Sherkat, “Optimization based methods for operations scheduling,” *Proceedings of the IEEE*, vol. 75, no. 12, pp. 1574–1591, 1987.
[28] S. K. Tong and S. M. Shahidehpour, “Combination of Lagrangian-Relaxation and linear-programming approaches for fuel-constrained unit commitment problems,” *Proc. Inst. Elect. Eng., Gen. Transm. Dist.*, vol. 136, pp. 162–174, May 1989.
[29] H. Okuno, T. Tominaka, S. Fujishima, T. Mitsumoto, T. Kubo, T. Kawaguchi, J.W. Kim, K. Ikegami, N. Sakamoto, S. Yokouchi, T. Morikawa, T. Tanaka, A. Goto, Y. Yano, Optimal scheduling of spinning reserve with ramp constraints, *IEEE Power Eng. Soc. (Winter Meeting)* 2 (1999) 1075–1077.
[30] S. Mukhtari, J. Singh, and B. Wollenberg, “A unit commitment expert system,” *IEEE Trans. Power Syst.*, vol. 3, pp. 272–277, Feb. 1988.
[31] X. Guan, P. B. Luh, and H. Yan, “An optimization based method for unit commitment,” *Int. J. Elect. Power Energy Syst.*, vol. 14, no. 1, pp. 9–17, Feb. 1992.
[32] N. P. Padhy, V. R. Ramachandran, and S. R. Paranjothi, “Fuzzy decision system for unit commitment risk analysis,” *Int. J. Power Energy Syst.*, vol. 19, no. 2, pp. 180–185, 1999.
[33] V.B.A. Kasangaki, H.M. Sendaula and S.K. Biswas, “Stochastic hopfield artificial neural network for electric power production costing,” *IEEE Trans. Power Syst.,* vol. 10, no. 3, pp. 1525–1533, 1995.
[34] M. P.Walsh and M. J. O. Malley, “Augmented Hopfield network for unit commitment and economic dispatch,” *IEEE Trans. Power Syst.*, vol. 12, pp. 1765–1774, Nov. 1997.
[35] H. Mori and O. Matsuzaki, “Embedding the priority into tabu search for unit commitment,” *Proc. IEEE (Winter Meeting)* 3 (2001) 1067–1072.
[36] X. Bai and S.M. Shahidehpour, “Hydro-thermal, scheduling by tabu search and decomposition method,” *IEEE Trans. Power Syst.*, vol. 11, no. 2, pp. 968–974, 1996.
[37] S. Kirkpatrick, C. D. Gelatt, and M. P. Vecchi, “Optimization by simulated annealing,” *Science*, 220(4598): 671–680.
[38] A. H. Mantawy, Y. L. Abdel-Magid, and S. Z. Selim, “A simulated annealing algorithm for unit commitment,” *IEEE Trans. Power Syst.*, vol. 13, pp. 197–204, Feb. 1998.
[39] K. P.Wong and Y.W.Wong, “Short term hydro thermal scheduling part I: simulated annealing approach,” *Proc. Inst. Elect. Eng., Gen. Transm. Dist.*, vol. 141, pp. 497–501, 1994.
[40] J. H. Holland, “Outline for a logical theory of adaptive systems,” *J. Assoc. Comput.,* Mach. 3, 1962.

[41] K.S. Swarup, S. Yamashiro, "Unit commitment solution methodology using genetic algorithm," *IEEE Trans. Power Syst.*, vol. 17, pp. 87–91, 2002.
[42] G. B. Sheble et al., "Unit commitment by genetic algorithm with penalty methods and a comparison of Lagrangian search and genetic algorithm - economic dispatch example," *Int. J. Elect. Power Energy Syst.*, vol. 18, no. 6, pp. 339–346, Feb. 1996.
[43] H. Yang, P. Yang, and C. Huang, "A parallel genetic algorithm approach to solving the unit commitment problem: implementation on the transputer networks," *IEEE Trans. Power Syst.*, vol. 12, pp. 661–668, May 1997.
[44] A. H. Mantawy, Y. L. Abdel-Magid, and S. Z. Selim, "Integrating genetic algoritms, Tabu search and simulated annealing for the unit commitment problem," *IEEE Trans. Power Syst.*, vol. 14, pp. 829–836, Aug. 1999.
[45] H.T. Yang, P.C. Yang and C.L. Huang, "Evolutionary programming based economic dispatch for units with non-smooth fuel cost functions," *IEEE Trans. Power Syst.,* vol. 11, no. 1, pp. 112–117, 1996.
[46] K. Deb, *Multi-Objective Optimization Using Evolutionary Algorithms*. New York: Wiley, 2001.
[47] J. Horn, N. Nafploitis, and D. E. Goldberg, "A Niched Pareto genetic Algorithm for Multiobjective Optimization," in *Proceedings of the First IEEE Conference on Evolutionary Computation*, Z. Michalewicz, Ed. Piscataway, NJ: IEEE Press, 1994, pp. 82–87.
[48] N. Srinivas and K. Deb, "Multiobjective function optimization using nondominated sorting genetic algorithms," *Evol. Comput.*, vol. 2, no. 3, pp. 221–248, Fall 1995.
[49] E. Zitzler, "Evolutionary algorithms for multiobjective optimization: Methods and applications," Doctoral dissertation ETH 13398, Swiss Federal Institute of Technology (ETH), Zurich, Switzerland, 1999.
[50] J. Knowles and D. Corne, "The Pareto archived evolution strategy: A new baseline algorithm for multiobjective optimization," in *Proceedings of the 1999 Congress on Evolutionary Computation*. Piscataway, NJ: IEEE Press, 1999, pp. 98–105.
[51] K. Deb, A. Pratap, S. Agarwal and T. Meyarivan, "A fast and elitist multi-objective genetic algorithm: NSGA-II," *IEEE Trans. Evol. Comput.*, vol. 6, no. 2, pp. 182–197, 2002.
[52] E. Zitzler, M. Laumanns, and L. Thiele, "SPEA2: Improving the strength pareto evolutionary algorithm for multiobjective optimization," *Evolutionary Methods for Design, Optimisation and Control*, CIMNE, Barcelona, Spain, 2002
[53] S. Bandyopadhyay, S. Saha, U. Maulik, and K. Deb, "A Simulated Annealing-Based Multiobjective Optimization Algorithm: AMOSA," *IEEE Trans. Evol. Comput.*, vol. 12, no. 3, pp. 269–283, June 2008.
[54] B. KRALJ, N. RAJAKOVIC: 'Multi-objective programming in power system optimization: new appraoch to generator maintenance scheduling', *Int. J. Elect. Power Energy Syst.*, 1994, 16, (4), pp. 211–220.
[55] H.D. Chiang, and R. Jean-Jumeau, "Optimal network reconfigurations in distribution systems: Part 2: Solution algorithms and numerical results," *IEEE Trans. Power Deliv.*, 1990, 5, (3), pp. 1568–1574
[56] M. Muslu, "Economic dispatch with environmental considerations: tradeoff curves and emission reduction rates," *Elect. Power Syst. Res.*, 2004, 71, (2), pp. 153–158
[57] Tankut Yalcinoz and Onur Köksoy, "A multi-objective optimization method to environmental economic dispatch," *Int. J. Electr. Power Energy Syst.*, 2007, 29, (1), pp. 42–50.

[58] W. B. Liao, Y. L Chen, S. C. Wang, "Goal-attainment method for optimal multi-objective harmonic filter planning in industrial distribution systems," *IEE Proceedings C-Generation, Transmission and Distribution,* vo. 149, Iss. 5, pp. 557 – 563, Sep 2002.
[59] W. D. Rosehart, C. A. Cañizares, and V. H. Quintana, "Multiobjective optimal power flows to evaluate voltage security costs in power networks," *IEEE Trans. Power Syst.*, vol. 18, no. 2, pp. 578–587, May 2003.
[60] M.A. Abido, "A niched Pareto genetic algorithm for multiobjective environmental/economic dispatch," *Int. J. Electr. Power Energy Syst.*, 2003, 25, (2), pp. 97–105.
[61] M.A. Abido and J.M. Bakhashwain, **"**Optimal VAR dispatch using multi-objective evolutionary algorithm," *Int. J. Electr. Power Energy Syst.*, 2005, 27, (1), pp. 13–20.
[62] D. Li, S. Das, and A. Pahwa, "Two-phase multi-objective evolutionary approaches for optimal generation scheduling with environmental considerations," *41th Annual North American Power Symposium*, Starkville, Mississippi, 2009.
[63] D. Li, A. Pahwa, and S. Das, "A new optimal dispatch method for the day-ahead electricity market using a multi-objective evolutionary approach," *39th Annual North American Power Symposium*, Las Cruces, New Mexico, 2007.
[64] F. Yang and C.S. Chang, "Optimisation of maintenance schedules and extents for composite power systems using multi-objective evolutionary algorithm," *IET Gener. Transm. Distrib.*, vol. 3, Iss. 10, pp. 930–940, 2009.
[65] J. Kennedy and R. Eberhart, "Particle Swarm Optimization," *Proc. of IEEE Int. Conf. on Neural Network*, vol. 4, pp. 1942-1948. 1995.
[66] N.M. Pindoriya and S.N. Singh, "MOPSO based day-ahead optimal self-scheduling of generators under electricity price forecast uncertainty," *Power & Energy Society General Meeting, IEEE 2009*, pp. 1–8.
[67] L. Slimani and T. Bouktir, "Economic power dispatch of power system with pollution vontrol using multiobjective ant colony optimization," *International Journal of Computational Intelligence Research*, vol. 3, no. 2, pp. 145–153, Apr. 1995.
[68] A. Ahuja, S. Das, A. Pahwa, "An AIS-ACO hybrid algorithm for multi-objective distribution system configuration problem," *IEEE Trans. Power Syst.*, vol. 22, no. 3, pp. 1101–1111, Aug. 2007.
[69] K. P. Wong; B. Fan; C.S. Chang, A.C., Liew, "Multi-objective generation dispatch using bi-criterion global optimisation Power Systems," *IEEE Trans. Power Syst.*, vol. 10 , no. 4, pp. 1813–1819, 1995.
[70] B. Suman, "Study of self-stopping PDMOSA and performance measure in multiobjective optimization," *Comput. Chem. Eng.*, vol. 29, no. 5, pp. 1131–1147, Apr. 15, 2005.
[71] Eckart Zitzler, Marco Laumanns and Stefan Bleuler, "A tutorial on evolutionary multiobjective optimization," *Metaheuristics for Multiobjective Optimisation (2004)* Volume: 535, Publisher: Springer-Verlag, Pages: 3–38.
[72] G. Rudolph, "Convergence of evolutionary algorithms in general search spaces," *Proceedings of IEEE International Conference on Evolutionary Computation*, 1996., pp. 50–54.
[73] M. Dorigo, Optimization, Learning and Natural Algorithms, PhD thesis, Politecnico di Milano, Italie, 1992.
[74] D. Martens, M. De Backer, R. Haesen, J. Vanthienen, M. Snoeck, B. Baesens, Classification with Ant Colony Optimization, *IEEE Trans. Evol. Comput.*, vol. 11, no. 5, pp. 651–665, 2007.

[75] P. Toth, D. Vigo, "Models, relaxations and exact approaches for the capacitated vehicle routing problem," *Discrete Applied Mathematics*, vol. 123, pp. 487–512, 2002.
[76] K. Deb and R. B. Agrawal, "Simulated binary crossover for continuous search space," *Complex Syst.*, vol. 9, pp. 115–148, Apr. 1995.
[77] L.J. Eshelman and J.D. Schaer, "Real-coded genetic algorithms and interval-schemata," *Foundations of Genetic Algorithms,* 2, pp. 187–202 (1993).
[78] S. Tsutsui, M. Yamamura and T. Higuchi, "Multi-parent recombination with simplex crossover in realcoded genetic algorithms," *Proceedings of the Genetic and Evolutionary Computing Conference (GECCO-1999)* pp. 657–664.
[79] G. P. Granelli, M. Montagna, G. L. Pasini, and P. Marannino, "Emission constrained dynamic dispatch," *Elect. Power Syst. Res.*, vol. 24, pp. 55–64, 1992.
[80] K.P. Wong and J. Yuryevich, "Evolutionary-programming-based algorithm for environmentally-constrained economic dispatch," *IEEE Trans. Power Syst.*, vol. 13, no. 2, pp. 301–306, May 1998.
[81] M. Shahidehpour, H. Yamin, and Z. Y. Li, *Market Operations in Electric Power Systems*. New York: Wiley, 2002.
[82] A. A. El-Keib. H. Ma. and J. L. Hart. "Economic dispatch in view of the clean air act of 1990," *IEEE Trans. Power Syst.*, vol. 9, no. 2, pp. 972–978, 1994.
[83] I. H. Talaq, F. El-Hawary, and M. E. El-Hawary. "A summary of environmental/economic dispatch algorithms," *IEEE Trans. Power Syst.*, vol. 9, no. 3, pp. 1508–1516, 1994.
[84] A. Aulisi, A. E. Farrell, J. Pershing, and S. Vandeveer, "Greenhouse gas emissions trading in U.S. States: Observations and lessons from the OTC NOx budget program," [Online] Available: http://pdf.wri.org/nox_ghg.pdf.
[85] J. Alan Beamon, Tom Leckey and Laura Martin, "Power plant emission reductions using a generation performance standard," [Online]. Available: http://www.eia.doe.gov/oiaf/servicerpt/gps/gpsstudy.html.
[86] R. Yokoyama, S. H. Bae, T. Morita, and H. Sasaki, "Multiobjective generation dispatch based on probability security criteria," *IEEE Trans. Power Syst.*, vol. 3, pp. 317-324, Feb. 1988.
[87] R.T.F. Ah King, H.C.S. Rughooputh, K. Deb, "Stochastic evolutionary multiobjective environmental/economic dispatch," in *Proceedings of the IEEE Congress on Evolutionary Computation*, Vancouver, BC, Canada, pp. 946–953, July 2006.
[88] Paul J. Miller and Chris Van Atten, "North american power plant air emissions," Report from Commission for Environmental Cooperation of North America, [Online]. Available: http://www.cce.cec.org/files/PDF/POLLUTANTS/PowerPlant_AirEmission_en.pdf.
[89] K. P. Wong and C. C. Fung, "Simulated annealing based economic dispatch algorithm," *IEE Proceedings C-Generation, Transmission and Distribution,* 140(6) pp. 509–515. Nov 1993.
[90] K. Deb and M. Goyal, "A combined genetic adaptive search (geneas) for engineering design," *Computer Science and Informatics*, 26(4):30–45, 1996.
[91] A. K. Jain and R. C. Dubes, *Algorithms for Clustering Data*. Englewood Cliffs, NJ: Prentice-Hall, 1988.
[92] S. A. Kazarlis, A. G. Bakirtzis, and V. Petridis, "A genetic algorithm solution to the unit commitment problem," *IEEE Trans. Power Syst.*, vol. 11, pp. 83–92, Feb. 1996.
[93] T. Senjyu, T. Miyagi, A. Y. Saber, N. Urasaki, and T. Funabashi, "Emerging solution of large-scale unit commitment problem by stochastic priority list," *Elect. Power Syst. Res.*, vol. 76, pp. 283–292, Mar. 2006.

[94] T. Senjyu, K. Shimabukuro, K. Uezato, and T. Funabashi, "A fast technique for unit commitment problem by extended priority list," *IEEE Trans. Power Syst.*, vol. 18, no. 2, pp. 882–888, May 2003.
[95] D. Srinivasan and J. Chazelas, "A priority list-based evolutionary algorithm to solve large scale unit commitment problem," in *Proc. Int. Conf. Power System Technology*, Nov. 2004, pp. 1746–1751.
[96] B. Zhao, C. X. Guo, B. R. Bai, and Y. J. Cao, "An improved particle swarm optimization algorithm for unit commitment," *Int. J. Elect. Power Energy Syst.*, vol. 28, pp. 482–490, Sep. 2006.
[97] T. O. Ting, M. V. C. Rao, and C. K. Loo, "A novel approach for unit commitment problem via an effective hybrid particle swarm optimization," *IEEE Trans. Power Syst.*, vol. 21, no. 1, pp. 411–418, Feb. 2006.
[98] C. P. Cheng, C. W. Liu, and G. C. Liu, "Unit commitment by Lagrangian relaxation and genetic algorithms," *IEEE Trans. Power Syst.*, vol. 15, no. 2, pp. 707–714, May 2000.
[99] W. Ongsakul and N. Petcharaks, "Unit commitment by enhanced adaptive Lagrangian relaxation," *IEEE Trans. Power Syst.*, vol. 19, no. 1, pp. 620–628, Feb. 2004.
[100] I. G. Damousis, A. G. Bakirtzis, and P. S. Dokopoulos, "A solution to the unit commitment problem using integer-coded genetic algorithm," *IEEE Trans. Power Syst.*, vol. 19, no. 2, pp. 1165–1172, May 2004.
[101] T. Senjyu, H. Yamashiro, K. Uezato, and T. Funabashi, "A unit commitment problem by using genetic algorithm based on unit characteristic classification," in *Proc. 2002 IEEE Power Eng. Soc. Winter Meeting*, vol. 1, pp. 58–63.
[102] T. Sum-im and W. Ongsakul, "Ant colony search algorithm for unit commitment," in *Proc. 2003 IEEE Int. Conf. Industrial Technology*, pp. 72–77.
[103] T. A. A. Victoire and A. E. Jeyakumar, "Unit commitment by a tabu search-based hybrid-optimisation technique," *Proc. Inst. Elect. Eng., Gen., Transm., Distrib.*, vol. 152, no. 4, pp. 563–574, Jul. 2005.
[104] J. Valenzuela and A. E. Smith, "A seeded memetic algorithm for large unit commitment problems," *J. Heurist.*, vol. 8, pp. 173–195, Mar. 2002.
[105] L. Sun, Y. Zhang, and C. Jiang, "A matrix real-coded genetic algorithm to the unit commitment problem," *Elect. Power Syst. Res.*, vol. 76, pp. 716–728, Jun. 2006.
[106] S. H. Hosseini, A. Khodaei, and F. Aminifar. "A novel straightforward unit commitment method for large-scale power systems," *IEEE Trans. Power Syst.*, vol. 22, no. 4, pp. 2134–2143, May 2007.
[107] U.S. Environmental Protection Agency, "NOx budget trading program: compliance and environmental results 2007," December 2008, [Online] Available: http://www.epa.gov/airmarkets/progress/docs/2007-NBP-Report.pdf.
[108] CantorCO2e's NOx Market Price Indicator (MPI), 2008. [Online] Available: http://www.emissionstrading.com/.
[109] Zwe-Lee Gaing, "Particle swarm optimization to solving the economic dispatch considering the generator constraints," *IEEE Trans. Power Syst.*, vol. 18, no. 3, pp. 2134–2143, Aug. 2003.
[110] Michalewicz Z, *Genetic algorithms + data structures = evolution programs*. Springer, New York, 1992.